Ai miei nonni

Contents

Introduction

The numerical study of quantum field theories (QFT) on a lattice is a technique recent, born in '74 by Wilson. In most cases this is the only known tool to investigate non-perturbative aspects of QFT, like phase transitions and critical phenomena. This makes the lattice investigation more and more accepted and used by the scientific community. The mutual interest between lattice investigation and thermodynamical study of phase transitions is two-fold. Indeed, if the Feynman quantization leads to expressions for the vacuum expectation values of any observable formally equivalent to those of thermodynamical averages in statistical mechanics, criticality is needed on the lattice to recover the continuum limit in QFT.

With the aim of exploring some critical properties in lattice gauge theories, I present in this work the collection of the numerical studies carried out during my PhD. A special look is devoted to the concept of universality which is the link between all these works.

The Chapter 1 is a brief review of the theory of phase transitions in which the main aspects of a critical phenomenon are explained.

The Chapter 2 is devoted to the study of field theories on the lattice and their simulation through Monte Carlo technique.

In Chapter 3 the reader will find a universality check for first order transitions; this is done by comparing the mass spectra in $3d$ 3-state Potts model and $4d$ SU(3) pure gauge theory at finite temperature. Moreover it is verified the conjecture of universality of the mass spectrum, considering the Potts model in an external field.

In Chapter 4 the universality class of the $3d$ U(1) lattice gauge theory is investigated in the particular case of vanishing spatial coupling. First results on the more interesting

case of non-zero spatial coupling are discussed. This work has been done in collaboration with prof. Oleg Borisenko from the Bogolyubov Institute for Theoretical Physics of Kiev in Ukraine.

Chapter 5 contains the first data about a numerical study of the phase diagram of QED with Wilson fermions. This work comes out from a training period of 7 months carried on at the Muenster University in Germany, in collaboration with prof. Owe Philipsen and Pushan Majumdar.

Chapter 1

Critical systems

1.1 Phase transitions and universality

The phenomenon of phase transition is very important for scientists since a longtime. Our life is full of examples of systems changing their physical properties under variation of some external parameter; the most famous is water, known even in three different phases: solid, liquid and gaseous. In general, phase transitions have fundamental applications in several scientific fields, from chemistry to particles physics. Moreover the proper understanding of the transition mechanism promises to provide new technology and to clarify open questions like the evolution of the universe slightly after the Big Bang, when subsequent phase transitions occurred.

The classical approach to phase transitions was localized on the study of the equation of state, a relation like $f(x, y, z, \ldots) = 0$, where $x, y, z, \ldots$ are thermodynamical parameters. An equation of state defines several surfaces in the parameters space, separating the different phases of the system under consideration. Projecting opportunely these surfaces, one obtains a *phase diagram* of the theory.

In order to introduce the main quantities needed in our description and clarify their physical meaning (see [1, 2]), let us refer to the familiar case of water. In Fig. 1.1 it is shown a very simplified version of its phase diagram; in this case the parameters are

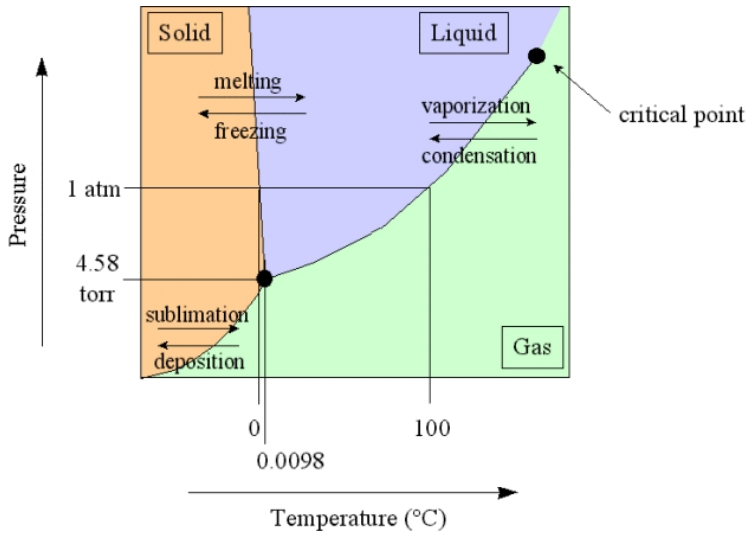

Figure 1.1: Phase diagram of water.

pressure P and temperature T. Phases are separated by transition lines, projection of the surfaces in the (P, T) plane. Let us suppose, for example, to cross the upper-right line under variation of temperature, keeping the pressure fixed at a value large enough: physical and chemical properties of the matter change; water liquid becomes water vapor and the phase transition occurs.

In general, the position of a phase transition is found by varying some parameter, for instance the temperature T, and looking for a jump of some quantity very sensible to the transition: the *order parameter* M. At the same place one observes a peak in the response function (χ) of the order parameter with respect to another parameter, for instance an external field h, *i.e.* $\chi = (\partial M)/(\partial h)|_T$.

In our example the order parameter is the density, which undergoes a sharp decrease when the liquid becomes vapor, while the susceptibility is the compressibility.

Depending on the way in which the order parameter jumps, one talks about the *order* of the transition; since in our example the density jumps discontinuously, one says that transition is first order. But, what does one observe exactly in the water at transition? We know that bubbles are produced, heating up enough liquid water. The new phase

manifests in regions of extension ξ, the *correlation length*, which is the extension of bubbles and a measure of the typical correlation distance between points. The fact that ξ keeps finite, as well as the height of the peak of χ, are further general features of the first order transition occurrence.

Besides this heuristic introduction, in general one has to study thermodynamics using the mathematical tool of *statistical mechanics*. In this context one studies the partition function

$$Z(\beta) = \sum_{\{s\}} e^{-\beta E(s)} = \mathrm{Tr}_s e^{-\beta(s)} \quad , \tag{1.1}$$

where the sum over s is to be understood as a sum over all possible configurations in which the system can be found, and E is the corresponding energy, depending on the nature of microscopic composition of the system; $\beta = \frac{1}{KT}$ where K is the Boltzmann constant and T is the temperature. Thus, partition function is the link between microscopic interactions and the collective macroscopic behavior: thermodynamics. Indeed the partition function is directly connected to the free energy, F, of the system:

$$F = -\frac{1}{\beta} \ln Z(\beta) \quad . \tag{1.2}$$

¿From that one obtains any other thermodynamical potential after suitable derivation of the free energy. In particular the order parameter is found after a first derivative of the free energy, while susceptibility after a second one. This procedure provides a way to distinguish the order of the transition, known as Ehrenfest classification; one says that the order of the transition is k if the free energy of the system is differentiable $(k-1)$ times. In general the thermodynamical average at temperature T of a physical observable Q is defined as

$$\langle Q \rangle = \frac{\sum_s Q(s) e^{-\beta E}}{\sum_s e^{-\beta E}} \quad . \tag{1.3}$$

In the last century new observations required scientists for a modern approach to critical phenomena. They saw that many critical systems could be put in few *classes*, characterized by a common set of indices, *critical exponents*, which govern the behavior of

thermodynamical observables near the transition; this fact is known as *universality*. Let us give an example; let us suppose that a system is showing a phase transition under variation of temperature T; a physical observables, Q, can be expressed in terms of a reduced temperature $\epsilon \equiv \frac{T-T_c}{T_c} = \frac{T}{T_c} - 1$, so that $Q = Q(\epsilon)$, where T_c is the transition temperature. Then a critical exponent is defined as [1, 2]

$$\lambda \equiv \lim_{\epsilon \to 0} \frac{\ln Q(\epsilon)}{\ln \epsilon} \tag{1.4}$$

and this implies that

$$Q(\epsilon) \sim \epsilon^{\lambda} \quad . \tag{1.5}$$

This means that the behavior of the observable is dominated by the power term; (1.5) makes very easy the extraction of the critical exponent and very simple the classification of the observable near the transition.

The most important quantities used for the characterization of the transition in our description are the order parameter, the susceptibility and the correlation length. The corresponding critical indices are β, γ and ν:

$$M \sim \epsilon^{\beta} \quad , \tag{1.6}$$

$$\chi \sim \epsilon^{-\gamma} \quad , \tag{1.7}$$

$$\xi \sim \epsilon^{-\nu} \quad . \tag{1.8}$$

It is evident from the last definitions that one expects that χ and ξ diverges at criticality.

As stated above, physicists noticed that many systems show the same set of critical indices; they belong to the same universality class. These classes depend on

1. The number of degrees of freedom of the microscopic field and the symmetry of the system.
2. The number of dimensions of the space.

To account for this strange cataloging, a symmetry braking mechanism is introduced.

Systems, defined through some particular interaction, exhibit at the same time a global symmetry which is broken at transition. The order parameter, which is in general a quantity not invariant under this symmetry, should vanish by symmetry; it takes a non-zero value when the symmetry is broken, thus indicating that transition occurred.
At criticality, where the correlation length becomes very large, the long-distance properties of the system do not depend anymore on the particular microscopic interaction. The only relevant informations are contained in the mechanism of breaking of the global symmetry. Systems characterized by the breaking of the same global symmetry present the same long-distance behavior (*scaling*), *i.e.* the same critical exponents. Scaling theory and universality find a theoretical basis in the *renormalization group* theory (RG); the reader is reminded to the next section for a rigorous treatment of this topic.
Even though the symmetry breaking mechanism is the most used to explain critical phenomena, one should keep in mind that this is not the only one. Indeed, in the following, we will explore also the Berezinskii-Kosterlitz-Thouless transition where the symmetry breaking is forbidden by the energetics of the system, even though one observes a change in the behavior of the potential: a phase transition. In this case the transition is understood as the unbinding of topological objects.

1.2 Renormalization group

What follows is inspired to [3]. For a review on the main applications see [4] and references therein. All renormalization group studies have in common the idea of re-expressing the parameters which define a problem in terms of some other set, perhaps simpler, while keeping unchanged those physical aspects of the problem which are of interest.
Let us consider a particular model, specified through its action. This will show a cut-off somewhere, like, for instance, a lattice spacing a for theories living on a lattice. The original action S with cut-off Λ is considered to be embedded in an infinite-space of

actions

$$S = \sum_i K_i S_i \quad . \tag{1.9}$$

A renormalization group transformation R_λ is a mapping $S \to S^{(\lambda)}$ in this space so that both S and $S^{(\lambda)}$ describe the same physics at large distances, but the cut-off Λ gets lowered by a factor $\lambda > 1$:

$$\Lambda \to \frac{1}{\lambda}\Lambda \quad . \tag{1.10}$$

$R^{(\lambda)}$ can be described in terms of the change of coefficients $K_i \to K_i^{(\lambda)}$.

The most important points in the space of actions are the fixed points S^*:

$$R_\lambda S^* = S^* \quad , \tag{1.11}$$

in particular those where ξ is infinite. Here the action of R_λ can be linearized and diagonalized such that in a suitable basis

$$K_\alpha = K_\alpha^* + \delta K_\alpha \tag{1.12}$$

it reads

$$K_\alpha^{(\lambda)} = K_\alpha^* + \lambda^{d_\alpha} \delta K_\alpha \quad . \tag{1.13}$$

Those terms with negative *scaling dimension* d_α die out after repeated application of RG transformation and are called *irrelevant* since their presence does not affect the long-distance physics. The terms with $d_\alpha > 0$ are *relevant* and coefficients are decisive for long-distance physics. Repeated RG iterations drive the system away from its fixed point. Terms with $d_\alpha = 0$ are called *marginal*. We cannot tell from linearized equations whether the system will move away from the point or towards it.

Universality emerges in the following way. Two actions S' and S'' which belong to the domain of the same fixed point, are mapped under the action of the RG into the neighborhood of the same low-dimensional manifold

$$S = S^* + \sum_{\substack{\text{relevant} \\ \alpha}} K_\alpha S_\alpha \quad , \tag{1.14}$$

assuming that no marginal operators are present.

The critical behavior is determined only by the few relevant operators in the vicinity

of the fixed point. In particular it can be shown that the critical indices are simple algebraic combinations of the dimensions d_α belonging to them. Thus the fixed points of the RG determine the universality classes of actions.

As an example, let us consider a system in a d-dimensional space with a relevant thermal scaling variable u_t with eigenvalue d_t and a relevant magnetic scale variable u_h with eigenvalue d_h. The relevant variables (u_t, u_h) must vanish at the critical point, chosen so that $t = h = 0$. They must have the form

$$u_t = t/t_0 + O(t^2, h^2) \tag{1.15}$$

$$u_h = h/h_0 + O(th) \quad , \tag{1.16}$$

where t_0 and h_0 are non-universal constants. Thus, close to the critical point, we can take u_t and u_h to be proportional to t and h respectively.

Let us notice that the partition function $Z = \mathrm{Tr}_s e^{-H(s)}$ does not change under RG transformation which, in general, acts as a projection operator

$$e^{-H'(s')} = \mathrm{Tr}_s T(s', s) e^{-H(s)} \quad , \tag{1.17}$$

with $\sum_{s'} T(s', s) = 1$. As a consequence

$$Z' = \mathrm{Tr}'_s e^{-H'(s')} = \mathrm{Tr}_s e^{-H(s)} = Z \quad . \tag{1.18}$$

Consider now the free energy per site, $f(\{X\}) = -N^{-1} \ln Z$, as a function of the couplings $\{X\}$. Under renormalization one changes the global extension of the system, $N' \to b^{-d} N$, and correspondingly the couplings, $\{X\} \to \{X'\}$, in order to keep the physics fixed. This gives the fundamental transformation law for the singular part of the free energy per site:

$$f_s(X) = b^{-d} f_s(X') \quad , \tag{1.19}$$

while for the correlation length

$$\xi(X) = b^{-1} \xi(X') \quad . \tag{1.20}$$

Close to the fixed point, we may write (1.19) in terms of the scaling variables

$$f_s(u_t, u_h) = b^{-d} f_s(b^{d_t} u_t, b^{d_h} u_h) = b^{-nd} f_s(b^{nd_t} u_t, b^{nd_h} u_h) \quad , \tag{1.21}$$

where we have iterate RG n times. Let choose to halt the iteration at the point $|b^{nd_t} u_t| = u_{t0}$, where u_{t0} is arbitrary fixed to a value sufficiently small so that the linear approximation is still valid. Solving this equation for n, we then find that

$$f_s(u_t, u_h) = |u_t/u_{t0}|^{d/d_t} f_s(\pm u_{t0}, u_h |u_t/u_{t0}|^{-d_h/d_t}) \quad . \tag{1.22}$$

Rewriting this in terms of the reduced physical variables t and h, we see that u_{t0} may be incorporated into a redefinition of the scale factor t_0, and that

$$f_s(t, h) = |t/t_0|^{d/d_t} \Phi\left(\frac{h/h_0}{|t/t_0|^{d_h/d_t}} \right) \quad , \tag{1.23}$$

where Φ is a *scaling function*. This function may appear to depend on u_{t0}, but since the left hand side of (1.23) cannot, this is illusory, and, in fact, such scaling function turns out to be *universal*. The only dependence on the particular system is through the *scale factors* t_0 and h_0.

¿From the scaling law (1.23) for the singular part of the free energy, all the thermodynamic exponents follow. For example, for the spontaneous magnetization, $\partial f/\partial h|_{h=0} \propto (-t)^{(d-d_h)/d_t}$, so that

$$\beta = \frac{d - d_h}{d_t} \quad . \tag{1.24}$$

For susceptibility, $\partial^2 f/\partial h^2|_{h=0} \propto |-t|^{(d-2d_h)/d_t}$, one finds

$$\gamma = \frac{2d_h - d}{d_t} \quad . \tag{1.25}$$

1.3 Some important examples

In this section two important physical theories are discussed: the Ising model and the XY model. These are the most simple spin models in which it is possible to show easily the meaning of a symmetry breaking; in particular it is stressed the fact that the

possibility of having a phase transition depends strictly on the nature of the symmetry group characterizing the theory as well as on the dimensionality in which the system is considered. This is the main topic of the Mermin-Wagner theorem.

1.3.1 The Ising model

Despite its simplicity, the Ising model [2] shows all the most important features of a phase transition; in this framework it is particularly easy to appreciate the physical meaning of the concepts relevant in the description of criticality. Moreover, the Ising models considered in different dimensions of the space define very wide universality classes, in which a great number of systems falls in. That is why it is worth to dedicate a section to this model.

Let us consider a system of N spins on a lattice. The dynamics is defined by the microscopic interaction

$$E = -\sum_{i=1}^{N} h s_i - J \sum_{\langle ij \rangle} s_i s_j, \tag{1.26}$$

where s_i is the spin on the i-th site and can take the values $\{+1, -1\}$. J is the coupling constant, while the sum over $\langle ij \rangle$ is extended over all pairs next-to-neighbor on the lattice and h is an external magnetic field. Let us refer to the ferromagnetic case, $J > 0$, where configurations of parallel spins are favored.

Thermodynamics is derived from the partition function

$$Z(\beta, N, h) = \sum_{s_1=\pm 1} \sum_{s_2=\pm 1} \cdots \sum_{s_N=\pm 2} \exp\left(\beta h \sum_i s_i + \beta J \sum_{\langle ij \rangle} s_i s_j\right) \quad , \tag{1.27}$$

which has to be evaluated in the thermodynamical limit $N \to \infty$. ¿From the previous formula one can calculate macroscopic quantities like

$$\langle E \rangle = \frac{\sum_s E(s) e^{-\beta E}}{\sum_s e^{-\beta E}} = -\frac{\partial \ln Z}{\partial \beta} \tag{1.28}$$

and

$$\langle M \rangle = \frac{\sum_s M(s) e^{-\beta E}}{\sum_s e^{-\beta E}} = -\frac{1}{\beta N} \frac{\partial \ln Z}{\partial h} \quad , \tag{1.29}$$

where the magnetization

$$M(s) = \frac{1}{N}\sum_{i=1}^{N} s_i \quad , \tag{1.30}$$

represents the global spin on the lattice. The last thermodynamical average measures the order of the system at a fixed temperature T.

Let us notice that if the external source is set to zero, *i.e.* $h = 0$, it turns out that E is invariant under a global flip of the spins on the lattice. In other words, the system presents the global symmetry $Z(2)$. Under the same transformation, (1.30) changes sign. As a consequence configurations connected by a $Z(2)$ transformation present the same statistical weight in (1.29) and corresponding terms in the sum compensate, giving $\langle M \rangle = 0$ by symmetry. The system should be disordered at any temperature, independently from the dimensionality d of the space. Let us anticipate that, for temperatures small enough and for some value of d, a spontaneous magnetization appears: $\langle M \rangle \neq 0$. This indicates that the system is ordered in spite of the prediction of total order; this means that the $Z(2)$ symmetry is broken. Let T_c denote the transition or critical temperature.

Evaluating partition functions like (1.1) is, in general, a very difficult task; in most cases this cannot be done and one is obliged to study numerically the system. In the case of Ising model, (1.27) can be summed in the cases $d = 1$ and $d = 2$.

In one dimension one finds [2]

$$Z(\beta, N, h) = \left[e^{\beta J} (\cosh \beta h + (\cosh^2 \beta h - 2e^{-2\beta J} \sinh 2\beta J)^{1/2}) \right]^N \quad . \tag{1.31}$$

After application of (1.29) one has

$$\langle M \rangle = \frac{\sinh \beta h}{(\cosh^2 \beta h - 2e^{-2\beta J} \sinh 2\beta J)^{1/2}} \quad , \tag{1.32}$$

which in the limit $h \to 0^+$ gives

$$\langle M \rangle = 0 \tag{1.33}$$

for any finite temperature. Thus the symmetry is not broken in $d = 1$.

In $d = 2$ the situation is radically different. The partition function has been summed

giving [5]

$$Z(\beta, N, 0) = (2\cosh(\beta J)e^I)^N \quad , \tag{1.34}$$

where

$$I = (2\pi)^{-1} \int_0^\pi d\phi \, \ln\left[\frac{1}{2}(1 + (1 - k^2 \sin^2\phi)^{\frac{1}{2}})\right] \tag{1.35}$$

with

$$k = 2\sinh(2\beta J)/\cosh^2(2\beta J) \quad . \tag{1.36}$$

¿From previous formulas one finds that the magnetization becomes

$$M \sim (T_c - T)^\beta \quad , \quad T < T_c \tag{1.37}$$

where $\beta = 1/8$ and $T_c \approx 2.269J$. Thus the first derivative of the free energy turns out to be continuous. This is not the case of quantities related to the second derivative of the free energy, like heat capacity or susceptibility: they diverge at T_c. This means that transition is second order. Correlation length is also divergent. In particular one has $\gamma = 7/4$ and $\nu = 1$.

In three dimensions nobody has solved the Ising model. Nevertheless the system has been studied numerically revealing the presence of a second order transition, just like in $d = 2$. The universal critical indices in this case are [4]

$$\beta = 0.3265(3) \quad , \quad \gamma = 1.2372(5) \quad , \quad \nu = 0.6301(4) \quad .$$

These examples show that the presence of a transition is strictly related to the dimension d in which the system lives.

1.3.2 The Mermin-Wagner theorem

For the Ising model (and, more generally, for systems with discrete symmetries) a phase transition is possible only for $d > d_c = 1$. d_c is called the *lower critical dimension*. It turns out that for most systems with continuous symmetry the fluctuations are more severe because the order parameter may easily change its direction with little cost in the free energy. As a result, the value of the lower critical dimension is increased to $d_c = 2$.

There exist rather simple arguments [3] based on the free energy cost of destabilizing the ordered phase which lead to the above results. Suppose that a magnetic fields acts on the boundary of the system in such a way as to favor energetically a particular ordered state. What, then, is the cost in the free energy of introducing a domain, of size l, within which the spins are in another possible ground state? Consider first the Ising-like system. In $d = 1$, there will be a finite energy $2J$ associated with each domain wall which may occupy $O(l)$ different positions, so that the set of configurations has an entropy $\sim \ln l$. The free energy cost is therefore roughly $4J - 2KT \ln l$, and so forming such a domain of sufficiently large size will always lower the free energy. Thus the ordered phase cannot be stable. This is a simplified version of Landau's argument for the absence of equilibrium order in one dimension. In $d = 2$, a domain wall of size l will have energy $O(Jl)$. To estimate its entropy we may imagine it has a closed random walk, which, at each step, on a square lattice, for example, has at most three choices of which way to go, since it must avoid itself. We therefore expect the number of possible configurations to go roughly as μ^l, where $\mu < 3$. As a result the free energy cost is roughly $2Jl - KTl \ln \mu$. For sufficiently low temperatures, therefore the ordered phase should be stable against the formation of large domains of reversed spins. At some temperature $T_c = O(J/K)$, this is no longer true and the system breaks up into many domains. This is the Peierls argument for the existence of a phase transition in the two-dimensional Ising model. Similar arguments apply for other model with discrete symmetries.

For system with a continuous symmetry, however, the energetics of domain walls is quite different. If we form a domain of size l by insisting that the spins near the center of the domain point in the opposite direction from those away, then the intervening spins have a distance $O(l)$ over which to relax. Since they may do this in a continuous fashion, the relative angle between two neighboring spins will be $O(1/l)$, and the energy density of such a configuration is $O(1/l^2)$. This yields a total energy $O(l^{d-2})$ for a domain whose volume is $O(l^d)$, as compared with $O(l^{d-1})$ in the discrete case. This means that the entropic effects will always win for $d \leq d_c = 2$.

This heuristic argument is supported by the *Mermin-Wagner theorem* [6] which states

that there cannot be any spontaneous braking of continuous symmetry in $d \leq 2$ dimensions.

1.3.3 $2d$ XY model

The $2d$ XY model describes a set of two components classical spins (S_x, S_y) normalized to unit length $S_x^2 + S_y^2 = 1$, and interacting with their nearest neighbors. The corresponding global symmetry is O(2) (or U(1)). After some transformations, this model also describes a classical Coulomb gas, a set of fluctuating surfaces, or superfluid films (see [7] and references therein). It undergoes a remarkable transition, so that the free energy and all its derivatives remain continuous: the Berezinskii-Kosterlitz-Thouless transition [8, 9]. Here there is no macroscopic spontaneous magnetization because of the Mermin-Wagner theorem. Spin variables can also be described by angles, defined modulo 2π, with the partition function written as

$$Z = \int \prod_i \frac{d\theta_i}{2\pi} \exp\left(\beta \sum_{\langle ij \rangle} \cos(\theta_i - \theta_j)\right) \quad , \tag{1.38}$$

where, as usual, $\beta = 1/(KT)$. The interaction is ferromagnetic, in the sense that the configurations with equal θ_i's are favored. The global rotational symmetry appears here as a translational invariance $\theta_i \to \theta_i + \alpha$.

Following [10], each factor of (1.38) can be expanded on the basis of irreducible characters of the group $O(2)$:

$$\begin{aligned} e^{\beta \cos\theta} &= I_0(\beta) + \sum_{n=1}^{\infty} I_n(\beta)(e^{in\theta} + e^{-in\theta}) \\ &= I_0(\beta)(1 + \sum_{n \neq 0} b_n(\beta) e^{in\theta}) \quad , \end{aligned} \tag{1.39}$$

where the coefficients are expressed in terms of modified Bessel functions

$$b_n(\beta) = b_{-n}(\beta) = \frac{I_n(\beta)}{I_0(\beta)} \tag{1.40}$$

with the following behavior for small and large β

$$b_n(\beta) \sim \begin{cases} \frac{\beta^n}{2^n n!} & \beta \to 0 \\ e^{-n^2/2\beta} & \beta \to \infty \end{cases} . \tag{1.41}$$

For a lattice with N sites and $2N$ links, one has

$$\frac{Z}{I_0^{2N}(\beta)} = \int \prod_i \frac{d\theta_i}{2\pi} \prod_{\langle ij \rangle} (1 + \sum_{n_{ij} \neq 0} b_{n_{ij}} e^{i n_{ij}(\theta_i - \theta_j)}) \quad . \tag{1.42}$$

The interest of the expansion (1.41) is clear for small β, the high temperature expansion, since the coefficients b_n decrease very rapidly with n and since integrations can be performed explicitly over each term in the expansion of the product (1.42). The result is

$$\frac{Z}{I_0^{2N}(\beta)} = \sum_{\{n_{ij}\}} \prod_{\langle ij \rangle} b_{n_{ij}}(\beta) \quad . \tag{1.43}$$

One sums over all configurations of relative integers n_{ij}, with the notations $b_0 = 1$ and $n_{ji} = -n_{ij}$. These configurations satisfy the zero divergence condition $(\partial n)_i = \sum_j n_{ij} = 0$. One can, then, compute the correlation function

$$\langle \vec{S}_1 \vec{S}_2 \rangle = \mathrm{Re} \langle e^{i(\theta_1 - \theta_1)} \rangle \tag{1.44}$$

and more generally

$$\langle e^{im(\theta_1 - \theta_2)} \rangle = \frac{\sum_{\{n_{ij}\}, (\partial n)_i = m(\delta_{i1} - \delta_{i2})} \prod_{\langle ij \rangle} b_{n_{ij}}(\beta)}{\sum_{\{n_{ij}\}, (\partial n)_i = 0} \prod_{\langle ij \rangle} b_{n_{ij}}(\beta)} \tag{1.45}$$

The point 1 acts as a source and the point 2 as a sink of intensity m for the "field" n_{ij}. For $m = 1$, the dominant term in (1.45) at high temperature is $N_{12} t_1(\beta)^{d_{12}}$, where d_{12} is the minimal distance on the lattice between points 1 and 2, and N_{12} is the number of corresponding paths of minimal length. Hence correlations decrease exponentially at high temperature to lowest order, and this extends to all orders because the high temperature series has a finite radius of convergence. In particular

$$G(x) \sim e^{-x/\xi(\beta)} \quad . \tag{1.46}$$

At low temperature, the energetic term favors the alignment of spins, and one is tempted to expand $\cos(\theta_i - \theta_j)$ near $\theta_i - \theta_j = 0$, loosing the periodic character of the angles. In this case the partition function becomes the one of a pure Gaussian model

$$Z_{SW} = \int \prod_i \frac{d\theta_i}{2\pi} \exp \left[-\frac{1}{2} \beta \sum_{\langle ij \rangle} (\theta_i - \theta_j)^2 \right] \tag{1.47}$$

and the model is replaced by the so-called *spin wave* approximation. It is easy to calculate the correlation

$$G_{SW}(x) \sim \frac{1}{x^{\eta(\beta)}} \quad , \qquad \eta(\beta) = \frac{1}{2\pi\beta} \quad . \tag{1.48}$$

The spin wave approximation predicts a decrease according to a power law behavior, qualitatively different from the high temperature exponential decrease. This suggests the existence of a transition at an intermediate temperature. The exponent characterizing the decrease of $G(x)$ varies with temperature and vanishes linearly at zero temperature. We have thus here a whole continuous zone of critical temperatures. Fluctuations of the angles increase logarithmically at large distance. Hence the approximation neglecting their periodic character might become unjustified. Indeed, as Berezinskii, Kosterlitz and Thouless have shown, the topological effects resulting from this periodicity play an essential role. They combine with the spin wave fluctuation and increase disorder, so that correlation functions acquire an exponential decrease beyond some critical temperature. Let us study the variation of the angle between the spin and a fixed direction as one follows a simple closed curve. Implicitly, fluctuations are supposed to be weak, so that this angle varies continuously along the path. If the spins are almost aligned, the variation of course vanishes. However, one can imagine configurations such that this angle varies by an integer multiple of 2π, let us say q. This is a topological invariant, in the sense that it does not change when the curve or the configuration changes continuously. This simplest case corresponds to a *vortex* of intensity $n = \pm 1$ (see Fig. 1.2). This particular configuration corresponds to an extremum of the classical action which is the continuous counterpart of (1.47):

$$S_{class} = \frac{1}{2}\beta \int d^2x (\nabla\theta)^2 \quad . \tag{1.49}$$

This action is singular in a vortex configuration. As a regularization, let us exclude from the integration domain a small region, for instance a disk of radius r_0 centered on each singular point and small with respect to the distance between vortices. We denote the intensities of vortices with q_j located in the points z_j. After some calculations [3] one

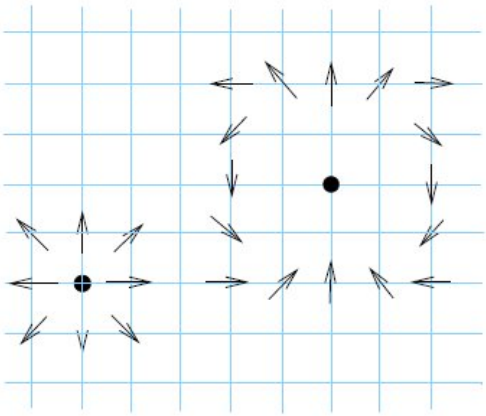

Figure 1.2: A vortex of charge 1 (left) and vortex of charge 2 (right).

has

$$S_{class} = -2\pi\beta \sum_{\langle ij \rangle} q_i q_j \ln |z_i - z_j| + \sum_i q_i^2 \pi\beta \ln 1/r_0 \quad , \tag{1.50}$$

describing a gas of classical particles, globally neutral and with a Coulomb interaction, logarithmic in two dimensions. Consider the case of a vortex pair, at distance r_{12}. Its statistical weight is $\exp(-2\pi\beta \ln r_{12}/r_0)$ (according to (1.50)). In a box of linear dimension L, the global contribution of one vortex pair to the total energy is, for dimensional reasons, of the form

$$\begin{aligned} \exp F_{pair} &\sim \int_{|x_1 - x_2| > r_0} d^2x_1 d^2x_2 \exp(-2\pi\beta \ln \frac{|x_1 - x_2|}{r_0}) \\ &\sim L^4 \exp\left(-2\pi\beta \ln L/r_0\right) \quad . \end{aligned} \tag{1.51}$$

Hence

$$F_{pair} \sim (4 - 2\pi\beta) \ln L \quad . \tag{1.52}$$

If $2\pi\beta > 4$, this contribution is negligible in the limit $L \to \infty$. On the other hand, if $2\pi\beta < 4$, an instability appears. The creation of well-separated vortices is favored and disorder increases. This explains that transition is related to the unbinding of vortices. A first estimate of the critical temperature is

$$2\pi\beta_c = 4 \quad , \tag{1.53}$$

which gives, from (1.48), $\eta(\beta_c) = 1/4$. Actually, after a complete RG treatment [10] one finds that (1.48) should present logarithmic corrections and be replaced by

$$G(x) \sim \frac{1}{|x|^{\eta}} (\ln |x|)^{r} \quad , \tag{1.54}$$

where the critical exponents take the values $\eta = 1/4$ and $r = 1/8$. Furthermore a very particular behavior for correlation length is found just above the transition

$$\xi(\beta) \sim e^{b(\beta - \beta_c)^{-\nu}} \quad , \quad \beta \to \beta_c^{+} \quad , \tag{1.55}$$

where b is a non-universal constant and the critical exponent is $\nu = 1/2$. This law is called *essential scaling* and it is one of the most important evidence of the presence of a BKT transition.

Chapter 2

Field theories on the lattice

2.1 Path integrals

As stated above, the lattice provides a very powerful tool, specially to explore non-perturbative aspects of field theories. Often this method is the only one known. The possibility of simulating quantum field theories on a lattice relies on a particular way of define quantization: the path integral formalism [11, 12]. Let us introduce $|\phi(\vec{x})\rangle$ as the eigenstate of the field operator $\hat{\phi}(\vec{x})$ with eigenvalue $\phi(\vec{x})$:

$$\hat{\phi}(\vec{x})|\phi(\vec{x})\rangle = \phi(\vec{x})|\phi(\vec{x})\rangle \qquad . \tag{2.1}$$

The time evolution of the state reads

$$|\phi(\vec{x}), t\rangle = e^{i\hat{H}t}|\phi(\vec{x})\rangle. \tag{2.2}$$

A procedure of discretization of space and time leads to the following representations for the transition matrix elements

$$\langle\phi_F, t_F|\phi_I, t_I\rangle = \langle\phi_F|e^{-i\hat{H}(t_F-t_I)}|\phi_I\rangle = C\int[d\phi]\exp\left(i\int_{t_I}^{t_F}dt\int d^3x\mathcal{L}\right) \tag{2.3}$$

and for the matrix element of the product of n fields

$$\langle\phi_F, t_F|T[\hat{\phi}(x_1)\cdots\hat{\phi}(x_n)]|\phi_I, t_I\rangle = C\int[d\phi]\phi(x_1)\cdots\phi(x_n)\exp\left(i\int_{t_I}^{t_F}dt\int d^3x\mathcal{L}\right) \quad . \tag{2.4}$$

Here x represent the 4-vector $(t, \vec{x})$. The labels F and I refers to the final and initial state, while C is an irrelevant constant and $\mathcal{L}$ is the classical Lagrangian density. The notation $\int[d\phi]$ means a sum over all possible configurations for the fields and T represents the time-ordered product. It is defined formally by

$$[d\phi] = \prod_{t,\vec{x}} d\phi(t, \vec{x}) \quad . \tag{2.5}$$

In the case of two fields, one has

$$T[\hat{\phi}(x_1)\hat{\phi}(x_2)] = \theta(t_1 - t_2)\hat{\phi}(x_1)\hat{\phi}(x_2) + \theta(t_2 - t_1)\hat{\phi}(x_2)\hat{\phi}(x_1) \quad . \tag{2.6}$$

Now we are able to extract the contribution of the ground state to (2.3) and (2.4). To do this, let us develop the eigenstate of $\hat{\phi}(\vec{x})$, $|\phi(\vec{x})\rangle$, in terms of the eigenstates $|E_m\rangle$ of the Hamiltonian operator:

$$|\phi(\vec{x})\rangle = \sum_m |E_m\rangle\langle E_m|\phi(\vec{x})\rangle \quad , \tag{2.7}$$

where $\hat{H}|E_m\rangle = E_m|E_m\rangle$ with $E_0 = 0$. $|E_0\rangle \equiv |0\rangle$ is the ground state or vacuum state. After a time evolution (2.2) one has

$$\langle\phi_F, t_F|T[\hat{\phi}(x_1)\cdots\hat{\phi}(x_n)]|\phi_I, t_I\rangle$$

$$= \sum_{mm'} e^{iE_m t_I - iE_{m'} t_F}\langle\phi_F|E_{m'}\rangle\langle E_m|\phi_I\rangle\langle E_{m'}|T[\hat{\phi}(x_1)\cdots\hat{\phi}(x_n)]|E_m\rangle \quad . \tag{2.8}$$

At this point, let us apply the analytical continuation to the imaginary time. This consists in doing

$$t_I = i\tau, \qquad t_F = -i\tau \tag{2.9}$$

and then $\tau \to \infty$. The exponential in (2.8) becomes real and, consequently, the dominant contribution will be due to the ground state $E_m = E_{m'} = 0$.

Then

$$\langle\phi_F, t_F|T[\hat{\phi}(x_1)\cdots\hat{\phi}(x_n)]|\phi_I, t_I\rangle \longrightarrow \langle\phi_F|0\rangle\langle 0|\phi_I\rangle\langle 0|T[\hat{\phi}(x_1)\cdots\hat{\phi}(x_n)]|0\rangle \ , \quad \tau \to \infty \ . \tag{2.10}$$

The same procedure applied to (2.3) leads to

$$\langle \phi_F, t_F | \phi_I, t_I \rangle \longrightarrow \langle \phi_F | 0 \rangle \langle 0 | \phi_I \rangle \quad \tau \to \infty \quad . \tag{2.11}$$

In the limit $\tau \to \infty$ one has

$$\langle 0 | T[\hat{\phi}(x_1) \cdots \hat{\phi}(x_n)] | 0 \rangle = \frac{\int [d\phi] \phi(x_1) \cdots \phi(x_n) e^{-S_E(\phi)}}{\int [d\phi] e^{-S_E(\phi)}} \quad , \tag{2.12}$$

with

$$S_E(\phi) = \int_{-\tau}^{\tau} d\tau L_E(\phi(\tau), \dot{\phi}(\tau)) \quad , \tag{2.13}$$

where S_E e L_E are euclidean versions, calculated at complex time, of the action and lagrangian respectively.

In this way it is possible to represent any Green function

$$G(x_1, x_2, \cdots, x_n) = \langle 0 | T[\hat{\phi}(x_1) \cdots \hat{\phi}(x_n)] | 0 \rangle \quad , \tag{2.14}$$

without introducing any operator. Equation (2.12) is formally equivalent to thermodynamical averages in statistical mechanics and the Green function acquires the form of the correlation function of a statistical system defined by the partition function

$$Z = \int [d\phi] e^{-S(\phi)} \quad . \tag{2.15}$$

On a general ground, an important result comes from the application of the generating functional mechanism [13, 14]. In fact, putting the action in the suitable form

$$S = \sum_{n,m} \phi_n M_{nm} \phi_m \quad , \tag{2.16}$$

one finds that the green function turns out to be

$$\langle \phi_n \phi_m \rangle = M^{-1}_{nm} \quad , \tag{2.17}$$

independently on the bosonic or fermionic nature of the field ϕ.

Hence it has been established a link between QFT and thermodynamics. As a consequence, it is possible to use all mathematical tools developed in statistical mechanics for the study of field theories. In particular, considering the field theory on a *lattice*, it is possible to treat (2.12) with numerical simulations. Since (2.12) is derived directly from first principles, numerical simulations are very useful to extract non-perturbative informations on the Green function, specially where perturbation theory fails.

2.2 Gauge theories on the lattice

Writing a theory on a lattice means that one has to discretize the original continuous theory. Moreover, in numerical simulations, one is forced to deal with a finite lattice, instead of the infinite and continuous space-time. A very delicate point is the extraction of the continuum physics, after simulation on a discrete space. Let us present this procedure in the case of *gauge theories*, which are very relevant in particle physics since they are used to describe the fundamental interactions [15].

2.2.1 QED on the lattice

QED, quantum electrodynamics, is the gauge theory which describes electromagnetism. It represents the most important case which supports the use of gauge theories in the particles physics. Indeed, it has never been contradicted by experiments, rather predicting very precisely experimental results. Like any gauge theory, QED is described by the lagrangian [14, 16]

$$\mathcal{L} = -\frac{1}{4}F_{\mu\nu}F^{\mu\nu} + \overline{\psi}(i\gamma^{\mu}D_{\mu} - M)\psi \quad , \tag{2.18}$$

where

$$D_{\mu} = \partial_{\mu} + ieA_{\mu} \tag{2.19}$$

and

$$F_{\mu\nu} = \partial_{\mu}A_{\nu} - \partial_{\nu}A_{\mu} \quad . \tag{2.20}$$

The Dirac γ matrices satisfy the usual anticommutation relations

$$\{\gamma^{\mu}, \gamma^{\nu}\} = 2g^{\mu\nu} \quad . \tag{2.21}$$

The lagrangian is invariant under local U(1) transformations $G = e^{i\Lambda(x)}$. This means that it is invariant under the following transformations for matter fields (ψ) and gauge fields (A_{μ}):

$$\psi(x) \rightarrow G(x)\psi(x) \quad , \tag{2.22}$$

$$\overline{\psi}(x) \to \overline{\psi}(x)G^{-1}(x) \quad , \tag{2.23}$$

$$A_\mu(x) \to G(x)A_\mu(x)G^{-1}(x) - \frac{i}{e}G(x)\partial_\mu G^{-1}(x) \quad . \tag{2.24}$$

Notice that $x \equiv x_\mu$ is the 4-vector position in the space-time.

Before discretizing the lagrangian, let us write the euclidean version of the action

$$S_{QED} = \int d^4x \mathcal{L} = \frac{1}{4}\int d^4x F_{\mu\nu}F_{\mu\nu} + \int d^4x \overline{\psi}(i\gamma^\mu D_\mu + M)\psi \quad . \tag{2.25}$$

This is realized by an analytical continuation of any 0-component of each 4-vector, *i.e.* $x^0 \to -ix_4$, $A^0 \to +iA_4$. The euclidean version of the γ matrices is $\gamma^0 = \gamma_4^E$, $\gamma^i = i\gamma_i^E$. What follows is inspired to [13]. Let us introduce, now, a space-time lattice with lattice spacing a. Each point of the lattice will be singled out by a set of four integer numbers $n \equiv (n_1, n_2, n_3, n_4)$. Any quantity should be made dimensionless to be considered on the lattice. The transition from the continuum to the lattice is made by the following substitutions:

$$\begin{aligned} x_\mu &\to n_\mu a \quad , \\ \int d^4x &\to a^4 \sum_n \quad , \\ [d\phi] &\to \prod_n d\phi(na) \quad , \end{aligned} \tag{2.26}$$

where symbol with the hat are dimensionless. Let us look first at the free fermionic part of the action ($A_\mu = 0$); this will require

$$\begin{aligned} M &\to \frac{1}{a}\hat{M} \quad , \\ \psi(x) &\to \frac{1}{a^{3/2}}\hat{\psi}(n) \quad , \\ \overline{\psi}(x) &\to \frac{1}{a^{3/2}}\overline{\hat{\psi}}(n) \quad , \\ \partial_\mu\psi(x) &\to \frac{1}{a^{5/2}}\hat{\partial}_\mu\hat{\psi}(n) \quad , \end{aligned} \tag{2.27}$$

where $\hat{\partial}_\mu$ is the lattice derivative, defined as

$$\hat{\partial}_\mu\hat{\psi}(n) = \frac{1}{2}[\hat{\psi}(n+\hat{\mu}) - \hat{\psi}(n-\hat{\mu})] \quad . \tag{2.28}$$

Thus the lattice version of the corresponding part in the euclidean action reads

$$S_f = \sum_{n,m\alpha,\beta} \overline{\hat{\psi}}_\alpha(n) K_{\alpha,\beta}(n,m) \hat{\psi}_\beta(m) \quad , \tag{2.29}$$

where

$$K_{\alpha,\beta}(n,m) = \sum_\mu \frac{1}{2}(\gamma_\mu)_{\alpha\beta}[\delta_{m,n+\hat{\mu}} - \delta_{m,n-\hat{\mu}}] + \hat{M}\delta_{mn}\delta_{\alpha\beta} \quad . \tag{2.30}$$

α and β are the 4-spinor labels, while $\hat{\mu}$ is the unit vector in the direction μ. ¿From (2.17) one gets

$$\langle \overline{\hat{\psi}}_\alpha(n) \hat{\psi}_\beta(m) \rangle = K^{-1}_{\alpha,\beta}(n,m) \quad . \tag{2.31}$$

Unfortunately this naive discretization of the fermionic action fails. To see this, let us carry out the continuum limit $a \to 0$

$$\langle \overline{\psi}_\alpha(x) \psi_\beta(y) \rangle = \lim a \to 0 \frac{1}{a^3} \langle \overline{\hat{\psi}}_\alpha(n) \hat{\psi}_\beta(m) \rangle \quad . \tag{2.32}$$

Here the factor $\frac{1}{a^3}$ arises from the scaling of the fields according to (2.27). Switching to the momentum space and using some Fourier algebra, it turns out that

$$\langle \overline{\psi}_\alpha(x) \psi_\beta(y) \rangle = \lim_{a\to 0} \int_{-\pi/a}^{\pi/a} \frac{d^4p}{(2\pi)^4} \frac{[-i\sum \gamma_\mu \tilde{\tilde{p}}_\mu + M]_{\alpha\beta}}{\sum_\mu \tilde{\tilde{p}}^2_\mu + M^2} e^{ip(x-y)} \quad , \tag{2.33}$$

where

$$\tilde{\tilde{p}}_\mu = \frac{1}{a}\sin(p_\mu a) \quad . \tag{2.34}$$

What destroys the correct continuum limit are the zeros of the sine-function in the last equation, at the edges of the Brillouin zone. Thus there exist sixteen region of integration in the above integral, where p_μ takes a finite value in the limit $a \to 0$. Of these, fifteen regions involve high momentum excitations of the order of π/a (and $-\pi/a$), which give rise to a momentum distribution function having the characteristic form of a single particle propagator. Hence the above lattice theory actually contains sixteen species of fermions. In a d space-time dimensions the number would be 2^d; it doubles for each additional dimension. In fact, this problem is known as *fermion doubling*. To obtain the correct continuum limit, we must therefore eliminate the extra fermions species.
A possible solution is provided by the *Wilson fermions* [17]. The strategy is based on the

modification of the action (2.29) in such a way that the zeros of the denominator of the above integral at the edges of the Brillouin zone are lifted by an amount proportional to the lattice spacing. Let us, then, modify the previous action by a term which vanishes in the continuum limit:

$$S_f^{(W)} = S_f - \frac{r}{2}\sum_n \overline{\hat{\psi}}(n)\ \widehat{\Box}\ \hat{\psi}(n) \quad . \tag{2.35}$$

Here r is the Wilson parameter and $\widehat{\Box}$ is the lattice Laplacean defined as

$$\widehat{\Box}\ \phi(na) = \sum_\mu (\phi(na+\hat{\mu}a) + \phi(na-\hat{\mu}a) - 2\phi(na)) \quad , \tag{2.36}$$

with $a = 1$. Setting $\hat{\psi} = a^{3/2}$ and $\widehat{\Box} = a^2\Box$, we see that the additional term in the action vanishes linearly with a in the naive continuum limit. Now we have

$$S_f^{(W)} = \sum_{n,m\alpha,\beta} \overline{\hat{\psi}}_\alpha(n) K^{(W)}_{\alpha,\beta}(n,m)\hat{\psi}_\beta(m) \quad , \tag{2.37}$$

where

$$K^{(W)}_{\alpha,\beta}(n,m) = (\hat{M}+4r)\delta_{nm}\delta_{\alpha\beta} - \sum_\mu \frac{1}{2}[(r-\gamma_\mu)_{\alpha\beta}\delta_{m,n+\hat{\mu}} + (r+\gamma_\mu)_{\alpha\beta}\delta_{m,n-\hat{\mu}}] \quad . \tag{2.38}$$

This action leads to the following two-point function of the continuum theory

$$\langle\overline{\psi}_\alpha(x)\psi_\beta(y)\rangle = \lim_{a\to 0}\int_{-\pi/a}^{\pi/a}\frac{d^4p}{(2\pi)^4}\frac{[-i\sum\gamma_\mu\tilde{\tilde{p}}_\mu + M]_{\alpha\beta}}{\sum_\mu \tilde{\tilde{p}}_\mu^2 + M(p)^2}e^{ip(x-y)} \quad , \tag{2.39}$$

where $\tilde{\tilde{p}}_\mu$ is given by (2.34) and

$$M(p) = M + \frac{2r}{a}\sum_\mu \sin^2(p_\mu a/2) \quad . \tag{2.40}$$

¿From the last equation we see that for any fixed value of p_μ, $M(p)$ approaches M for $a \to 0$. Near the corners of the Brillouin zone, however, $M(p)$ diverges as we let the lattice spacing go to zero.

This procedure eliminates the fermion doubling problem, but at the expense that the chiral symmetry of the original action (2.29) for $M = 0$ has been broken. Let us separate the matter field in the left-handed and right-handed parts

$$\psi_L = \frac{1}{2}(1-\gamma_5)\psi, \quad \psi_R = \frac{1}{2}(1+\gamma_5)\psi \quad ,$$

where $\gamma_5 = i\gamma^0\gamma^1\gamma^2\gamma^3$. It turns out that the original action is invariant under global SU(3) transformations on fields L and R separately, in the case $M = 0$. This is the so-called *chiral symmetry*.

Using Wilson fermions means loosing this original invariance. This is the price to pay to ensure a correct continuum limit and this makes this approach less attractive for studying such questions as spontaneous chiral symmetry breaking in lattice gauge theories. However, this is not the one scheme for the fermions simulation on the lattice. An alternative way for putting fermions on the lattice is the "staggered" [18] formulation which, for instance, preserves the original chiral symmetry of the continuous action.

Let us start from (2.37) where, for simplicity, we suppress all the hats in the notation, since we deal only with quantities on the lattice. The Wilson action for fermions is invariant under a global gauge transformation

$$\begin{aligned} \psi(n) &\to G\psi(n) \quad , \\ \overline{\psi}(n) &\to \overline{\psi}(n)G^{-1} \quad , \end{aligned} \tag{2.41}$$

with $G \in \mathrm{U}(1)$; the same action is not invariant under local gauge transformations. To understand how to realize this fundamental requirement of a gauge theory, let us consider the bilinear terms

$$\begin{aligned} \overline{\psi}(n)(r-\gamma_\mu)\psi(n+\hat{\mu}) &\to \overline{\psi}(n)(r-\gamma_\mu)U_{n,n+\hat{\mu}}\psi(n+\hat{\mu}) \quad , \\ \overline{\psi}(n+\hat{\mu})(r-\gamma_\mu)\psi(n) &\to \overline{\psi}(n+\hat{\mu})(r-\gamma_\mu)U_{n+\hat{\mu},n}\psi(n) \quad , \end{aligned} \tag{2.42}$$

where $U_{n+\hat{\mu},n} = U^\dagger_{n,n+\hat{\mu}}$ is an element of the U(1) group. Unlike the matter fields, the $U_{n,n+\hat{\mu}}$ elements do not live in a single site, but they connect two adjacent sites. This is why they are called "link" variable. Putting all in the action, one has

$$S_f = (\hat{M}+4r)\sum_n \overline{\psi}(n)\psi(n) - \frac{1}{2}\sum_{n,\mu}\left[\overline{\psi}(n)(r-\gamma_\mu)U_{n,n+\hat{\mu}}\psi(n+\mu) + \overline{\psi}(n+\mu)(r+\gamma_\mu)U^\dagger_{n,n+\hat{\mu}}\psi(n)\right] \quad . \tag{2.43}$$

The interaction matrix is often expressed as

$$K_{\alpha,\beta}[U]^{(W)}(n,m) = \delta_{nm} - \kappa\sum_{\mu>0}[(r-\gamma_\mu)U_\mu(n)\delta_{m,n+\hat{\mu}} + (r+\gamma_\mu)U^\dagger_\mu(n-\hat{\mu})\delta_{m,n-\hat{\mu}}] \quad , \tag{2.44}$$

so that (2.37) becomes

$$S_f^{(W)} = \sum_{n,m} \overline{\hat{\psi}}_\alpha(n) K^{(W)}(n,m) \hat{\psi}_\beta(m) \quad , \tag{2.45}$$

with the so-called hopping parameter κ

$$\kappa = \frac{1}{2\hat{M} + 2rN_f} \tag{2.46}$$

and rescaled fermions fields by the coefficient $\sqrt{2\kappa/a^3}$. ¿From the last expression one sees that for the free theory in 4 dimensions the fermion mass is given in terms of the lattice parameters κ and r as

$$Ma = \frac{1}{2\kappa} - 4r = \frac{1}{2\kappa} - \frac{1}{2\kappa_c} \quad , \tag{2.47}$$

where $m = 0$ at $\kappa = \kappa_c = 1/8r$.

To conclude the discretization of the continuum action we have to consider the gauge part. Let us build the product of link variables around an elementary plaquette, a square of unitary side, for instance in the plane $\hat{\mu}\hat{\nu}$:

$$U_{\mu\nu}(n) = U_\mu(n) U_\nu(n+\hat{\mu}) U_\mu^\dagger(n+\hat{\nu}) U_\nu^\dagger(n) \quad . \tag{2.48}$$

Using $U_\mu(n) \equiv U_{n,n+\hat{\mu}} = e^{ieaA_\mu(n)}$, by which (2.43) has the right continuum limit, one gets $U_{\mu\nu}(n) = e^{iea^2 F_{\mu\nu}}$. As a consequence, for $a \to 0$

$$S_G \simeq \frac{1}{e^2} \sum_n \sum_{\mu,\nu;\mu<\nu} \left[1 - \frac{1}{2}(U_{\mu\nu}(n) + U_{\nu\mu}^\dagger(n)) \right] \simeq \frac{1}{4} \sum_{n,\mu,\nu} a^4 F_{\mu\nu} F_{\mu\nu} \quad . \tag{2.49}$$

Finally one can write the last equation in a compact form as

$$S_G(U) = \frac{1}{e^2} \sum_P \left[1 - \frac{1}{2}(U_P + U_P^\dagger) \right] \quad , \tag{2.50}$$

where U_P is the plaquette variable (see Fig. 2.1).

2.2.2 Continuum limit

The above arguments by which the previous action really describe QED in the continuum limit, were based on the observation that lattice action reproduces the correct

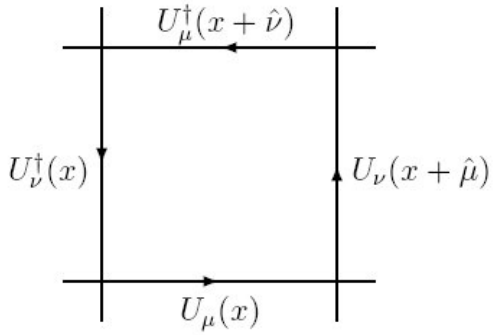

Figure 2.1: The plaquette: the product of links around an elementary square on the lattice.

expression in the naive continuum limit. But it there exists an infinite number of lattice actions which have the same naive continuum limit. We have merely chosen the simplest one. There is no a priori reason why any choice of lattice action satisfying the above requirement will ensure that the theory presents a continuum limit corresponding to QED. For this to be the case the lattice theory must exhibit first of all a critical region in parameters space where correlation lengths diverge. To see this, let us consider the case of a U(1) pure gauge theory, which in the lattice formulation resembles to the statistical mechanical system described by the partition function

$$Z = \int DU e^{\frac{1}{g^2}\sum_P \left[1-\frac{1}{2}\left(U_P+U_P^\dagger\right)\right]} \quad . \tag{2.51}$$

Suppose that this lattice theory possesses a continuum limit, and that we want to extract from it the mass spectrum of the corresponding field theory by studying the appropriate correlation function for large euclidean time. The largest correlation length is then determined by the lowest mass, m, is to be finite, then the mass measured in the lattice units, $\hat{m}$, must necessarily vanish in the continuum limit. This, in turn, implies that correlation length measured in the lattice units, $\hat{\xi}$, must diverge. Hence the continuum field theory can only be realized at a critical point of the statistical mechanical system described by the previous partition function. This, of course, is to be expected, since

only if the correlation lengths diverge does the system loose its memory of the underlying lattice structure. It follows that if the above system is not critical for any value of the coupling, it cannot possibly describe QED or any other continuum field theory.

Now studying a system near criticality means tuning the parameters accordingly. In the case considered above, the only parameter is the bare coupling g_0, a dimensionless quantity which is void of any direct physical meaning. The correlation length in lattice units will depend on this parameter. Hence the continuum limit will be realized for $g \to g_0^*$, where

$$\hat{\xi} \stackrel{g \to g_0^*}{\longrightarrow} \infty \quad . \tag{2.52}$$

We wanted to emphasize that (2.52) followed from the general requirement that physical quantities should be finite in the limit of zero lattice spacing a. To arrive to this conclusion we have implicitly introduced a scale from the outside, in terms of which dimensioned observables can be measured.

Consider an observable Θ, such as the correlation length or the string tension σ, with mass dimension d_Θ. Let $\hat{\Theta}$ denote the corresponding lattice quantity which can in principle be determined numerically. $\hat{\Theta}$ will depend on the bare parameters of the theory (coupling, masses, etc.) which in the simple case considered here is just the dimensionless coupling g_0. The existence of a continuum limit then implies that

$$\Theta(g_0, a) = \Big(\frac{1}{a}\Big)^{d_\Theta} \hat{\Theta}(g_0) \tag{2.53}$$

approaches a finite limit for $a \to 0$, if g_0 is tuned with in an appropriate way, with $g_0(a)$ approaching the critical coupling g_0^*:

$$\Theta(g_0(a), a) \stackrel{a \to 0}{\longrightarrow} \Theta_{phys} \quad . \tag{2.54}$$

Hence if the functional dependence of $\hat{\Theta}$ on g_0 is known, we can determine $g_0(a)$ from (2.53) for sufficiently small lattice spacing by fixing the left-hand side at its physical value Θ_{phys}. This determines g_0 as a function.

The above discussion did not make use of any particular observable. ¿From (2.52) and (2.53) it may appear, however, that the functional dependence of $g_0(a)$ will depend on

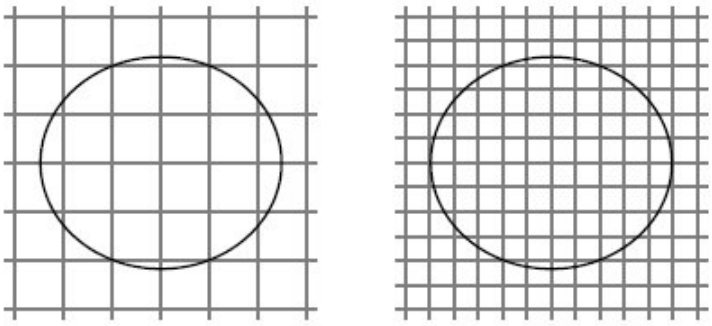

Figure 2.2: Tuning the lattice spacing a in order to keep physics the same.

the observable considered. For a finite lattice spacing this will, in fact, be true. For sufficiently small a, however, a universal function $g_0(a)$ should exist, which ensures the finiteness of any observable. A corresponding statement is expected to hold if the action depends on several parameters. like bare coupling constant and fermions' masses. We want to emphasize that it is not surprising that the bare parameter will depend on the lattice spacing. Just to make an example, suppose that the number of lattice points within the enclosing circle in in Fig. 2.2 corresponds to a bare quantity living on the lattice, like a physical length d (equal, for instance to 1 fm). We want to hold the quantity d (represented by the circle) fixed by its physical value. As we make the lattice finer and finer, more and more lattice points migrate into the circle to keep the quantity d constant. Thus, if physics is to remain the same at all lattice spacings, the bare parameters of the theory must to be tuned to a in a way depending on the dynamics of the theory.

2.2.3 QCD

The quantum cromodynamics (QCD) is the gauge theory which describes the strong interaction, responsible for the formation of hadronic systems [16]. In agreement with the gauge principle, it is required that the lagrangian would be invariant under the SU(3) gauge transformation. The number 3 reminds the number of different strong charges, the colors. The gauge transformations act on particles carrying the color: quarks (matter field) and gluons (gauge field). At the moment, six different species of quarks are known:

$$up \qquad down \qquad strange \qquad charm \qquad top \qquad bottom.$$

The SU(3) gauge group is non-Abelian. This is the most important difference with the case of QED, which generates all the peculiar features of the hadronic world, like *confinement*. Indeed, colored charges have never been seen in nature. They are confined. As a postulate of the theory, any physical observable must be colorless, neutral; it must be invariant under the gauge transformation, *i.e. singlet*. As a consequence, the only possible combinations of quarks are $|qqq\rangle$ and $|q\overline{q}\rangle$. These correspond to the two ways of having hadrons: the barions and the meson, respectively.

In analogy with QED, the classical lagrangian of QCD with N_f species of Dirac fields ψ (quark) is

$$\mathcal{L} = -\frac{1}{4}F^a_{\mu\nu}F^{a\mu\nu} + \sum_{\alpha\beta}\sum_{k=1}^{N_f}\overline{\psi}^k_\alpha(i\gamma^\mu D_\mu - m_k)_{\alpha\beta}\psi^k_\beta \quad , \tag{2.55}$$

where

$$F^a_{\mu\nu} = \partial_\mu A^a_\nu - \partial_\nu A^a_\mu + g f^{abc} A^b_\mu A^c_\nu \quad , \tag{2.56}$$

$$D_\mu = \partial_\mu - igT^a A^a_\mu \quad , \tag{2.57}$$

with $a = 1, 2, \ldots, 8$, f^{abc} structure constants of SU(3) and T^a generators of the gauge group in the fundamental representation. In particular, the algebra $[T^a, T^b] = if^{abc}T^c$ is verified. α and β are color indices and run from 1 to 3, while A^a_μ are gauge field (gluons). The above lagrangian is thus invariant under the set of gauge transformations (2.23), where now $G \in$ SU(3). For our purpose, let us quantize the QCD with the path integrals, exactly in the same way as in QED.

Let us discuss the more general case of a SU(N) theory. Formally the lagrangian is the same as in QCD. The discretization of the fermionic part of the action leads to the doubling problem, as in QED. Even in this case one can consider an extra term and build the Wilson action in analogy with (2.43). In this case the link variable $U_\mu(n)$ are elements of the SU(N) group in the fundamental representation, while the matter fields present an extra color degree of freedom. By building again the plaquette variable U_P, as in QED, the new gauge part of the action reads

$$S[U]_G = \frac{2N}{g_0^2} \sum_P \left[1 - \frac{1}{2N} \mathrm{Tr}(U_P + U_P^\dagger) \right] \quad . \tag{2.58}$$

2.3 Field theories at finite temperature

As stated many times, the thermodynamics of a system at temperature T is described by the canonical partition function

$$Z(T, V) = \mathrm{Tr} e^{-\frac{H}{T}} \quad , \tag{2.59}$$

where H is the hamiltonian and V the volume. For simplicity we set the Boltzman constant to 1. The expectation value of any observable at fixed T is given by

$$\langle O \rangle = \frac{1}{Z} \mathrm{Tr}(O e^{-\frac{H}{T}}) \quad . \tag{2.60}$$

Following the description of [13], let us consider a quantomechanical system described by a finite number of degrees of freedom q_i, $i = 1, 2, \cdots, N$. In the coordinate representation

$$Z(\beta, V) = \int \prod_i dq_i \langle q | e^{-\frac{H}{T}} | q \rangle \quad , \tag{2.61}$$

where $q = (q_1, \ldots, q_N)$ and $|q\rangle$ denotes the simultaneous eigenstates of the coordinate operators Q_i with eigenvalues q_i. The integrand of (2.61) presents the following representation in terms of path integrals, derived from the formal correspondence with (2.3)

$$\langle q | e^{-\frac{H}{T}} | q \rangle = \int_q^q [dq] e^{-\int_0^{\frac{1}{T}} dt L_E(q, \dot{q})} \quad , \tag{2.62}$$

where L_E is the euclidean version of the lagrangian describing the system. This path integral is a sum over all possible paths starting in q at "time" $\tau = 0$ and finishing in q at "time" $\tau = 1/T$. Inserting (2.62) in (2.61), one sees that the partition function is a sum over all possible closed paths in the space. The translation of these formulae to the case of a field theory is straightforward. Let $\phi(\tau, \vec{x})$ be a real scalar field, for instance, and $\mathcal{L}_E(\phi, \dot{\phi})$ the euclidean lagrangian density. The lagrangian is

$$L_E(\phi, \dot{\phi}) = \int d^3x \mathcal{L}_E(\phi, \dot{\phi}) \tag{2.63}$$

while the partition function (2.61) becomes

$$Z = \int [d\phi] e^{-\int_0^\beta d\tau \int d^3x \mathcal{L}_E(\phi, \dot{\phi})} \quad , \tag{2.64}$$

where β is the inverse of temperature

$$\beta = \frac{1}{T} \quad . \tag{2.65}$$

In analogy with the quantomechanical discussion, the path integral (2.64) has to be calculated over all fields $\phi(\tau, \vec{x})$ which satisfy the periodic boundary condition

$$\phi(0, \vec{x}) = \phi(\beta, \vec{x}) \quad . \tag{2.66}$$

In other words, introducing temperature in a field theory, means compactifying the euclidean temporal direction and identifying its extension with the inverse of T.
In the context of lattice gauge theory, one identifies $\beta = n_4$ e $n_1 = n_2 = n_3 \equiv n_s \to \infty$, being the integration (2.63) carried out over the whole space. In numerical simulations, the spatial extension will be, evidently, finite. Hence, one must work under the condition $n_s \gg n_4$ to approximate the thermodynamical limit. In the limit $n_4 \to \infty$ one recovers the zero T field theory.

2.3.1 Finite temperature QCD

The occurrence of a finite temperature phase transition for the strongly interacting matter is one of the most important non-perturbative aspects in QCD. One expects

that at sufficiently high temperatures and densities this matter is found in a new state, where quarks and gluons are no longer confined in hadrons, and which is therefore often referred to as a deconfined phase or Quark Gluon Plasma (QGP) [19]. The main goal of heavy ion experiments is to create such form of matter and study its properties. Lattice QCD can provide first principle calculation of such a quantities as transition temperature, equation of state and screening lengths, and help for the understanding about the nature of the transition. Beyond the particle physics interest, this is very important from several points of view. For example, it is believed that QGP can be found in the core of neutron stars, where the needed conditions of temperature and densities are reached. Still more interesting is the cosmological implication about the formation of the universe. In fact, at the Big Bang conditions, deconfinement could be realized. Then the universe had to cross a transition to the confinement phase giving rise to the hadronic world such as we know it. In view of that, it is very important to understand how this crossing occurred, *i.e.* knowing the nature of the transition.

For vanishing chemical potential ($\mu = 0$), this transition appears at $T \sim 270$ MeV in the pure gauge case (that is the limit of infinite massive quarks which corresponds to consider the theory in absence of quarks), while it appears at $T \sim 150 - 170$ MeV in QCD with fermions [20, 21].

In the case of pure gauge QCD, the discretized action to be considered is (2.58). Having the finite temperature means compactifying the temporal extension N_t of the lattice ($T = 1/(N_t a)$) and imposing periodic boundary conditions in this direction for gauge field. This implies for the link variable

$$U_\mu(\vec{n}, 0) = U_\mu(\vec{n}, \hat{\beta}) \quad . \tag{2.67}$$

Full lattice QCD is realized adding the fermionic contribution to the gauge action. In this case antiperiodic boundary condition in the temporal direction must be used.

Numerical simulations have shown several signals for the deconfinement transition. It turns out that its nature is strictly dependent on the number of quarks introduced (N_f) and on their bare masses (m_f).

When infinite massive quarks are considered (no quarks at all) transition is understood as a consequence of the center symmetry breaking. The center of a group is a subgroup of it, containing only those elements which commute with any other. In the case of QCD the symmetry group is SU(3), while the center is Z(3) which is formed by the three third root of the unity. The center symmetry is to be defined as the product of a slice of temporal links by an element z of the center

$$U_4 \to zU_4, \quad \forall \vec{n}, \text{ at fixed } n_4 \quad . \tag{2.68}$$

The order parameter is the *Polyakov loop*

$$L(\vec{n}) = \mathrm{Tr} \prod_{n_4} U_4(\vec{n}, n_4) \quad , \tag{2.69}$$

where the trace is made on the color indices. This quantity is not invariant under the center symmetry:

$$L(\vec{n}) \to zL(\vec{n}) \quad , \tag{2.70}$$

but configurations which are related by a center transformation presents the same action, thus the same statistical weight in the partition function. As a consequence, one finds that $\langle L \rangle = 0$ by symmetry. In the continuum theory it can be shown [22] that

$$e^{-\beta F_q} = \langle L \rangle \quad , \tag{2.71}$$

where F_q is the free energy of a single quark and β is the inverse of temperature. Hence the symmetric phase, under center symmetry, is related to the phenomenon of confinement, $F_q \to \infty$. Furthermore, there are arguments showing that the free energy of a static quark-antiquark pair can be extracted from the two-point correlator of Polyakov loops [13]:

$$\langle L(\vec{x}) L^\dagger(\vec{y}) \rangle \sim e^{-\beta F_{q\bar{q}}(\vec{x},\vec{y})} \quad . \tag{2.72}$$

It turns out that, for temperature large enough, one finds $\langle L \rangle \neq 0$. This is to be interpreted as the breaking of the center symmetry, indicating that deconfinement is occurred. Several numerical studies have shown that this transition is first order.

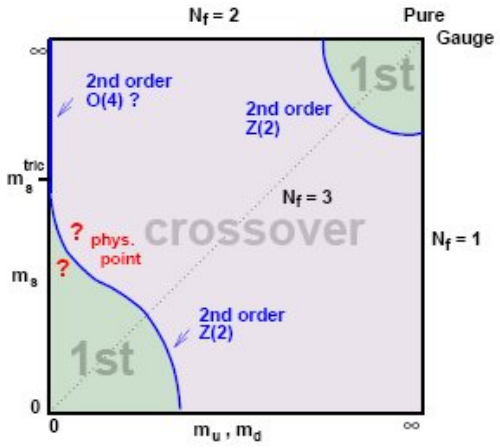

Figure 2.3: Phase diagram of QCD with three quarks (two degenerate) [23].

In the presence of quarks, the massless case is again well understood. Indeed, as a consequence of the chiral symmetry, one can conclude that the *chiral condensate*, $\langle\overline{\psi}\psi\rangle$, vanishes in the high temperature symmetric phase. At temperature low enough, one has $\langle\overline{\psi}\psi\rangle \neq 0$, thus indicating the chiral symmetry breaking. Even this transition has been shown to be of first order. For a review see [23] and references therein.

In the realistic situation of finite quark masses, neither the Polyakov loop nor the chiral condensate are good order parameter. In fact, it has not been singled out which is the symmetry or the mechanism responsible for confinement. I has been, however, noticed that both $\langle L\rangle$ and $\langle\overline{\psi}\psi\rangle$ present a strong change around transition. By studying these quantities it is possible to draw the phase diagram of QCD (Fig. 2.3), where the two first order corners are separated from a cross over central region by two second order critical lines. For values of the quark masses close to those extracted by experiments, it follows that in the real world the deconfinement it is not a true transition but only a rapid cross over. However, this result is not final. Indeed, to know the real nature of the deconfinement transition one should, in principle, identify the symmetry broken at transition for any value of the quark mass, and then identify the true order parameter of the transition.

2.3.2 Svetitsky-Yaffe conjecture

A fundamental link between spin systems and gauge theories can be established with the Svetitsky-Yaffe conjecture [24]. The deconfinement transition in the SU(N) pure gauge theories would be related to the order-disorder transition in spin models presenting the center of SU(N) as global symmetry, *i.e.* Z(N).

Any SU(N) pure gauge theory present a high temperature deconfined phase. As a consequence, any theory which is in the confined phase at zero temperature must present a finite temperature phase transition separating confined and deconfined phase. The conjecture states that the deconfinement transition of a $(d+1)$ SU(N) pure gauge theory at finite temperature belongs to the same universality class as the Z(N) spin model in d dimensions, if correlation length diverges. Since quantum field theory at finite theory corresponds to a compactification with periodic boundary conditions in the euclidean time direction, the high temperature gauge theories can be treated in such a way as they effectively live in one dimension less; this is known as *dimensional reduction*. In particular, one can integrate any degree of freedom except the order parameter associated to the confinement. This generates an effective theory for the order parameter which, for an initial $d+1$ gauge theory, is a d scalar spin model.

Let us consider a theory which presents a second order deconfinement phase transition: SU(2) $(3+1)d$. According to the Svetitsky-Yaffe conjecture, the relevant universality class will be the $3d$ Z(2) spin model, *i.e.* the $3d$ Ising model. The equivalence between the two transition has been verified with high accuracy by comparing several universal quantities as critical exponents [25, 26].

Unfortunately for the most relevant case, the QCD with infinite quark mass, the conjecture does not hold since transition is not critical. Correlation length does not diverge. Nevertheless, it turns out that the order of the transition is the same for both theories. Transitions are weakly first order. This means that the correlation length keeps finite but becomes very large compared with the lattice spacing a.

2.4 Monte Carlo methods

Calculating the expectation value of an observable O, means carrying out a huge number of integrations

$$\langle O \rangle = \frac{\int DUO[U]e^{-S[U]}}{\int DUe^{-S[U]}} \quad . \tag{2.73}$$

Where $S[U]$ is the action and U the dynamical variables. In practice, this can be done only using statistical methods. Let us follow the description of [13]. Since the most of configurations present a very large action, only few of them contribute significantly to (2.73). An effective way for calculating the average is then generating a sequence of configurations of dynamical variables with a probability distribution given by the Boltzman factor $\exp(-S[U])$. This technique is known as *importance sampling*. In this case the the generated set is representative and the ensemble average $\langle O \rangle$ will be done by

$$\langle O \rangle \approx \overline{O} = \frac{1}{N} \sum_{i=1}^{N} O(C_i) \quad , \tag{2.74}$$

where C_i $(i = 1, \ldots, N)$ is the *chain* of configurations.

We need to build an algorithm to generate our representative ensemble. The general ground in which these topics are theoretically introduced is the *Markov process* [27, 28]. This consists in a stochastic procedure in which configurations are generated one after the other with some transition probability $P(C \to C')$ to go from the configuration C to C'. The transition probability has to depend only on the previous configuration for a chain to be Markovian. It holds the normalization condition

$$\sum_{C'} P(C \to C') = 1 \quad . \tag{2.75}$$

In practice, starting for an arbitrary configuration, letting the algorithm work, after a first set of bad configurations, the process starts to provide configurations belonging to the desired ensemble. This is known as *thermalization* and in general, one has to wait that the algorithm reaches the thermalized region, where configurations present the right statistical weight, *i.e.* the right occurrence. In this region the following relation holds

$$P_{eq}(C) = \sum_{C'} P_{eq}(C')P(C' \to C) \quad , \tag{2.76}$$

while (2.73) becomes

$$\langle O \rangle = \sum_C P_{eq}(C) O(C) \quad , \tag{2.77}$$

where $P_{eq}(C)$ denotes the probability density of finding the configuration C at the equilibrium.

Let us show now that it is sufficient to require that the transition probability satisfies the *detailed balance*

$$e^{-S(C)} P(C \to C') = e^{-S(C')} P(C' \to C) \quad , \tag{2.78}$$

in order to generate the distribution $e^{-S(C)}$. Indeed, let us consider the following probability density

$$P_{eq}(C) = \frac{e^{-S(C)}}{\sum_{C''} e^{-S(C'')}} \quad . \tag{2.79}$$

Using the normalization condition and assuming (2.78), one has

$$\begin{aligned} P_{eq}(C) &= \sum_{C'} P_{eq}(C') P(C' \to C) = \sum_{C'} \frac{e^{-S(C')}}{\sum_{C''} e^{-S(C'')}} P(C' \to C) \\ &= \sum_{C'} \frac{e^{-S(C)}}{\sum_{C''} e^{-S(C'')}} P(C \to C') = \frac{e^{-S(C)}}{\sum_{C''} e^{-S(C'')}} \sum_{C'} P(C \to C') \\ &= \frac{e^{-S(C)}}{\sum_{C''} e^{-S(C'')}} \quad . \end{aligned} \tag{2.80}$$

The requirement of the detailed balance does not determine the transition probability in a single way. One can use this freedom to invent more and more efficient algorithms.

2.4.1 The Metropolis algorithm

As an example, let us present the Metropolis algorithm [29], proposed in the 1953. This can be, in principle, be applied to any system. Let C be the configuration to be updated. First, a new configuration C' is proposed, with the only requirement of *microreversibility* for the transition probability

$$P_0(C \to C') \to P_0(C' \to C) \quad . \tag{2.81}$$

Now it is to be chosen whether this proposed configuration should be accepted. The answer depends on the actions $S(C)$ and $S(C')$. In particular, if $\exp(-S(C')) >$

$\exp(-S(C))$, that is the action gets lower, then C' is accepted. If, conversely, the action gets higher, C' will be accepted with probability $e^{-S(C')}/e^{-S(C)}$. To realize this, one has only to generate a random number R in the interval [0,1] and take C' as the new configuration only if

$$R \leq \frac{e^{-S(C')}}{e^{-S(C)}} \quad . \tag{2.82}$$

Otherwise C' is rejected and one restarts this procedure with the old configuration C. Let us verify that the Metropolis algorithm effectively satisfies the detailed balance. Let us that the probability for the transition $C \to C'$ is nothing but the product between the probability of suggesting the new configuration, $P_0(C \to C')$, and that of accepting it. Then, if $\exp(-S(C')) > \exp(-S(C))$, one has

$$P(C \to C') = P_0(C \to C') \tag{2.83}$$

and

$$P(C' \to C) = P_0(C' \to C)\frac{e^{-S(C)}}{e^{-S(C')}} \quad . \tag{2.84}$$

Since $P_0(C \to C') = P_0(C' \to C)$ it is evident that the detailed balance (2.78) is satisfied. If, otherwise, $\exp(-S(C')) < \exp(-S(C))$, then

$$P(C \to C') = P_0(C \to C')\frac{e^{-S(C')}}{e^{-S(C)}} \tag{2.85}$$

and

$$P(C' \to C) = P_0(C' \to C) \quad ; \tag{2.86}$$

(2.78) is satisfied again.

Even though this algorithm is very popular, its biggest limit is that, in general, it can be used only to update one variable at time. This is the so-calles locality for an algorithm. In fact, updating many variables can product a big variation in the action and a consequent low probability for the new configuration to be accepted. The system would move very slowly in the configuration space, deteriorating the goodness of the method. The algorithm turns out to be even slower, when the action depends non-locally on the spatial coordinates, as in the case of the fermions on the lattice.

2.4.2 Data analysis

In numerical simulations the updating process creates a sampling of N configurations, from which extracting the expectation values of any quantity. The simplest type are the function of dynamical variables, $O(C)$. As already stated, the estimation of its expectation value is the arithmetic average (2.74). Since we are not recovering all possible field configurations, but only a part of them, we expect that the average value will be accompanied by an error. In the ideal case of statistically independent configurations, the error σ_O could be calculated by the ordinary variance

$$\sigma_{\overline{O}}^2 = \frac{\overline{O^2} - \overline{O}^2}{N-1} = \frac{\overline{(O-\overline{O})^2}}{N-1} \quad . \tag{2.87}$$

This evaluation turns out to be too optimistic. In real simulations subsequent configurations are not independent, but rather they are autocorrelated. One must wait some steps in the updating in order to have independent configurations. The autocorrelation function is defined as

$$\begin{aligned} (O_n O_{n+\tau}) &\equiv \langle O_n O_{n+\tau}\rangle - \langle O_n\rangle\langle O_{n+\tau}\rangle \\ &= \langle O_n O_{n+\tau}\rangle - \langle O\rangle^2 = \langle (O_n - \overline{O})(O_{n+\tau} - \overline{O})\rangle \quad . \end{aligned} \tag{2.88}$$

The true variance becomes

$$\begin{aligned} \sigma_{\overline{O}}^2 &= \left\langle \left[\frac{1}{N}\sum_{n=1}^{N} (O_n - \langle O\rangle) \right]^2 \right\rangle = \sum_{\tau=-N}^{N} \frac{N-|\tau|}{N^2} (O_n O_{n+\tau}) \\ &\to (OO)\frac{2\tau_{int,O}}{N} \simeq (\overline{O^2} - \overline{O}^2)\frac{2\tau_{int,O}}{N} \quad , \quad N \to \infty \quad , \end{aligned} \tag{2.89}$$

where the *integrated autocorrelation time* [30] is

$$\tau_{int,A} \equiv \frac{1}{2}\sum_{\tau=-\infty}^{+\infty} \frac{(A_n A_{n+\tau})}{(AA)} \quad . \tag{2.90}$$

The number of independent measurements turns out to be $N/(2\tau_{int,A})$. The autocorrelation effect gets worse if one studies a statistical system near the critical region. In fact, introducing the dynamical critical exponent z, one has

$$\tau_{int,A} \propto \xi^{z(O)} \quad , \tag{2.91}$$

where ξ is the correlation length and where z depends on the particular observable and on the particular algorithm. For example, for local algorithms one has typically $z \sim 2$. This deteriorates very much simulations, just where they are more interesting, in order to extract continuum physics, so that at criticality. This fact is known as *critical slowing down*.

Another method very useful is the *binning*. It consists in building blocks in the string of measurements and in averaging in each block. If the amplitude of blocks is larger than the autocorrelation time, these new average variables can be considered as independent. The binning, however, needs for a very large sample. If this condition is not verified, one can use the *jackknife* method for the estimation of the true variance. This procedure is particularly useful when one studies *secondary quantities* ($y(O)_J$), as correlators, for instance. These quantities cannot be calculated directly from simulation, but they are to be extracted from the *primary* ones. One omits any single measure in all possible way

$$O_J \equiv \frac{1}{N_s - 1} \sum_{r \neq s} O_r \quad . \tag{2.92}$$

The estimator for the secondary quantity is then

$$\overline{y_J} \equiv \frac{1}{N_s} \sum_{s=1}^{N_s} y_J \quad , \tag{2.93}$$

while a good estimation for the variance is

$$\sigma_J^2 \equiv \frac{N_s - 1}{N_s} \sum_{s=1}^{N_s} (y_J - \overline{y_J})^2 \quad . \tag{2.94}$$

In general, to increase the goodness of the error analysis, one can mix binning and jackknife, using the averages in the blocks as entries of the jackknife, and studying the behavior of the jackknife estimation for the variance as a function of the extension of blocks. When this variance stabilizes, one can be optimistic to have a good determination of the error.

Chapter 3

Universality for first order transitions: mass spectrum of $3d$ 3-state Potts model

3.1 Introduction

Universality is a powerful concept since it establishes the common long-distance behavior of theories characterized by different microscopic interactions, but possessing the same underlying global symmetry. A remarkable example is provided by $(d+1)$-dimensional SU(N) pure gauge theories at finite temperature which undergo a confinement/deconfinement phase transition associated with the breaking of the center of the gauge group, Z(N), the order parameter being the Polyakov loop [33, 34]. When the transition is second order, the long-range critical behavior of $(d+1)$-dimensional SU(N) pure gauge theories at finite temperature is conjectured to be the same as the d-dimensional Z(N) spin model in the critical region near the order/disorder phase transition [24]. As a consequence, the gauge theory and the spin model are predicted to have the same critical indices, amplitude ratios and correlation functions at criticality. This prediction has been accurately verified in several cases - see, for instance,

Refs. [35, 36, 37, 38, 39, 40, 41] and, for a review, Ref. [42].

A few years ago a study of the broken symmetry phase of the $3d$ Z(2) (Ising) class has brought compelling evidence that universality has a much wider and reach than usually expected. In particular, it has been shown that the Ising model and the lattice regularized ϕ^4 theory both exhibit a rich spectrum of massive excitations and that mass ratios coincide in the scaling region [43, 44]. This result is quite far from obvious: since only the lowest mass contributes to the free energy, there is no simple reason why higher masses in the spectrum should be universal. Later on, numerical evidence has been given that the same spectrum characterizes finite temperature SU(2) gauge theory in the scaling region above the deconfinement temperature [45, 46]. In the deconfined phase of the SU(2) gauge theory the counterpart of the massive excitations in the broken phase of the $3d$ Ising model are the so-called *screening masses*, i.e. the inverse exponential decay lengths of correlation functions between suitably defined operators, built from the Polyakov loops [45, 46].

It would be quite interesting to extend the test of the universality of the spectrum in two different directions: (1) by considering a theory with a global symmetry different from Z(2), which, however, presents in its phase diagram a second order critical point in the $3d$ Ising class; (2) by verifying if and to what extent the universality of the spectrum holds also in the broken symmetry phase near a first order *weak* phase transition.

The $3d$ 3-states Potts model with external magnetic field model provides a good test-field for both these investigations. Indeed, its phase diagram in the temperature - magnetic field (T, h) plane (see Fig. 3.1) exhibits a line of first order phase transitions which starts at $(0, 0)$, moves along the T-axis up to a transition temperature T_t and then bends in the positive h-plane up to reaching a second order endpoint, which belongs to the Ising class [47]. The $3d$ 3-states Potts model near this critical endpoint should exhibit a mass spectrum in the Ising universality class. Instead, the mass spectrum of the $3d$ 3-states Potts model at zero magnetic field, in the broken phase near T_t, should reproduce the spectrum of screening masses of the finite temperature SU(3) pure gauge theory in the deconfined phase near criticality, *if* universality holds also in the case of

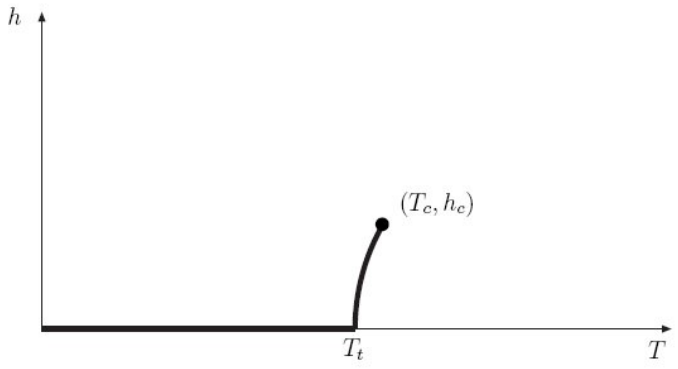

Figure 3.1: Qualitative phase diagram of the $3d$ 3-states Potts model: the solid line in bold is the line of first order phase transitions. T_t is the order/disorder transition temperature at zero magnetic field, (T_c, h_c) is the endpoint in the $3d$ Ising class.

first order weak phase transitions.

In this work [31] we determine the low-lying masses of the spectrum of the $3d$ 3-state Potts model in two different sectors of parity and orbital angular momentum, 0^+ and 2^+, and in two different regions of the (T, h) phase diagram, (a) near the critical Ising endpoint, (b) near the transition temperature T_t at zero magnetic field. For the determinations in the region (a), the comparison between the resulting mass ratios and the corresponding ones in the $3d$ Ising model [43] will provide a check of validity of the ansatz of universality of the spectrum. The mass ratios determined in the region (b) are instead the quantities to be compared with the corresponding screening masses in the finite temperature SU(3) gauge theory [32] in order to verify the validity of the ansatz near a weakly first order transition point.

This chapter is organized as follows: in Section 3.2 we briefly review the $3d$ 3-states Potts model and describe its phase diagram on the temperature - magnetic field plane; in Section 3.3 we describe the method used to extract the massive excitations near the two critical points in which we are interested; in Section 4.4 we present our numerical results and in the last Section we draw our conclusions.

3.2 The 3d 3-state Potts model

The 3-d 3-states Potts model [48, 49] is a spin theory in which the fundamental degree of freedom, s_i, defined in the site i of a 3-dimensional lattice, is an element of the Z(3) group, *i.e.*

$$s_i = e^{i\frac{2}{3}\pi\sigma_i}, \quad \sigma_i = \{0, 1, 2\} \quad . \tag{3.1}$$

The Hamiltonian of the model is

$$H = -\frac{2}{3}\beta \sum_{\langle ij \rangle} (s_i^\dagger s_j + s_j^\dagger s_i) = -\beta \sum_{\langle ij \rangle} \delta_{\sigma_i, \sigma_j} \ , \tag{3.2}$$

up to an irrelevant constant. Here, β is the coupling in units of the temperature and the sum is done over all the nearest-neighbor pairs of a cubic lattice with linear size L.

The Hamiltonian (3.2) is invariant under the Z(3) transformation

$$s_i \longrightarrow s_i' = e^{i\frac{2\pi}{3}\sigma} s_i \ , \tag{3.3}$$

where σ is fixed at any of the values $\{0, 1, 2\}$. It is well known that this system undergoes a *weakly* first order phase transition [50], associated with the spontaneous breaking of the Z(3) symmetry. The order parameter of this transition is the magnetization,

$$\langle S \rangle = \langle \frac{1}{L^3} \sum_i s_i \rangle \ , \tag{3.4}$$

which, in the thermodynamic limit, is zero above the transition temperature T_t (or below the transition coupling β_t) and takes a non-zero value below T_t (or above β_t).

In presence of an external magnetic field it is convenient to work with an Hamiltonian written in terms of the σ_i degrees of freedom, instead of the s_i ones. For a uniform magnetic field along the direction σ_h with strength h in units of the temperature, the Hamiltonian is

$$H = -\beta \sum_{\langle ij \rangle} \delta_{\sigma_i, \sigma_j} - h \sum_i \delta_{\sigma_i, \sigma_h} \equiv -\beta E - hM \ , \tag{3.5}$$

where E is the internal energy and M is the magnetization. The magnetic field breaks explicitly the Z(3) symmetry. However, first order transitions still occur for values of the magnetic field strength h below a critical value h_c, the transition temperature increasing

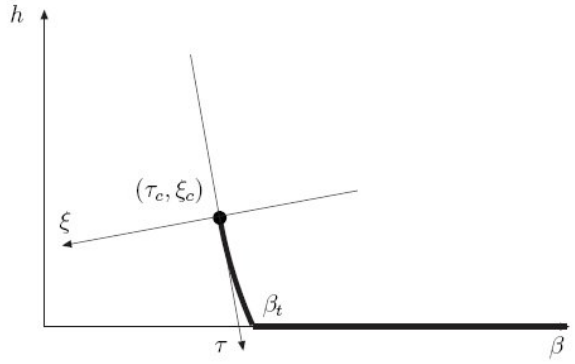

Figure 3.2: Qualitative phase diagram of the $3d$ 3-states Potts model in the (β, h)-plane: ξ and τ are the symmetry-breaking and the temperature parameters of the Ising theory (3.6).

with increasing h. The line of first order phase transitions ends in a second order critical point $P_c = (T_c, h_c)$ (see Fig. 3.1), belonging to the $3d$ Ising class [47]. The Hamiltonian in the scaling region of the critical point P_c can be written as

$$H = -\tau \tilde{E} - \xi \tilde{M} \ , \tag{3.6}$$

where $\tilde{E}$ and $\tilde{M}$ are the Ising-like energy and magnetization operators and τ and ξ the corresponding temperature-like and symmetry-breaking-like parameters. This means that $\langle \tilde{M} \rangle$ is the new order parameter. Close enough to P_c, the following relations hold,

$$\tilde{M} = M + sE \ , \qquad \tilde{E} = E + rM \ , \tag{3.7}$$

where the mixing parameters (r, s) have been determined numerically for several lattice sizes L in Ref. [47]. The τ-direction identifies the first order line (see Fig. 3.2). In Ref. [47] the location of the critical point P_c has been accurately determined: $P_c = (\beta_c, h_c)$=(0.54938(2),0.000775(10)) or, equivalently, $P_c = (\tau_c, \xi_c)$=(0.37182(2),0.25733(2)).

3.3 Massive excitations and Universality

Among the quantities relevant in the description of a phase transition there is the correlation function of local order parameter: in our case of the $3d$ 3-states Potts model this is just the local spin s_i. The point-point correlation function is defined as

$$\Gamma_{i_0}(r) = \langle s_i^\dagger s_{i_0} \rangle - \langle s_i^\dagger \rangle \langle s_{i_0} \rangle \ , \tag{3.8}$$

where i and i_0 are the indices of sites and r is the distance between them. The large-r behavior of the point-point correlation function is determined by the correlation length of the theory, ξ_0, or, equivalently, by its inverse, the fundamental mass. In order to extract the fundamental mass it is convenient to define the wall-wall correlation function, since numerical data in this case can be directly compared with exponentials in r, without any power prefactor. The connected wall-wall correlator in the x-direction is defined as

$$G(x) = \frac{1}{L} \sum_{x_0} \langle w(x_0 + x)^\dagger w(x_0) \rangle - \langle w(x + x_0)^\dagger \rangle \langle w(x_0) \rangle \ , \tag{3.9}$$

where

$$w(x) = \frac{1}{L^2} \sum_{y,z} s_{\{x,y,z\}} \tag{3.10}$$

represents the spin average over the "wall" at the coordinate x.

The general behavior for the function $G(x)$ is

$$G(x) = \sum_n a_n e^{-m_n x} \ , \tag{3.11}$$

where m_0 is the fundamental mass, while m_1, m_2, ... are higher masses with the same angular momentum and parity (0^+) quantum numbers of the fundamental mass. On a periodic lattice the above equation must be modified by the inclusion of the so called "echo" term:

$$G(x) = \sum_n a_n \left[e^{-m_n x} + e^{-m_n (L-x)} \right] \ . \tag{3.12}$$

Mass excitations in channels different from 0^+ can be determined by a suitable redefinition of the wall average (3.10). The fundamental mass in a definite channel can be extracted from wall-wall correlators by looking for a plateau of the effective mass,

$$m_{\text{eff}}(x) = \ln \frac{G(x)}{G(x-1)} \ , \tag{3.13}$$

at large distances. Excited masses in the given channel can be found by the variational method [51, 52], which consists in defining several wall-averaged operators with the given quantum numbers and building the matrix of cross-correlations between them. The eigenvalues of this matrix are single exponentials of masses in the given channel. The possibility to determine masses above the fundamental one in a given channel relies on the ability to define operators which have a large overlap with the excited states. Usually, these operators are defined in order to probe different length scales. In the present work we considered only the 0^+ and the 2^+ channels; the local variables to be wall-averaged as in (3.10) have been defined in the following way:

$$\begin{aligned} s^{0^+}_{\{x,y,z\}}(n) &= s_{\{x,y,z\}}(s_{\{x,y+n,z\}} + s_{\{x,y,z+n\}}) \, , \\ s^{2^+}_{\{x,y,z\}}(n) &= s_{\{x,y,z\}}(s_{\{x,y+n,z\}} - s_{\{x,y,z+n\}}) \, . \end{aligned} \tag{3.14}$$

Typically, we have used about ten operators in each channel, with the largest n almost reaching L. We can anticipate that we have not been able to extract masses higher than the fundamental one in any of the two channels. However, the use of the variational method has improved considerably the evaluation of the fundamental 2^+ mass. Needless to say that the determination of the fundamental mass in the 0^+ channel by the definition (3.14) turned out to be in perfect agreement with that from (3.9).

A few years ago it has been proposed [43] that ratios between massive excitations in the broken phase are universal quantities, i.e. mass ratios must be equal in theories where the same mechanism of symmetry breaking at the transition is active. One of the motivations of the present work is to check whether this statement holds also for the broken phase of the Ising theory (3.6) near the critical endpoint P_c of the $3d$ 3-states Potts model. This would provide us with a non-trivial check of validity of the conjecture of universal mass spectrum.

For the $3d$ Ising universality class, a definite prediction exists for the ratio between the fundamental 0^+ and 2^+ masses, $m_{2^+}/m_{0^+} = 2.56(4)$ [43]. We can estimate the same ratio near the Ising endpoint of the $3d$ 3-state Potts model and verify if it is consistent with this prediction. The procedure to determine the fundamental masses in the two

channels of interest is the same outlined above, with the only difference that we need to use the correct local order parameter to build correlators. We have defined this local variable, $\tilde{m}_i$, in such a way that it reconstructs the global magnetization operator $\tilde{M}$ after summation over the whole lattice:

$$\tilde{m}_i = \delta_{\sigma_i \sigma_h} + \frac{s}{2} \sum_{\hat{\mu}} \delta_{\sigma_i \sigma_{i+\hat{\mu}}} \ . \tag{3.15}$$

Indeed, it is easy to see that $\tilde{M}_i = \sum_i \tilde{m}_i$.

The second, and probably most important, aim of the present work is to study mass ratios also in the broken phase of the $3d$ 3-state Potts model at zero magnetic field near the transition point. It is known that this transition is weakly first order, a signature of this being the fact that the correlation length ξ, though finite at the transition point, becomes much larger than the lattice spacing. This fact could open the door to universality effects, such as the above-mentioned conjecture on mass ratios. If this claim is true, an important consequence would be that mass ratios in the broken phase near criticality of the $3d$ 3-state Potts model at zero magnetic field should reproduce the corresponding ratios in the phase of broken Z(3) symmetry of the (3+1)d SU(3) pure gauge theory at finite temperature. This is the deconfined phase of the SU(3) gauge theory and the counterparts of the massive excitations of the spin model are the so-called *screening* masses, i.e. the inverse decay lengths of the Yukawa-like interaction potential between static color sources.

As a probe for the check of consistency of this scenario, we can consider again the mass ratio m_{2^+}/m_{0^+}. If it will turn out that its value near the transition coupling β_t in the broken phase of the $3d$ 3-state Potts model is compatible with the corresponding ratio of screening masses in the deconfined phase near transition of (3+1)d SU(3) at finite temperature, this could be taken as an indication that the conjecture of universal spectrum can be extended also to the case of weakly first order transition.

Summarizing, we have to calculate the m_{2^+}/m_{0^+} ratio in two regions of interest in the temperature - magnetic field phase diagram: (a) in the broken phase near the critical Ising endpoint, (b) in the broken phase near the transition point of the model

in absence of magnetic field. In the case (a), we have to compare the result with the predicted value from universality in the $3d$ Ising class, given in Ref. [43]; in the case (b), our determination is to be compared with the corresponding one in the SU(3) pure gauge theory [32].

3.4 Numerical results

We have performed numerical Monte Carlo simulations of the $3d$ 3-states Potts model using a cluster algorithm [53, 54] to reduce the autocorrelation effects. In order to minimize the finite volume effects, we have imposed periodic boundary conditions. Data analysis has been done by the jackknife method applied to bins of different lengths.

For the simulations near the critical endpoint P_c (region (a)) we used lattices with size $L = 70$; near the transition coupling β_t at zero magnetic field (region (b)) we chose instead $L = 48$. In both cases we have seen tunneling between degenerate minima near the transition point. This finite volume effect can spoil mass measurements in the scaling region and must be treated carefully. Depending on the order of the transition, tunneling effects show up differently and must be removed accordingly.

3.4.1 The cluster algorithm

A radical reduction of the *critical slowing down* (see 2.4.2) is reached using, when it is possible, cluster algorithms in numerical simulations. They show, indeed, a value for the dynamical critical exponent close to zero, *i.e.* $z \sim 0$.

The force of this improvement relies on the construction of a more general system where a spin model and a random cluster model are mixed. Beside the spin variables, one introduces the bond variables $n_{ij} = n_{ji} = 0, 1$ between pairs of sites on the lattice. The partition function of this joint system is

$$Z_{SB} \equiv \mathrm{Tr}_{\{\sigma,n\}} \prod_{\langle ij \rangle} \{(1-p_{ij})\delta_{n_{ij},0} + p_{ij}\delta_{n_{ij},1}\delta_{\sigma_i\sigma_j}\} \prod_{\langle ik \rangle} \{(1-p_h)\delta_{n_{ik},0} + p_h\delta_{n_{ik},1}\delta_{\sigma_i\sigma_h}\} \quad , \quad (3.16)$$

where in the second product the external field σ_h is considered nearest neighbor of any other spin on the lattice. It is easy to verify that after a summation over the spin variables one recovers the partition function of a random cluster model, while after a summation over the bond variables (3.16) reduces to the partition function of the $3d$ 3-state Potts model, where

$$p_{ij} = 1 - e^{-J_{ij}} \quad , \quad p_h = 1 - e^{-h} \quad . \tag{3.17}$$

In particular (3.17) represent the probabilities of the bond activation between nearest neighbor sites which present the same spin. This procedure leads to a bond configuration under the spin one, where the system is partitioned in different clusters. These are nets between sites where the same value of spins are located. A new spin configuration is found by attributing randomly a new spin value to each cluster, keeping fixed the the spins belonging to the cluster of the external field. One can easily prove that the detailed balance is verified.

Evidently the improvement in terms of autocorrelation effects is based on the simultaneous change of a cluster of spins in the production of spin configurations, rather than the single change as in the local algorithms.

3.4.2 Region (a): critical endpoint

We have performed simulations on 70^3 lattices for which the mixing parameters appearing in (3.7) turn to be $s(L = 70) = -0.689(8)$ and $r(L = 70) = 0.690(3)$ [47].

First of all we have considered the distribution of the order parameter $\tilde{M}$ in the broken phase of the Ising theory (3.6) near P_c. Fig. 3.3 shows the structure, typical for a second-order phase transition, with two peaks corresponding to the two degenerate minima in the broken phase which separate while moving away from P_c along the first order Ising critical line. This double-peak structure is the signal of tunneling. The last plot in Fig. 3.3, obtained for Ising couplings $\xi = \xi_c$ and τ=0.37248, shows two almost completely separated peaks. We have decided to choose this as our working point and performed here simulations with statistics 200k.

We have removed here tunneling effects by the brute force method of analyzing separately data belonging to each peak. In Figs. 3.4 and 3.5 we show the behavior of the effective masses in the 0^+ and in the 2^+ channels at $\xi = \xi_c$ and τ=0.37248, as functions of the separation between walls, for the configurations in the "right-peak". Similar plots have been obtained for the configurations in the "left-peak". In each case, the *plateau mass* is taken as the effective mass (with its error) belonging to the *plateau* and having the minimal uncertainty. We define *plateau* the largest set of consecutive data points, consistent with each other within 1σ. This procedure is more conservative than identifying the plateau mass and its error as the results of a fit with a constant on the effective masses $m_{\rm eff}(x)$, for large enough x. We have found

"right-peak" (statistics 115K)

$$am_{0^+} = 0.0725(63)\ , \qquad am_{2^+} = 0.1981(87)\ , \qquad \frac{m_{2^+}}{m_{0^+}} = 2.73(36)\ ; \tag{3.18}$$

"left-peak" (statistics 85K)

$$am_{0^+} = 0.0714(40)\ , \qquad am_{2^+} = 0.1959(80)\ , \qquad \frac{m_{2^+}}{m_{0^+}} = 2.74(27)\ . \tag{3.19}$$

The uncertainty on the mass ratios has been determined by usual propagation of errors. The two determinations of the masses and, therefore, of the mass ratios are consistent, as expected. Moreover, they are compatible with the value of the $3d$ Ising class [43], $m_{2^+}/m_{0^+} = 2.59(4)$.

3.4.3 Region (b): transition point at zero magnetic field

We have performed simulations on 48^3 lattices for several values of the coupling β in the broken phase of the $3d$ 3-state Potts model at zero magnetic field. A summary of the Monte Carlo simulations is presented in Table 3.1.

Close enough to $\beta_t(L = 48)$=0.550538, determined in Ref. [50], the scatter plot of the complex order parameter $\langle S\rangle$ shows the coexistence of the symmetric phase (points around (0,0) in the Im$\langle S\rangle$ - Re$\langle S\rangle$ plane in Fig. 3.6) and of the broken phase (points

around the three roots of the identity in Fig. 3.6). Notice that the peaks in the distribution of points in Fig. 3.6 are well separated, as it must be for first order dynamics. In the thermodynamic limit this would occur only at the transition point; at finite volume, tunneling between broken minima and the symmetric phase occurs in a small region around the transition. The amplitude of this region decreases with the volume. For L=48 it is of the order of 10^{-4} in β [50].

Moving away from β_t the symmetric phase becomes less and less important, up to disappearing. For β=0.5508 there are only the three broken minima, as shown in Fig. 3.7(top). For larger β values the tunneling between broken minima survives. However, the three peaks are totally separated and it is therefore possible to "rotate" unambiguously all of them to the real sector (see Fig. 3.7(bottom)). Working only in one sector allows us to optimize statistics. With this approach we have calculated the fundamental masses in the 0^+ and 2^+ channels for several β values, up to 0.60 ($(T_t - T)/T_t \sim 0.08$). In Figs. 3.8 and 3.9 we show the behavior of the effective masses in the 0^+ and in the 2^+ channel at $\beta = 0.554$, as functions of the separation between walls. Similar plots have been obtained for the other β values. The plateau mass values have been determined as described in the previous Subsection. In Table 3.1 we present our results, whereas in Fig. 3.10 we have plotted the behavior of m_{0^+} and m_{2^+} versus β.

We have determined the ratio m_{2^+}/m_{0^+} for several β values near the transition, in the region $[\beta_t, 0.56]$; the results are presented in Table 3.1 and plotted in Fig. 3.11. This ratio remains practically constant in the considered region, this suggesting that the correlation length ξ_2 associated to the channel 2^+ ($\xi_2 = 1/m_{2^+}$) scales in the same way of the fundamental one ($\xi_0 = 1/m_{0^+}$). We can take as our estimation of the mass ratio the value

$$\frac{m_{2^+}}{m_{0^+}} = 2.43(10) \ , \tag{3.20}$$

determined, as discussed above, by taking value and error of the point with the smallest error belonging to the plateau ($\beta = 0.56$, see Fig. 3.11). A fit of the data with a constant gives for this ratio the value 2.353(49) with a χ^2/d.o.f.= 0.54.

The result given in (3.20) is to be compared with the corresponding ratio of screening

Table 3.1: Fundamental masses in lattice units in the 0^+ and 2^+ channels and their ratio for β values in the broken phase near the weakly first order transition at L=48. The statistics of each simulation is also given.

β	m_{0^+}	m_{2^+}	m_{2^+}/m_{0^+}	statistics
0.5508	0.1556(36)	0.381(17)	2.45(17)	300K
0.550875	0.1565(56)	0.384(16)	2.45(19)	200K
0.551	0.1837(59)	0.444(18)	2.42(18)	100K
0.552	0.2375(42)	0.533(36)	2.24(19)	100K
0.553	0.2900(34)	0.660(27)	2.28(12)	200K
0.554	0.3258(60)	0.691(57)	2.12(21)	100K
0.555	0.3502(67)	0.847(29)	2.42(13)	200K
0.556	0.3996(85)	0.891(35)	2.23(14)	200K
0.56	0.4965(83)	1.204(30)	2.43(10)	200K
0.562	0.537(11)	-	-	200K
0.565	0.6324(85)	-	-	200K
0.57	0.702(12)	-	-	200K
0.575	0.8381(78)	-	-	200K
0.58	0.9358(97)	-	-	200K
0.60	1.170(20)	-	-	200K

masses calculated in the broken phase of the (3+1)d SU(3) pure gauge theory at finite temperature, which is $m_{2^+}/m_{0^+} = 3.214(64)$ [32]. The comparison is shown in Fig. 3.12 where one sees that the pure gauge ratio turns out to be larger than the ratio in the spin model.

3.5 Conclusions and outlook

In this work we have studied massive excitations of the $3d$ 3-states Potts model near the Ising critical point on the temperature - magnetic field phase diagram and near the transition point at zero magnetic field.

We have found evidence that the mass ratio m_{2+}/m_{0+} near the Ising critical point is compatible with the prediction from universality, thus supporting the conjecture of universal spectrum.

In the broken phase near the transition in absence of the external source, we have found m_{2+}/m_{0+}=2.43(10). This result is to be compared with the corresponding ratio between screening masses of (3+1)d SU(3) pure gauge theory at finite temperature in the broken phase near the deconfinement temperature [32] which turns out to be $\sim 30\%$ larger than the corresponding ration in the $3d$ 3-state Potts model. This can be taken as an estimate of the level of the approximation by which the Svetitsky-Yaffe conjecture, valid in strict sense only for continuous phase transitions, can play some role in this context of weakly first order transition.

The present analysis could be extended with the numerical determination of higher masses in the 0^+ and 2^+ channels and with masses in other channels, in order to carry out a more systematic study of universality effects.

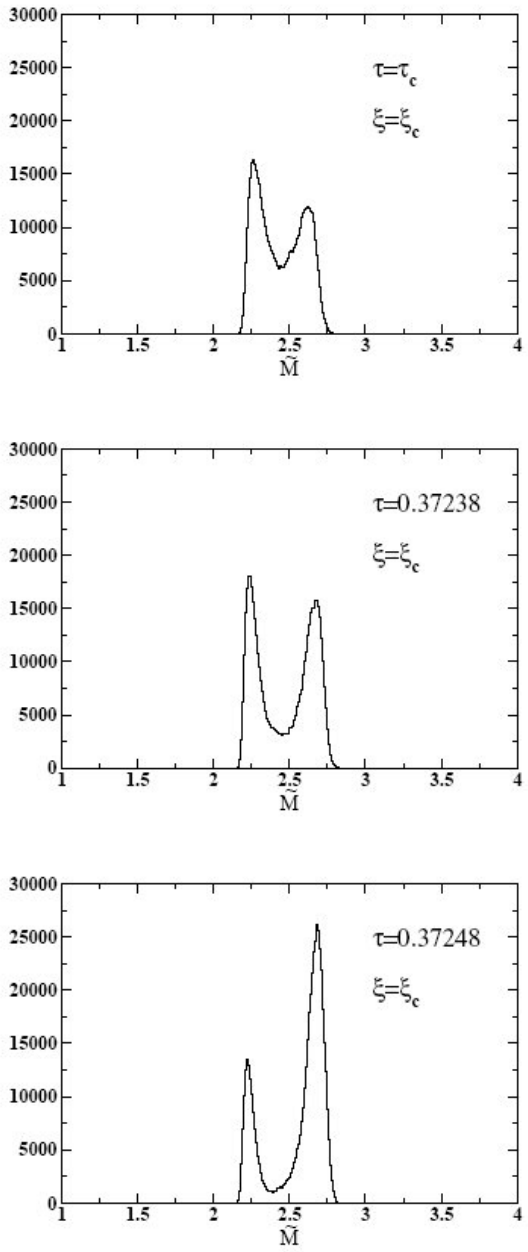

Figure 3.3: Distributions of the order parameter $\tilde{M}$ near P_c. The simulations have been done at the points (ξ_c, τ) with $\tau = 0.37182 \equiv \tau_c$, τ=0.37238 and τ=0.37248. These points lie on the first order line starting from P_c. The statistics is 500k in all cases.

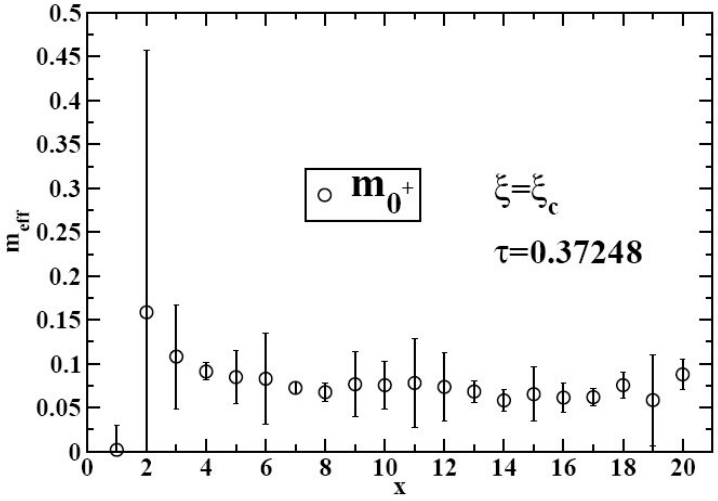

Figure 3.4: Effective mass in the 0^+ channel as a function of the separation between walls on the (y, z) plane at $\xi = \xi_c$ and τ=0.37248, determined from the configurations belonging to the "right-peak" in the thermal equilibrium ensemble.

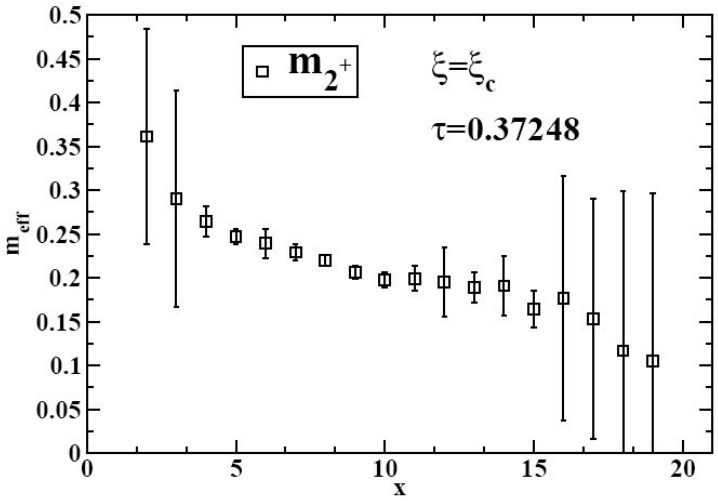

Figure 3.5: Effective mass in the 2^+ channel as a function of the separation between walls on the (y, z) plane at $\xi = \xi_c$ and τ=0.37248, determined from the configurations belonging to the "right-peak" in the thermal equilibrium ensemble.

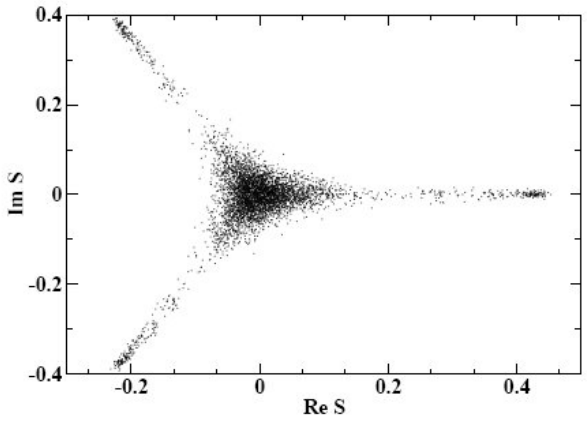

Figure 3.6: Scatter plot of the complex order parameter S at the transition point β_t=0.550538 [50] at zero magnetic field. Both the symmetric and the broken phases are present.

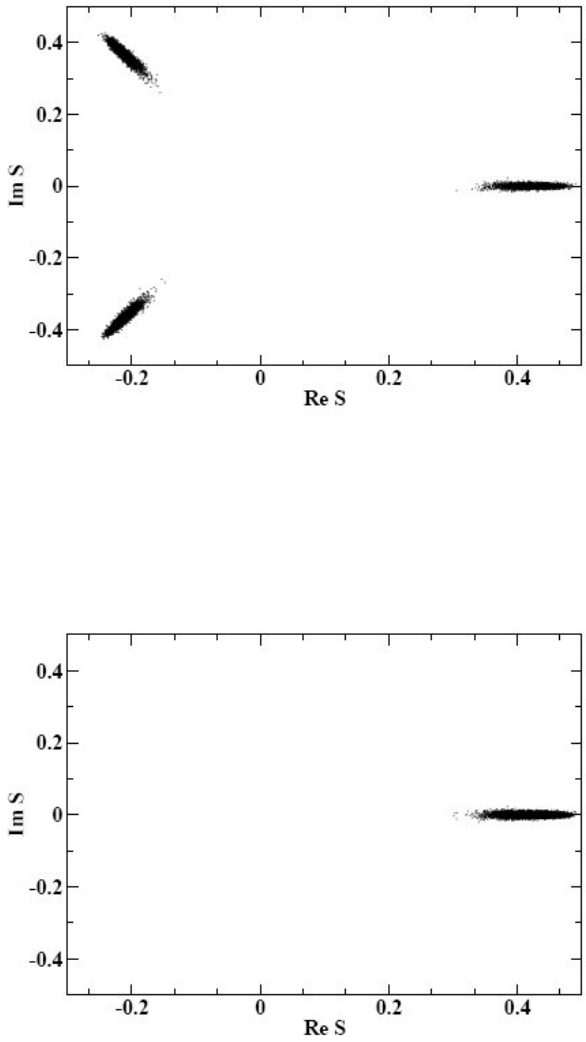

Figure 3.7: (Top) Typical scatter plot of the complex order parameter S for β larger than 0.5508 and zero magnetic field on a lattice 48^3. There are no states in the symmetric phase, but tunneling survives between the three broken minima.
(Bottom) Same as (Top) with the tunneling between broken minima removed by the "rotation" to the real phase.

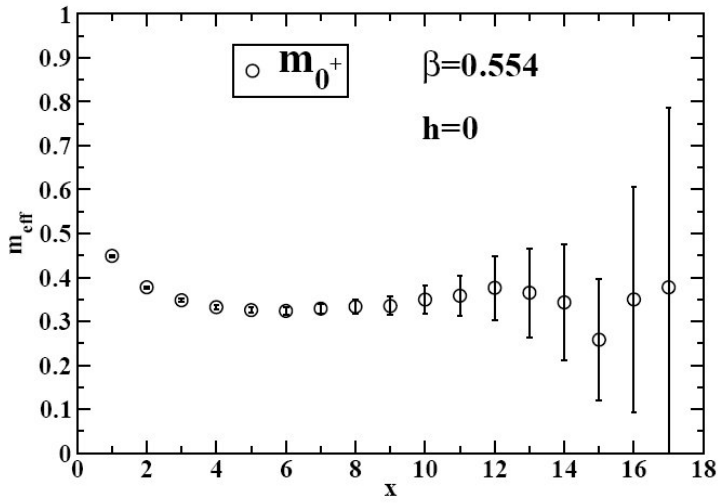

Figure 3.8: Effective mass in the 0^+ channel as a function of the separation between walls on the (y, z) plane at $\beta = 0.554$ and $h = 0$.

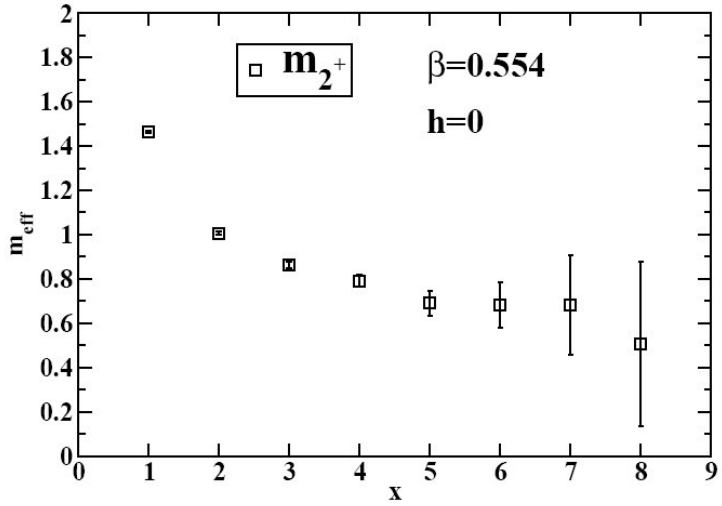

Figure 3.9: Effective mass in the 2^+ channel as a function of the separation between walls on the (y, z) plane at $\beta = 0.554$ and $h = 0$.

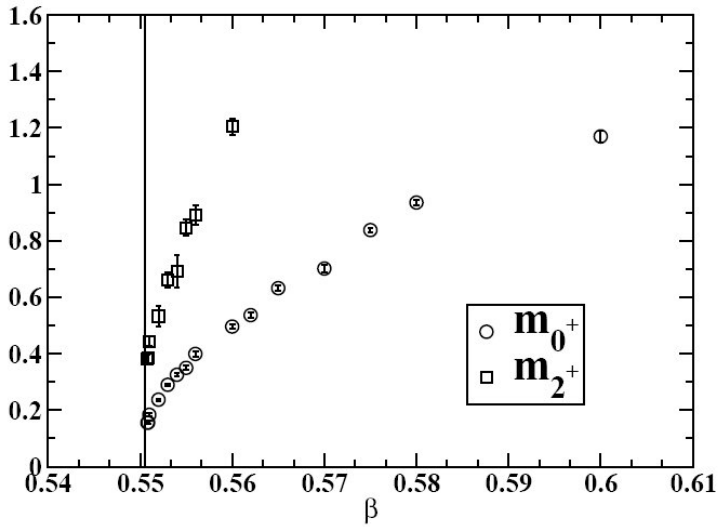

Figure 3.10: Fundamental masses in the 0^+ and 2^+ channels as functions of β, in the broken phase near T_t (vertical line).

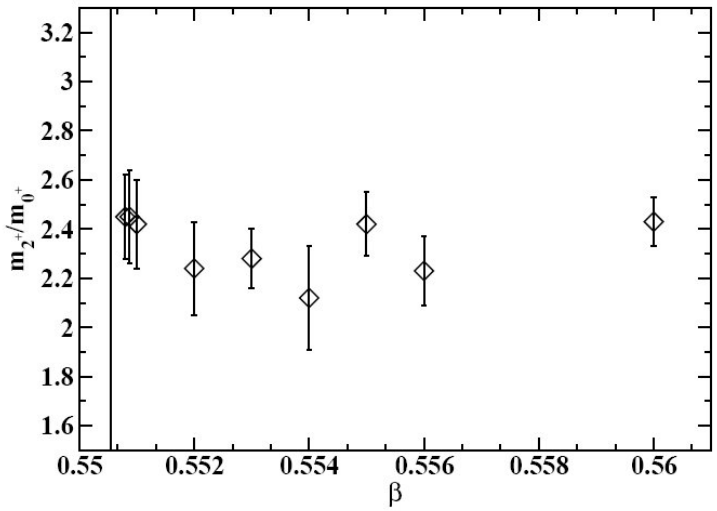

Figure 3.11: $m_{2^+}(\beta)/m_{0^+}(\beta)$ for β varying in the scaling region.

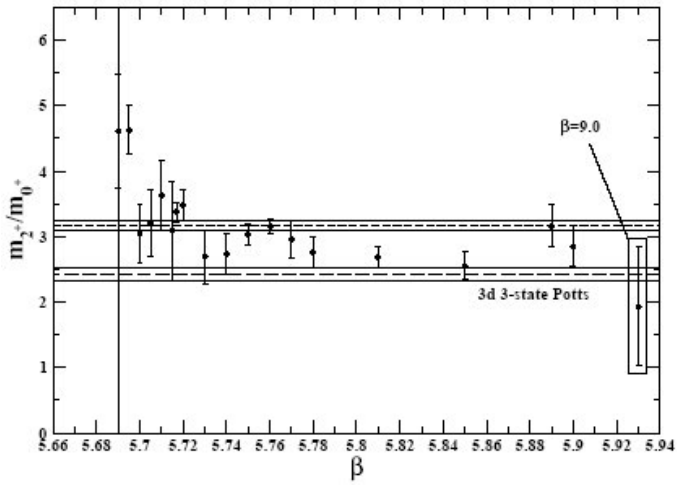

Figure 3.12: Ratio m_{2^+}/m_{0^+} as a function of β in the deconfined phase of 3+1)d SU(3) pure gauge theory at finite temperature. The three upper horizontal lines represent the constant (with its error) which fits the data of the ratio near the transition. This constant turns out to be $m_{2^+}/m_{0^+} = 3.214(64)$ [32]. The three lower horizontal lines represent the corresponding mass ratio (with its error) found in the $3d$ 3-state Potts model [31].

Chapter 4

Critical behavior of the compact $3d$ $U(1)$ theory in the limit of zero spatial coupling

4.1 Introduction

The finite temperature behavior of the compact three-dimensional ($3d$) $U(1)$ lattice gauge theory (LGT) is the subject of numerous investigations (see, e.g., Ref. [55] and references therein). It is well-known that at zero temperature the theory is confining at all values of the bare coupling constant [56]. At finite temperature the theory undergoes a deconfinement phase transition. Both phenomena are expected to take place in $4d$ QCD as well. Therefore, the $3d$ $U(1)$ gauge theory constitutes one of the simplest models with continuous gauge symmetry which possess the same fundamental properties as QCD. In view of these common features the critical properties of $3d$ $U(1)$ LGT deserve comprehensive qualitative and quantitative understanding.

On the theoretical side one should mention two results regarding the critical behavior of $3d$ $U(1)$ LGT. The first result states that the partition function of $3d$ $U(1)$ LGT in the Villain formulation coincides with that of the $2d$ XY model in the leading order

of the high-temperature expansion [57]. In particular, the monopoles of the original $U(1)$ gauge theory are reduced to vortices of the $2d$ system. The second result follows from the Svetitsky-Yaffe conjecture: the finite-temperature phase transition in the $3d$ $U(1)$ LGT should belong to the universality class of the $2d$ XY model if correlation length diverges [24]. Then, two possibilities arise: either the transition is first order or it is the same transition which occurs in the $2d$ XY model. The XY model is known to have Berezinskii-Kosterlitz-Thouless (BKT) phase transition of infinite order [8, 9]. Several important facts could be deduced from these results. First of all, the global $U(1)$ symmetry cannot be broken spontaneously even at high temperatures because of the Mermin-Wagner theorem. Consequently, a local order parameter does not exist. Secondly, one might expect the critical behavior of the Polyakov loop correlation function $\Gamma(R)$ to be governed by the following expressions

$$\Gamma(R) \asymp \frac{1}{R^{\eta(T)}} , \tag{4.1}$$

for $\beta \geq \beta_c$ and

$$\Gamma(R) \asymp \exp\left[-R/\xi(t)\right] , \tag{4.2}$$

for $\beta < \beta_c$, $t = \beta_c/\beta - 1$. Here, $R \gg 1$ is the distance between test charges and $\xi \sim e^{bt^{-\nu}}$ is the correlation length. Such behavior of ξ defines the so-called *essential scaling*. The critical indices $\eta(T)$ and ν are known from the renormalization-group analysis of the XY model: $\eta(T_c) = 1/4$ and $\nu = 1/2$, where T_c is the BKT critical point. Therefore, the critical indices η and ν should be the same in the finite-temperature $U(1)$ model if the Svetitsky-Yaffe conjecture holds in this case.

The first renormalization-group calculations of the critical indices, presented in [24], gave support to the conjecture even though they did not constitute a rigorous proof. The direct numerical check of these predictions was performed on lattices $N_s^2 \times N_t$ with $N_s = 16, 32$ and $N_t = 4, 6, 8$ in Ref. [58]. Though authors of Ref. [58] confirm the expected BKT nature of the phase transition, the reported critical index is almost three times that predicted for the XY model, $\eta(T_c) \approx 0.78$. More recent numerical simulations of Ref. [55] have been mostly concentrated on the study of the properties of the high-

temperature phase. We have to conclude that, so far, there are no numerical indications that the critical indices of $3d$ $U(1)$ LGT do coincide with those of the $2d$ XY model. Moreover, since a rigorous determination of the critical indices is not available even for the XY model one can hardly hope for a rigorous analysis of the critical behavior of $3d$ $U(1)$ LGT.

The absence of reliable results in the vicinity of the BKT critical point was our primary motivation to study the deconfinement phase transition in $3d$ $U(1)$ LGT. The difficulties in computations of critical indices of the XY model are well-known and we do not intend to discuss them here (see Ref. [59] for a summary of recent results and problems). It should be clear however, that in the context of the $3d$ theory a reliable determination of critical properties becomes even harder and requires simulations on very large lattices. We have decided therefore to attack the problem in a few steps. Consider the finite-temperature model on anisotropic lattice with different spatial and temporal coupling constants; as a first step, in this work we investigate the limit of vanishing spatial coupling. The major advantage of this limit is that the integration over spatial links can be performed analytically. The result of such integration is an effective two-dimensional spin model for the Polyakov loops. The latter can be studied numerically.

This chapter is organized as follows. In the next section we introduce the compact $U(1)$ LGT on anisotropic lattice and study it for vanishing spatial coupling. In the Section 3 we describe briefly our numerical procedure. The result of simulations are presented in the Section 4. Conclusions and perspectives are given in the Section 5.

4.2 The $3d$ U(1) lattice gauge theory

We work on a $3d$ lattice $\Lambda = L^2 \times N_t$ with spatial extension L and temporal extension N_t. Periodic boundary conditions on gauge fields are imposed in all directions. We

introduce anisotropic dimensionless couplings in a standard way as

$$\beta_t = \frac{1}{g^2 a_t} \ , \qquad \beta_s = \frac{\xi}{g^2 a_s} \ = \ \beta_t \ \xi^2 \ , \qquad \xi = \frac{a_t}{a_s} \ , \tag{4.3}$$

where a_t (a_s) is lattice spacing in the time (space) direction. g^2 is the continuum coupling constant with dimension a^{-1}. The finite-temperature limit is constructed as

$$\xi \to 0 \ , \qquad N_t \ , \ L \ \to \infty \ , \qquad a_t N_t = \frac{1}{T} \ , \tag{4.4}$$

where T is the temperature.

The $3d$ $U(1)$ LGT on the anisotropic lattice is defined through its partition function as

$$Z(\beta_t, \beta_s) = \int_0^{2\pi} \prod_{x \in \Lambda} \prod_{n=0}^{2} \frac{d\omega_n(x)}{2\pi} \ \exp S[\omega] \ , \tag{4.5}$$

where S is the Wilson action

$$S[\omega] = \beta_s \sum_{p_s} \cos \omega(p_s) + \beta_t \sum_{p_t} \cos \omega(p_t) \tag{4.6}$$

and sums run over all space-like (p_s) and time-like (p_t) plaquettes. The plaquette angles $\omega(p)$ are defined in the standard way. The correlation of two Polyakov loops can be written as, e.g.

$$\Gamma(R) \ = \ \left\langle \exp \left[i \sum_{x_0=0}^{N_t-1} (\omega_0(x_0, x_1, x_2) - \omega_0(x_0, x_1, x_2 + R)) \right] \right\rangle \ . \tag{4.7}$$

As stated in the Introduction we would like to explore the limit $\beta_s = 0$. Consider the strong coupling expansion at $\beta_s \ll 1$. The general form of such expansion reads

$$Z(\beta_t, \beta_s) = Z(\beta_t, \beta_s = 0) + \sum_{k=1} \beta_s^{2k} \ Z_{2k}(\beta_t) \ . \tag{4.8}$$

In this work we study the zero-order partition function $Z(\beta_t, \beta_s = 0)$ defined below. The series on the right-hand side of the last expression is known to be convergent uniformly in the volume, both for the free energy and for the gauge-invariant correlation functions. The uniform convergence guarantees the existence of the limit $N_t \to \infty$. The strong coupling expansion, done even in one parameter, might be far from the continuum limit.

Nevertheless, one expects that already the zero-order approximation captures correctly the critical behavior of the full theory. An example is given by the following Polyakov loop model

$$S_{\rm eff} = \beta_{\rm eff} \sum_{x,n} {\rm Re}\ W(x) W^*(x+n)\ , \tag{4.9}$$

derived at finite temperature for $(d+1)$-dimensional $SU(N)$ pure gauge theory in the limit $\beta_s = 0$. Here, $\beta_{\rm eff} \propto \beta_t^{N_t}$. As is well known, this model reveals correctly the critical behavior of the original theory thus supporting our approximation.

In the zero-order approximation the integration over spatial gauge fields can be easily done and leads to the following expression for the partition function

$$Z(\beta_t, \beta_s = 0) \ = \ \int_0^{2\pi} \prod_x \frac{d\omega_x}{2\pi} \prod_{x,n} \left[\sum_{r=-\infty}^{\infty} \ I_r^{N_t}(\beta_t) \ \exp\left[ir(\omega(x) - \omega(x+e_n))\right] \right] \ , \tag{4.10}$$

where x belongs to the two-dimensional lattice $\Lambda_2 = L^2$ and $\omega(x) \equiv \omega(x_1, x_2)$. Here, $I_r(x)$ are modified Bessel functions and $e^{ir\omega(x)}$ is the Polyakov loop in the representation r.

For $N_t = 1$ using the formula $\sum_r I_r(x) e^{ir\omega} = e^{x\cos\omega}$ one finds

$$Z(\beta_t, \beta_s = 0)|_{N_t=1} \ = \ \int_0^{2\pi} \prod_x \frac{d\omega(x)}{2\pi} \ \exp\left[\beta_t \sum_{x,n} \cos(\omega(x) - \omega(x+e_n)) \right] \tag{4.11}$$

which is the partition function of the $2d$ XY model. Thus, in this case the dynamics of the system is governed by the XY model with the inverse temperature β_t. For $N_t \geq 2$ the model (4.10) is of the XY-type, i.e. it describes interaction between nearest neighbors spins (Polyakov loops) and possesses the global $U(1)$ symmetry. Moreover, consider now two different limits - the strong coupling limit $\beta_t \ll 1$ and the weak coupling limit $\beta_t \gg 1$.

In the leading order of the strong coupling limit one can easily find from (4.10), up to an irrelevant constant,

$$Z(\beta_t \ll 1, \beta_s = 0) \ = \ \int_0^{2\pi} \prod_x \frac{d\omega(x)}{2\pi} \ \exp\left[h(\beta_t) \sum_{x,n} \cos(\omega(x) - \omega(x+e_n)) \right] \tag{4.12}$$

which is again the XY model with the coupling h given by

$$h(\beta_t) \ = \ 2 \left[\frac{I_1(\beta_t)}{I_0(\beta_t)} \right]^{N_t} \ .$$

The Polyakov loop vanishes while the correlations of the Polyakov loops are given, at the leading order, by

$$\Gamma(R) \;=\; \left[\frac{1}{2}\; h(\beta_t)\right]^R \;. \tag{4.13}$$

To study the weak coupling limit it is convenient to perform duality transformations which are well-known for the XY model. Taking then the asymptotics of the Bessel functions one obtains, up to an irrelevant constant,

$$Z(\beta_t \gg 1, \beta_s = 0) \;=\; \sum_{r(x)=-\infty}^{\infty} \exp\left[-\frac{1}{2}\tilde{\beta}\sum_x \sum_{n=1}^{2}(r(x) - r(x+e_n))^2\right] . \tag{4.14}$$

This is nothing but the Villain version of the XY model in the dual formulation with an effective coupling

$$\tilde{\beta} \;=\; N_t/\beta_t \;=\; g^2/T \;. \tag{4.15}$$

This shows that the region $\beta_s = 0$, $\beta_t \gg 1$ is also described by the XY model.

In the general case of arbitrary β_t the full effective action

$$S_{\text{eff}} \;=\; \sum_{x,n}\sum_{k}\; C_k \cos k(\omega(x) - \omega(x+e_n)) \tag{4.16}$$

will include all representations k of the Polyakov loops. In our case the coefficients C_k are given by

$$C_k \;=\; \int_0^{2\pi} \frac{d\omega}{2\pi}\; \cos k\omega\; \log\Big\{1 + 2\sum_{r=1}^{\infty}[b_r(\beta_t)]^{N_t}\cos r\omega\Big\} \;, \tag{4.17}$$

where $b_r(\beta_t) = I_r(\beta_t)/I_0(\beta_t)$. If there is a critical point at which the correlation length is divergent then on general grounds (universality, limiting behavior, etc.) one assumes that the model described by the effective action (4.16) indeed possesses the same critical behavior as the XY model. Nevertheless, we are not aware of any direct numerical check of the universality for models of the type (4.16) if $C_k \neq 0$ for $k = 2, 3, ...$ In the following sections we present numerical simulations which give support for the expected BKT behavior of the model (4.16). Our results hold only for the model with C_k defined by (4.17). We would like to stress that it is not obvious that for all possible C_k the

correlation length really diverges. For example, it was proven in Ref. [60] that the model with coefficients

$$C_k \;=\; \int_0^{2\pi} \frac{d\omega}{2\pi}\; \cos k\omega \;\left(\frac{1+\cos\omega}{2}\right)^p \;, \tag{4.18}$$

with sufficiently large p, exhibits a first order phase transition, so that one could expect that the correlation length stays finite across the phase transition point.

4.3 Numerical set-up

Determining the universality class of the $3d$ U(1) gauge theory discretized on a $L^2 \times N_t$ lattice means determining its critical indices. A convenient way to accomplish this task is to study the scaling with the spatial size L of the vacuum expectation value of suitable observables, determined through numerical Monte Carlo simulations.

For the special case $\beta_s = 0$, one can take advantage of Eq. (4.10) and describe the original gauge system with a two-dimensional spin model whose action S' is defined through

$$Z(\beta_t, \beta_s = 0) \equiv \int_0^{2\pi} \prod_x \frac{d\omega(x)}{2\pi} \exp S' \tag{4.19}$$

and reads

$$S' = \sum_{x,n} \log\Big\{1 + 2\sum_{r=1}^{\infty} [b_r(\beta_t)]^{N_t} \cos r(\omega(x) - \omega(x+e_n))\Big\} \,. \tag{4.20}$$

The infinite series in r can be truncated early, since the b_r's vanish very rapidly for increasing r. We studied the dimensionally reduced system with the Metropolis algorithm, taking the first twenty b_r couplings (notice that $b_{20}(\beta_t = 1) \sim 10^{-25}$).

Our goal is to bring evidence that the system exhibits BKT critical behavior *for any fixed* N_t. This is trivially verified in the case $N_t = 1$, since by inspection of Eqs. (4.19) and (4.20), the theory reduces exactly to the XY model. Therefore the case $N_t = 1$ can be used as a test-field for the description and the validation of our procedure.

Before presenting numerical results it is instructive to give some simple analytical predictions for the critical values β_t at different values of N_t. Such critical values can

be easily estimated if one knows β_t^{cr} for $N_t = 1$. Since the model with $N_t = 1$ coincides with the XY model one has $\beta_t^{cr}(N_t = 1) \approx 1.119$ and approximate critical points for other values of N_t can be computed from the equality

$$b_1(1.119) \;=\; [b_1(\beta_t^{cr})]^{N_t} \;. \tag{4.21}$$

Solving the last equation numerically one finds β_t^{cr}. The results are given in the Table 4.1. As will be seen below the predicted values are in a reasonable agreement with the numerical results.

Table 4.1: Analytical estimates of β_t^{cr} for several values of N_t (first row) compared with the numerical results obtained in Section 4.4 (second row).

N_t	2	4	8	16
β_t^{cr}	2.0003	3.39389	6.10642	11.6385
		3.42(1)	6.38(5)	

4.4 Results at $\beta_s = 0$

4.4.1 $N_t = 1$

What follows has been published in [61] The main indication of BKT critical behavior is a peculiar scaling of the pseudo-critical coupling with the spatial lattice size L, consequence of the *essential scaling*, [1]

$$\beta_{pc}(L) - \beta_c \sim \frac{1}{(\log L)^{1/\nu}} \;, \tag{4.22}$$

where $\beta_{pc}(L)$ is the pseudo-critical coupling on a lattice with spatial extent L, β_c is the (non-universal) infinite volume critical coupling and ν is the (universal) thermal critical index.

[1] Throughout this Section we use the notation $\beta_t \equiv \beta$.

The pseudo-critical coupling $\beta_{pc}(L)$ is determined by the value of β for which a peak shows up in the susceptibility of the Polyakov loop,

$$\chi = L^2\langle|P|^2\rangle \ , \qquad P = \frac{1}{L^2}\sum_x P_x \ ; \tag{4.23}$$

here the local Polyakov loop variable P_x corresponds to the spin $s_x = \exp i\omega(x)$ of the XY model. In Fig. 4.1 we show the behavior of the absolute value of the Polyakov loop $|P|$ (top) and of the susceptibility χ (bottom), for varying β on lattices with L= 32, 64, 128.

To extract $\beta_{pc}(L)$ in a more reliable way, we performed the multi-histogram technique [62] where errors were determined by the jackknife method. Results for $\beta_{pc}(L)$ are summarized in Table 4.2. Let us discuss the main idea of this procedure.

This multi-histogram technique allows for an interpolation between the set of simulation points carried out at the couplings β_i $(i = 1, \ldots, R)$ with a subsequent improvement in terms of error. First one has to measure the energy distributions for each coupling:

$$p_i(E) = H_i(E)/N_i \quad , \tag{4.24}$$

where $H_i(E)$ is the occurrence of the energy value E in the i-th simulation which is long N_i. The true distribution is given by

$$p_i(E) = n(E)e^{-\beta_i E + f_i} \quad , \tag{4.25}$$

where $n(E)$ is the density of state, which does not depend on E, while f_i are the free energies $f_i = -\log Z_{\beta_i}$. After some algebra, it can be shown that

$$n(E) = \frac{\sum_{i=1}^{R} H_i(E)}{\sum_{i=1}^{R} N_j e^{-\beta_j E + f_j}} \quad . \tag{4.26}$$

After the determination of the coefficients f_i by solving numerically the equation

$$e^{-f_i} = \sum_E n(E)e^{-\beta_i E} \quad . \tag{4.27}$$

one can calculate the thermodynamical average of any observable O at any β, at least in principle, with

$$\langle O \rangle_\beta = \frac{\sum_E O(E) n(E) e^{-\beta E}}{\sum_E n(E) e^{-\beta E}} \quad . \tag{4.28}$$

In practice, instead, the predictions of the interpolation are reliable only very close to the simulation points, but producing a substantial reduction of the errors. Furthermore the numerical extraction of the coefficients f_i is possible only if the simulation points are close enough each other. The bigger is the volume the closer the simulation points are to be taken. This could become prohibitive if one is working with big volumes.

Table 4.2: $\beta_{pc}(L)$ for N_t=1, 4, 8 and for several values of L. Errors are determined by a jackknife analysis.

L	$N_t = 1$	$N_t = 4$	$N_t = 8$
64	-	3.1250(51)	5.531(19)
128	1.0051(16)	-	5.754(22)
150	1.0094(26)	3.2190(40)	5.7945(59)
200	1.0227(15)	3.2368(39)	-
256	1.0278(20)	-	-

We determined $\beta_c(N_t = 1)$ by fitting the pseudo-critical coupling $\beta_{pc}(L)$ given in the second column of Table 4.2 with the law

$$\beta_{pc}(L) = \beta_c + \frac{A}{(\log L)^{1/\nu}} \ , \tag{4.29}$$

in which ν was fixed by hand at the XY value, $\nu = 1/2$. We got $\beta_c(N_t = 1) = 1.107(9)$ and $A(N_t = 1) = -2.4(2)$ (χ^2/d.o.f.=0.78), which is quite in agreement with the best known XY critical coupling, $\beta_c = 1.1199(1)$, given in Ref. [63].

The determination of β_c is crucial in order to extract critical indices; indeed, they enter scaling laws which hold just at β_c, such as, for example,

$$\chi(\beta_c) \sim L^{2-\eta_c} \quad , \tag{4.30}$$

where η_c is the magnetic critical index. Actually in Eq. 4.30 one should consider logarithmic corrections (see [64, 65] and references therein) and, indeed, recent works on the XY universality class generally include them:

$$\chi(\beta_c) \sim L^{2-\eta_c} (\log L)^r \quad , \tag{4.31}$$

where r is another universal critical index, which takes the value $-1/8$ in the XY universality class. However, taking these corrections into account for extracting critical indices calls for very large lattices even in the XY model; for the theory under consideration to be computationally tractable, we have no choice but to neglect logarithmic corrections.

We determined $\chi(\beta = 1.12)$ for L=64, 128, 150, 200, 256 – see Table 4.3 for a summary of the results. Fitting with the law (4.30), we found $\eta_c = 0.256(29)$ (χ^2/d.o.f.=0.2), in nice agreement with the XY value, $\eta_c = 1/4$. The same analysis repeated at $\beta = 1.107$, *i.e.* at the central value of our determination of β_c, on lattices with L=64, 128, 200, gave $\eta_c = 0.237(61)$ (χ^2/d.o.f.=0.01).

An alternative strategy to determine η_c uses the large distance behavior of the point-point correlator of the Polyakov loop,

$$C(R) = \sum_{x,n} \Re\Big(P_x^\dagger P_{x+R\cdot e_n} \Big) \quad , \tag{4.32}$$

where e_n is the unit vector in the n-th direction. Without logarithmic corrections, one has

$$C(R) \sim \frac{1}{R^{\eta_c}} \quad . \tag{4.33}$$

In Fig. 4.2 we plot $\log C(R)$ *vs* $\log R$ for L=200 at $\beta = 1.12$; linearity is clear up to $R \simeq 30$. Deviations at larger distances are due to finite size effects (echo terms are expected to be strong, since the correlator is long-ranged) and possibly to logarithmic corrections. In the linear regime ($5 < R < 30$), the naive fit with a power law gives

η= 0.22942(31) (χ^2/d.o.f.=0.83). The same analysis at $\beta = 1.107$ and L=200 gives η= 0.2380(20) (χ^2/d.o.f.=0.05) in the range $1 < R < 45$. On the same volume one sees that, for lower β's, η goes towards the expected value and that the linear region gets wider and wider.

The *effective* η_c index, defined as

$$\eta_{\rm eff}(R) \equiv \frac{\log[C(R)/C(R_0)]}{\log[R_0/R]} \quad , \tag{4.34}$$

must exhibit a plateau in the region where (4.33) holds. Fig. 4.3(top) shows that the larger the volume the larger the region in which there is a plateau at small distances. The chosen value of R_0 must belong to the linear region in order to minimize finite size effects. We have verified that varying R_0 in the linear region does not change the result and have chosen $R_0 = 10$ for all the cases considered here.

Since for the larger lattices (L=200 and L=256) plateaux are overlapping at small distances, one can conclude that thermodynamic limit is reached. We estimate the plateau value from the most precise data we have (L=200) as $\eta(\beta = 1.12) = \eta_{\rm eff}(R = 6) = 0.23101(49)$, since the latter is the value of $\eta_{\rm eff}$ in the linear region compatible with the largest number of subsequent points. Deviations from the expected value η=0.25 can be due either to logarithmic corrections or to the overestimation of β_c. Repeating the same procedure for slightly lower β's we find: $\eta(\beta = 1.115) = 0.23491(47)$ and $\eta(\beta = 1.107) = 0.24085(44)$. Notice that η approaches the expected value as β lowers. The relation between η and β is well described by a linear function (χ^2/d.o.f.=0.04) and this suggests that the β value at which η=0.25 is really close to those considered. Fig. 4.3(bottom) shows the correlation function $C(R)$ rescaled by $L^{-\eta}$ in units of R/L; it turns out that, when the best determination for η is used (in the present case, η = 0.23101) data from different lattices fall on top of each other over almost all the range of distances considered.

There are other observables which turned out to be useful in establishing the BKT scaling in the $2d$ XY model and which we do not use in the present work: the helicity modulus $\mathcal{Y}$ [66, 65], the second moment correlation length ξ_2 (see, for instance, [65])

and the U_4 cumulant, proposed in [67]. We plan to use them all when we will study the general case $\beta_s \neq 0$. For the purposes of the present work we have only tried to use the U_4 cumulant, but both lattice sizes and statistics seem to be not enough large to extract any useful information from this observable.

4.4.2 N_t=4 and 8

In this Subsection we extend the study performed in the $N_t = 1$ case to the cases of $N_t = 4$ and 8, with the aim of showing that the universal XY features are not lost increasing N_t at β_s=0.

In Table 4.2 we give the values of the pseudo-critical couplings $\beta_{pc}(L)$ obtained from the peaks of the Polyakov loop susceptibility for several values of L at $N_t = 4$ and 8. Fitting these values with the law (4.29) with $\nu = 1/2$ fixed, we get

$$\begin{aligned} \beta_c(N_t = 4) &= 3.42(1) , \quad A(N_t = 4) = -5.1(3) , \quad (\chi^2/\text{d.o.f.} = 0.43) \\ \beta_c(N_t = 8) &= 6.38(5) , \quad A(N_t = 8) = -15(1) , \quad (\chi^2/\text{d.o.f.} = 0.006) \quad .(4.35) \end{aligned}$$

This result shows that essential scaling is satisfied, *i.e.* in both cases transition is compatible with BKT. It is worth noting that these values of β_c are in nice agreement with the estimates given in Table 4.1. This suggests that the dynamics of the effective model near the transition point is indeed dominated by the lower representations, thus justifying the truncation of the series in Eq. (4.20).

Table 4.3: $\chi(L)$ for N_t=1, 4, 8. Errors are determined by a jackknife analysis.

L	$N_t = 1$	$N_t = 4$	$N_t = 8$
64	7.19(12)	9.30(57)	7.33(37)
128	24.6(1.3)	35.9(4.4)	25.1(1.5)
150	32.9(1.9)	42.5(2.5)	32.5(1.9)
200	51.4(2.7)	65.2(2.8)	58.4(3.3)
256	80.3(4.2)	101.7(5.4)	86.4(3.6)

In Table 4.3 we give the values of the Polyakov loop susceptibility for several values of L at $\beta = 3.42$ for $N_t = 4$ and at $\beta = 6.38$ for $N_t = 8$. Fitting with (4.30), we find

$$\begin{aligned} \eta_c(N_t = 4) &= 0.290(54) \quad (\chi^2/\text{d.o.f.} = 0.69) \\ \eta_c(N_t = 8) &= 0.212(46) \quad (\chi^2/\text{d.o.f.} = 0.28) \quad . \end{aligned} \tag{4.36}$$

Results agree with the universal XY value $\eta_c = 1/4$, although errors are quite large.

A more precise determination of the magnetic index can be achieved through the study of the point-point correlation function. In Figs. 4.4(top) and 4.5(top) we show $\eta_{\text{eff}}(R)$ for three values of the spatial size L for the cases of $N_t = 4$ and $N_t = 8$, respectively. Our estimated plateau values, taken from data at $L = 200$, are

$$\begin{aligned} \eta(\beta = 3.42) &= \eta_{\text{eff}}(N_t = 4, R = 2) = 0.2724(11) \ , \\ \eta(\beta = 6.38) &= \eta_{\text{eff}}(N_t = 8, R = 3) = 0.2499(11) \ . \end{aligned}$$

For $N_t = 4$, η overshoots by little the XY universal value, while for $N_t = 8$ it is in nice accord with it. The deviation for $N_t = 4$ is most likely washed out by a fine tuning of the critical coupling within its error bars.

One can observe, moreover, that the shape of the curve of values of $\eta_{\text{eff}}(R)$ changes qualitatively in the same way when the thermodynamic limit is approached for $N_t = 1$ and $N_t = 8$, while it has a different behavior for $N_t = 4$. This may be an indication that for $N_t = 1$ and $N_t = 8$ at the β's chosen for the simulation the system is in the same phase ($\beta > \beta_c$), *i.e.* correlators have the same behavior.

Figs. 4.4(bottom) and 4.5(bottom) show the correlation function $C(R)$ rescaled by $L^{-\eta}$ in units of R/L, with η fixed at the central value of our determinations ($\eta = 0.2724$ for $N_t = 4$ and $\eta = 0.2499$ for $N_t = 8$); one can see that data from different lattices fall on top of each other over a wide range of distances.

In summary, essential scaling is verified both for $N_t = 4$ and 8, thus indicating that indeed the occurring transitions are compatible with BKT. Moreover data point to values of the thermal and magnetic critical indices of the $2d$ XY universality class. This leads us to conclude that for $N_t = 4$ and 8 the $3d$ U(1) LGT at β_s=0 belongs to

the $2d$ XY universality class and this supports the conjecture that the same holds, in general, for any N_t at $\beta_s = 0$.

Since we do not study the correlation length, we are not allowed to rule out the possibility that it keeps finite and the transition is therefore first order. To this aim, we have performed a fit to the pseudo-critical couplings with the first order law

$$\beta_{pc}(L) = \beta_c + \frac{B}{L^2} \ , \tag{4.37}$$

finding

$$\begin{aligned} \beta_c(N_t = 4) &= 3.245(3) \ , \quad B(N_t = 4) = -500(30) \ , \quad (\chi^2/\text{d.o.f.} = 2.1) \\ \beta_c(N_t = 8) &= 5.852(8) \ , \quad B(N_t = 8) = -1300(100) \ , \quad (\chi^2/\text{d.o.f.} = 0.6) \end{aligned} \tag{4.38}$$

Looking at the χ^2/d.o.f., one can argue that for $N_t = 4$ first order should be ruled out, whereas $N_t = 8$ is compatible with first order scaling. [2] This can be due to the limited volumes ($L \leq 150$) considered for $N_t = 8$ and to the larger error bars in the determinations of the β_{pc}'s with respect to the $N_t = 4$ case. However, for $N_t = 8$ the good agreement between the numerical result for the magnetic critical index and the corresponding value in the $2d$ XY model supports the claim that, even for this N_t, the transition is BKT.

4.5 Conclusions and outlook

The purpose of this work has been to study the critical behavior of $3d$ U(1) LGT at finite temperatures, through the formulation on an asymmetric lattice. While the theory at zero-temperature is always in the confined phase, at finite temperatures it undergoes a deconfinement phase transition, just as it happens for $4d$ QCD. Analytical results from the high-temperature expansion suggest that this transition is of BKT type, but compelling numerical evidence is missing that indeed critical indices of $3d$ U(1) LGT coincide with those of the $2d$ XY model.

[2] The same conclusion can be reached by studying the scaling with the lattice size of the peak of the Polyakov loop susceptibility.

This work is the first step in the construction of the phase diagram of $3d$ U(1) LGT in the (β_t, β_s)-plane, where β_s (β_t) is the spatial (temporal) coupling. In particular, we restricted ourselves to the case $\beta_s = 0$ and, by means of numerical Monte Carlo simulations on a dimensionally reduced effective theory, found evidence that the theory belongs indeed to the same universality class of the $2d$ XY model. The key observations have been the appearance of essential scaling and the agreement of the magnetic critical index η with that from the $2d$ XY model.

The next step is the extension of the numerical procedure established in this work to the general case of $\beta_s \neq 0$.

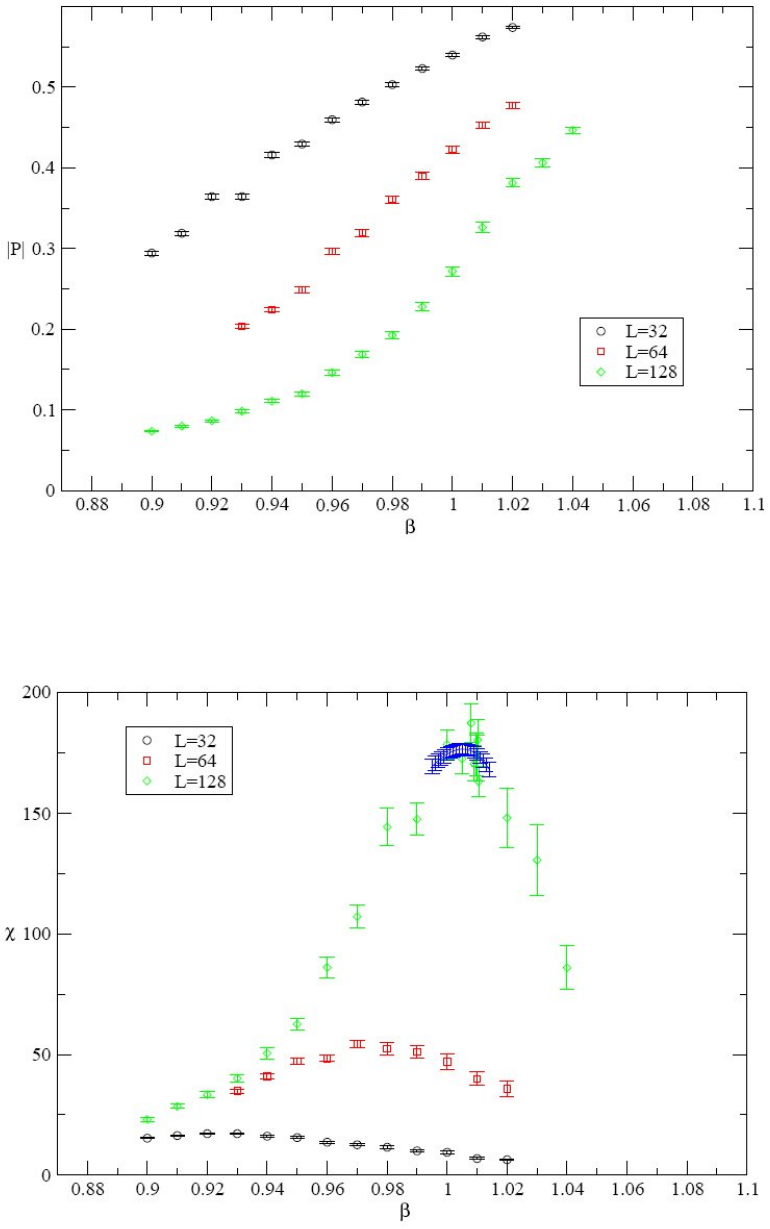

Figure 4.1: (Top) Absolute value of the Polyakov loop *vs* β on a $1 \times L^2$ lattice, with L=32, 64, 128. (Bottom) Susceptibility of the Polyakov loop *vs* β on a $1 \times L^2$ lattice, with L=32, 64, 128. For the L=128 case the multi-histogram interpolation around the peak is shown.

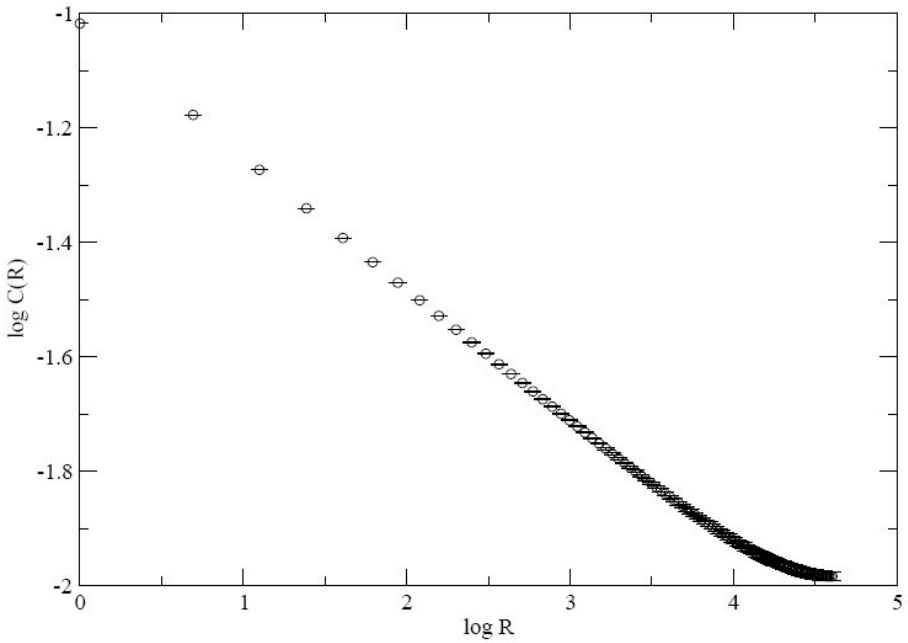

Figure 4.2: Log-log plot of point-point correlator for L=200 at $\beta = 1.12$.

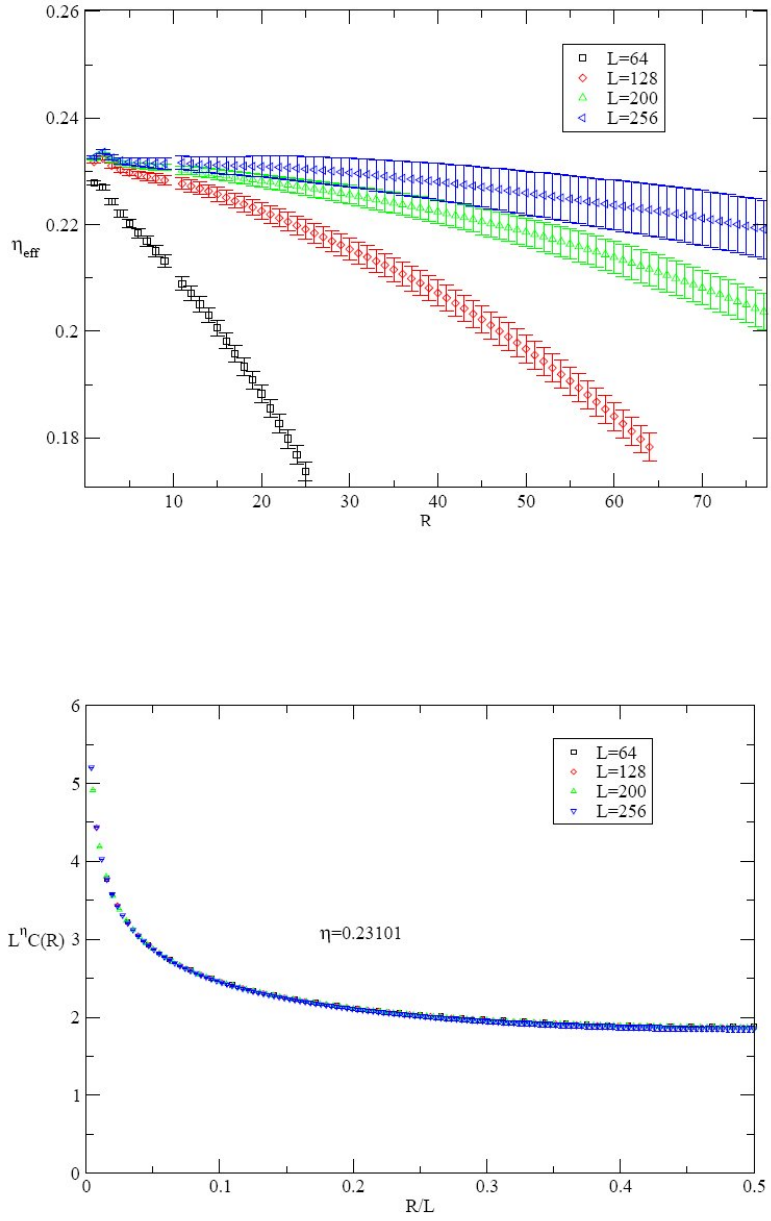

Figure 4.3: (Top) $\eta_{\rm eff}$ for $N_t = 1$ on lattices with several spatial sizes L at $\beta = 1.12$. For all lattices we fixed R_0=10. Errors are calculated with the jackknife method. (Bottom) $L^{\eta}C(R)$ versus R/L, with η fixed at the central value of our determination through the method of the effective $\eta_{\rm eff}$ (see the text).

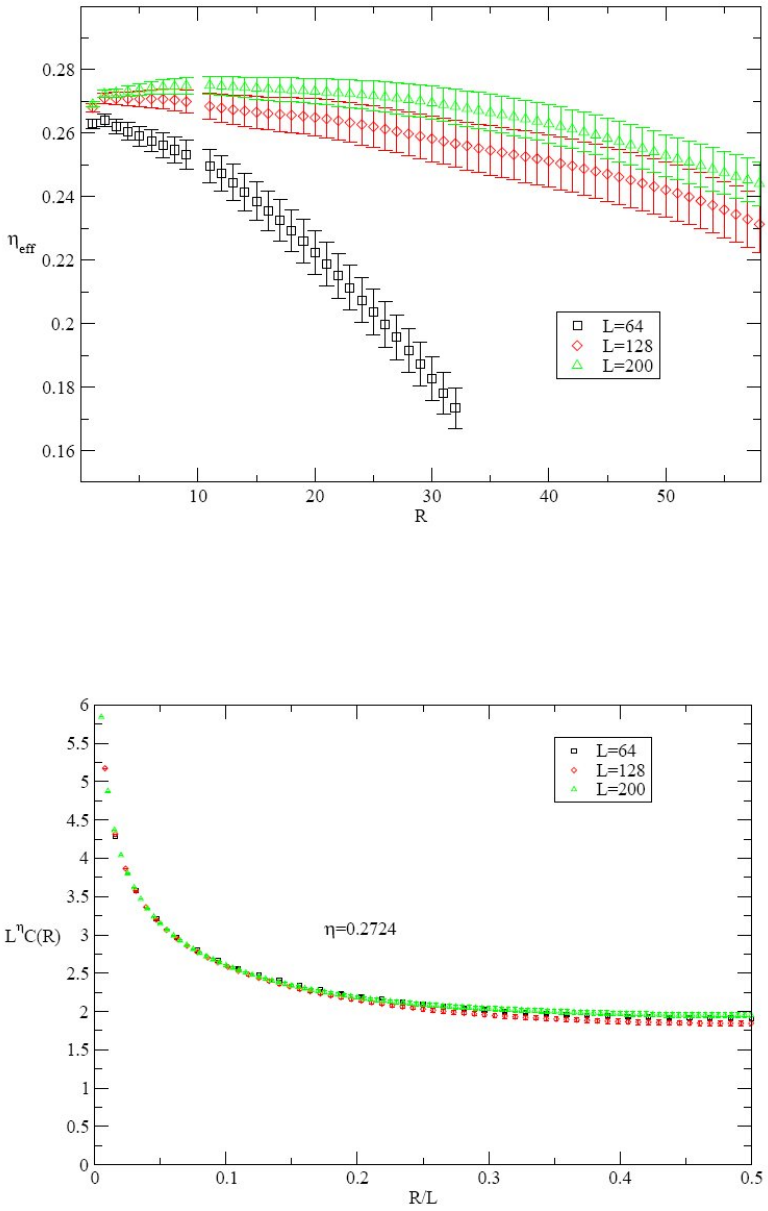

Figure 4.4: (Top) $\eta_{\rm eff}$ for $N_t = 4$ on lattices with L=64, 128, 200 at $\beta = 3.42$. For all lattices we fixed R_0=10. Errors are determined by the jackknife method. (Bottom) $L^\eta C(R)$ versus R/L, with η fixed at the central value of our determination through the method of the effective $\eta_{\rm eff}$ (see the text).

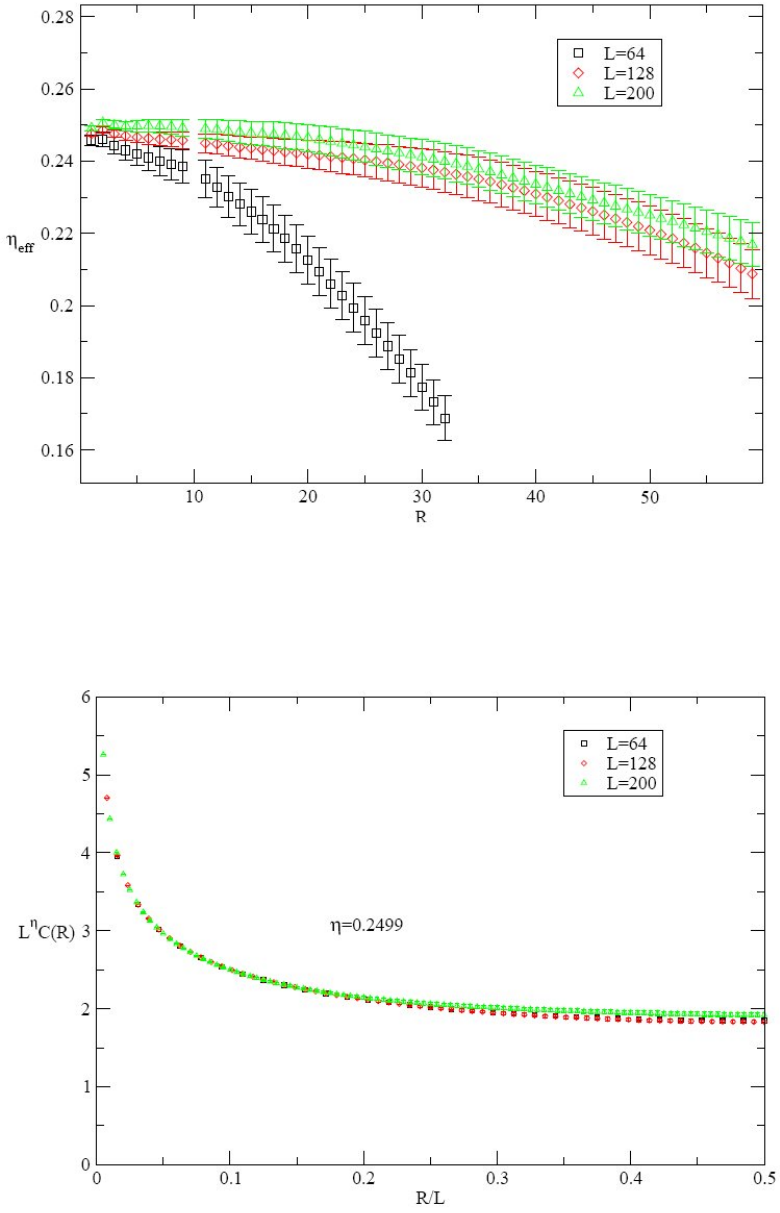

Figure 4.5: (Top) $\eta_{\rm eff}$ for $N_t = 8$ on lattices with L=64, 128, 200 at $\beta = 6.38$. For all lattices we fixed R_0=10. Errors are determined by the jackknife method. (Bottom) $L^{\eta}C(R)$ versus R/L, with η fixed at the central value of our determination through the method of the effective $\eta_{\rm eff}$ (see the text).

Chapter 5

Critical region in compact QED with two Wilson fermions

5.1 The Landau pole problem

An apparent mathematical inconsistency in QED is the existence of the so-called Landau pole. It appears in the perturbative behavior of the renormalized coupling constant as a function of the cut-off parameter.

The Callan-Symanzik β-function is defined as [14]

$$\beta(\alpha) = -\Lambda \left(\frac{\partial \alpha}{\partial \Lambda} \right)_{e, m_R} \quad , \tag{5.1}$$

where α is the renormalized fine structure constant, Λ the cut-off and the derivative is to be taken at fixed bare coupling e and renormalized m_R. The dependence of α on Λ is obtained from the differential equation

$$\frac{d\alpha}{d \ln \Lambda} = -\beta(\alpha) \tag{5.2}$$

and we obtain for the one-loop approximation to the β-function with only one fermion species

$$\alpha \left(\frac{\Lambda}{m_R} \right) = \frac{\alpha_0}{1 + \alpha_0 \beta_1 \ln(\Lambda / m_R)} \quad , \quad \beta_1 = \frac{2}{3\pi} \quad , \quad \alpha_0 = \frac{e^2}{4\pi} \quad . \tag{5.3}$$

Trying to send Λ to infinity while keeping α_0 fixed, α approaches zero and the theory would be trivial: the theory would be renormalizable only as a free theory. Two-loop contributions would not change the result qualitatively.

Consider now the renormalized coupling $e_R^2 = 4\pi\alpha$ instead of α. The β-function now determines the change of e_R^2 as a function of μ, the renormalization scale. The differential equation is obtained to be

$$\frac{de_R^2(\mu)}{d\log\mu} = \beta_{e^2}(e_R^2(\mu)) \quad , \quad \beta_{e^2} = 4\pi\beta \tag{5.4}$$

and in one-loop approximation we find

$$e_R^2(\mu) = \frac{e_R^2(\mu_0)}{1 - e_R^2(\mu_0)(\beta_1/4\pi)\ln(\mu/\mu_0)} \quad . \tag{5.5}$$

$e_R^2(\mu)$ has a pole at the scale

$$\mu_{\text{Landau}} = \mu_0 \exp\left(\frac{4\pi}{\beta_1 e_R^2(\mu_0)}\right) \quad , \tag{5.6}$$

if it is equal to $e_R^2(\mu_0)$ at the scale μ_0. The position of the Landau pole is changed by the two-loop contribution to

$$\mu_{\text{Landau}} = \mu_0 \left(\frac{\beta_2 e_R^2(\mu_0)}{4\pi\beta_1}\right)^{\frac{\beta_2}{\beta_1^2}} \exp\left(\frac{4\pi}{\beta_1 e_R^2(\mu_0)}\right)(1 + O(e_R^2(\mu_0))) \quad , \tag{5.7}$$

and substituting the physical information $e_R^2(\mu_0) = 4\pi/137$ we end up with a very high scale, far away from any reasonable scale. This mathematical inconsistency can be resolved if the full β-function has a zero at $e_R^2 = e_*^2$, an extra ultra-violet stable fixed point (see Fig.5.1).

This means that the solution of (5.4) for $e_R^2(\mu)$ always tends towards e_*^2 as μ goes to infinity. The zero of (5.2) implies that we can tune α_0 near $\alpha_{0*} = e_*^2/4\pi$ in a way such that for $\Lambda \to \infty$, α gets an arbitrary finite value. Thus, if such a fixed point exists, the continuum limit is non-trivial.

The zero of the β-function may be associated with a QED phase transition in the bare parameter space. At this critical point e_*^2, which is in the strong coupling regime, the

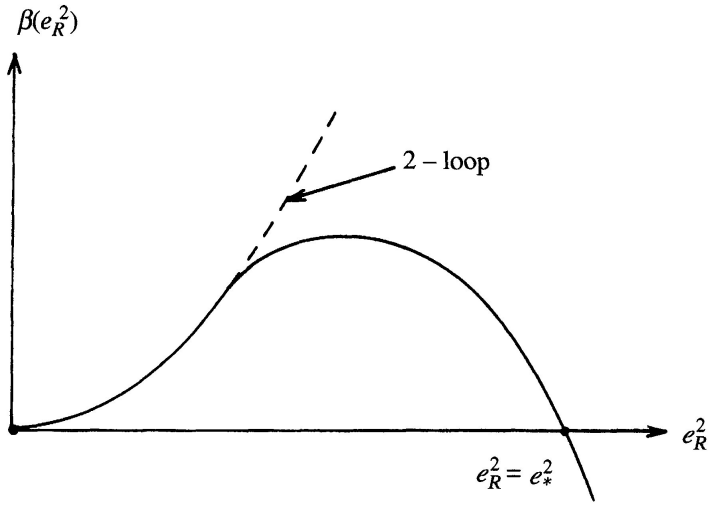

Figure 5.1: The β-function.

chiral symmetry of the massless theory is spontaneously broken and the chiral condensate $\langle\overline{\psi}\psi\rangle$ becomes non-zero. To find a solution to the Landau pole problem, QED has to be formulated in a non-perturbative way. Thus, it is evident to investigate the problem on the lattice. In particular, the existence of a critical region in the lattice formulation, where correlation length diverges, would indicate the presence of a point where one could eliminate the cut-off. This would mean that the theory would be renormalizable, thus suggesting the existence of the extra ultra-violet fixed point e_*^2.
It should be mentioned that QED is not the only theory showing the Landau pole problem. Every theory which is not asymptotically free suffers from this problem.

5.2 The phase structure of compact lattice QED

It has been stressed in section (2.2.2) that, in order to extract continuum physics from lattice simulations, a theory must present critical behavior at certain points in the parameter space. Thus, we are interested in the study of the phase diagram of compact lattice QED.
In the pure gauge case, that is in absence of fermions, for large values of the β pa-

rameter (weak coupling expansion) the system shows a phase with a massless photon and a Coulomb force between static charges. This can be studied in the framework of perturbation theory. This is the *Coulomb phase*. So far this sounds satisfactory, since those properties characterize electromagnetism as we know it. But, as we decrease β below some critical parameter $\beta_c \sim 1$, the theory exhibits properties quite different from those at large β. The expansion in this region is called the strong coupling expansion. In this phase, the *confining phase*, the static potential between static charges is directly proportional to the distance between them [17] and it amounts to the formation of monopole-antimonopole pairs [68].

Including charged fermions fields will bring about additional parameters to β. Here we will concentrate on Wilson fermions with the additional parameter κ, which itself will depend on β at the chiral critical line of the theory:

$$ma = \frac{1}{2}\left(\frac{1}{\kappa} - \frac{1}{\kappa_c}\right) \quad . \tag{5.8}$$

Now the vacuum contains additionally a fermion condensate. Starting with zero fermion mass and decreasing the parameter κ leads to a spontaneous breaking of the chiral symmetry; the fermions gain mass. All these effects lead to two phases with totally different properties, by varying β. For large values of β everything ever heard about abelian gauge theories holds. In the extreme case $\beta \to \infty$, perturbative calculations indicate that the fermion mass becomes equal to zero at the value $\kappa_c = 1/8$ [69]. But for small values of β the theory shows completely different properties, similarly to QCD. In the other extreme case $\beta \to 0$, the mass term for Wilson fermion vanishes at $\kappa_c = 1/4$ [70].

These two phases are separated by a phase transition in a region where both, the strong and weak coupling expansion, break down. This happens at $\beta \sim \beta_c$ where correlation lengths are large and perturbative methods do not hold. Investigation here is accessible only by numerical simulations. Above the chiral line $\kappa = \kappa_c$, two non-physical phases are present [71, 72]. In Fig. 5.2 we give a qualitative plot of the phase structure for compact lattice QCD.

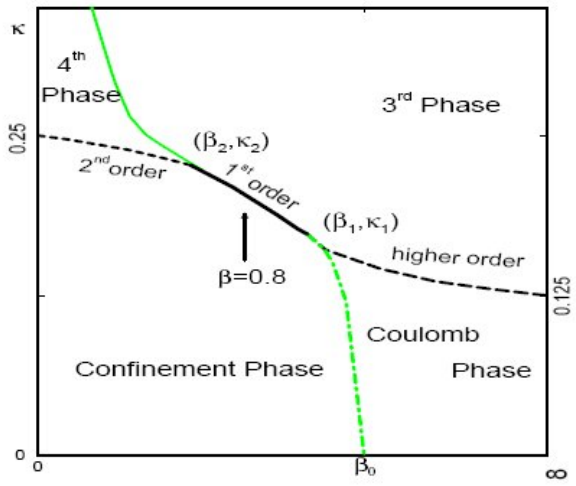

Figure 5.2: Phase diagram of QED with two Wilson fermions, taken from [72].

Many interesting questions emerge concerning the phase transition. First, one is interested in the question whether the Landau pole problem could be solved. No Landau pole occurs if the phase transition would be of second order.

Furthermore, about the presence of confinement, another question is whether it is possible to construct a continuum theory preserving the properties from confining phase. If this is the case there would exist a continuum theory which has not yet been formulated as a lagrangian continuum theory. In order to push the continuum limit the theory, again, needs a critical second order point.

For both questions, an obvious candidate would be the just mentioned confinement transition. It is of great interest whether the phase transition is a continuous second order one, or first order. For the Wilson fermions there are only indications that the transition is of weak first order [71]. There are more stringent arguments for the pure gauge case ($\kappa = 0$) [73, 74, 75] but still some calculations suggest a second order phase transition [76, 77].

It turns out that a more precise study of the critical properties for compact lattice QED with Wilson fermions is needed, in order to clarify the nature of the transition lines which are present in the phase diagram. This is the aim of this work.

5.3 The HMC algorithm

For the numerical simulation of our system we use the Hybrid Monte Carlo algorithm [78]. This was formulated on the base of the hybrid stochastic method suggested by Duane and Kogut [79], for the simulation of QCD on the lattice. We adapted the strategy to the case of compact QED with Wilson fermions.

Let us start by the path integral for the partition function in presence of two equal-mass Wilson fermions

$$Z = \int [dU d\psi d\overline{\psi}] e^{-S^{(W)}} \quad , \tag{5.9}$$

where $S^{(W)} = S_G + S_f^{(W)}$ is composed of the bosonic and fermionic contributions, (2.50) and (2.45) respectively. The fermionic matrix (5.10) is given by

$$K^{(W)}_{\alpha,\beta}[U](n,m) = \delta_{nm} - \sum_{\mu>0} [(r-\gamma_\mu)U_\mu(n)\delta_{m,n+\hat{\mu}} + (r+\gamma_\mu)U^\dagger_\mu(n-\hat{\mu})\delta_{m,n-\hat{\mu}}] \quad ; \tag{5.10}$$

setting $r = 1$ and $N_f = 2$, the hopping parameter becomes

$$\kappa = \frac{1}{2\hat{M}+4} \quad . \tag{5.11}$$

After integration over the Grassmann variables [13], the partition function reads

$$Z = \int [dU] e^{-S_G} \det{}^2 K^{(W)}(U) \quad . \tag{5.12}$$

Now, one can think $\det{}^2 K^{(W)} = \det K^{\dagger(W)} K^{(W)}$ and rewrite the determinant as the integration over one species of pseudo-fermionic variables ϕ:

$$Z = \int [dU d\phi] e^{-(S_G + \phi^* K^{\dagger(W)} K^{(W)} \phi)} = \int [dU] e^{-S_{eff}} \quad . \tag{5.13}$$

We used molecular dynamics to determine the evolution of the gauge fields [80]. We expect these deterministic equation to lead to a rapid movement of the fields through configuration space. In order for the link $U_\mu(n)$ to remain an element of $U(1)$, its equation of motion must have the form

$$\dot{U}_\mu(n) = i h_\mu(n) U_\mu(n) \quad , \tag{5.14}$$

where h is a real function. $\dot{U}$ is the derivative of U with respect to the "molecular dynamics" time, the time through which the fields evolve. The functions h play a role analogous to the canonical momenta in an ordinary molecular dynamics simulation. We therefore introduce an auxiliary field into the partition function by writing

$$Z = \int [dUdh] e^{-(1/2h^2 + S_{eff})} = \int [dUdh] e^{-H} \quad , \tag{5.15}$$

where $h^2 = \sum_{\mu,n} h_\mu^2(n)$. Clearly the introduction of the h field has no effect on correlation function involving U and ϕ.

We wish to generate a set of field configurations with a probability distribution proportional to $\exp(-H)$. To this end we employ three types of updating steps. The h and ϕ fields are updated using the heat baths [13]. We then simply equate each $h_\mu(n)$ to a real random number. To update the ϕ field we generate a complex vector of gaussian random numbers R with a probability distribution proportional to $\exp(-R^*R)$. We then form the vector $\phi = K^\dagger(U)R$. The probability distribution of ϕ is then proportional to $\exp(-\phi^*(K^\dagger K)^{-1}R)$.

The final type of updating is a molecular dynamics step in which we vary h and U for fixed ϕ in such a way as to keep H and the differential volume element in configuration space fixed. As will be clear from what follows, it suffices to find an equation of motion with these properties.

The equation of motion for the $U_\mu(n)$ is given in (5.14). This means that

$$U_\mu(n, t + \Delta t) = e^{ih(t + \frac{\Delta t}{2})\Delta t} U_\mu(n, t) \quad . \tag{5.16}$$

Setting $U_\mu(n,t) = e^{iA_\mu(n,t)}$, one has

$$A_\mu(n, t + \Delta t) = A_\mu(n, t) + \Delta t \; h\left(t + \frac{\Delta t}{2}\right) \quad , \tag{5.17}$$

which is the equation for the evolution of the field A, which requires the evolved field h. Notice that, from the last equation, $\dot{A}_\mu(n) = h_\mu(n)$.

To obtain an equation of motion for h we require that H be a constant of the motion, $\dot{H} = 0$. Hence

$$\dot{H} = \dot{h}h + \frac{\partial S_G(A)}{\partial A}\dot{A} + \phi^* \frac{d}{dt}(K^\dagger K)^{-1}\phi \quad . \tag{5.18}$$

Using the general formula for a matrix B

$$\frac{dB^{-1}}{dt} = -B^{-1}\frac{dB}{dt}B^{-1} \quad , \tag{5.19}$$

and after a little algebra, one has

$$\phi^* \frac{d}{dt}(K^\dagger K)^{-1}\phi = -2\mathrm{Re}\left(X_i^\dagger \left(\frac{\partial K}{\partial A}\right)_{ik} Y_k\right)\dot{A} \quad , \tag{5.20}$$

where

$$\begin{aligned} X &= (K^\dagger)^{-1}\phi \\ Y &= (K^\dagger K)^{-1}\phi = K^{-1}\phi \quad . \end{aligned} \tag{5.21}$$

The condition $\dot{H} = 0$ implies

$$h\left(\dot{h} + \frac{\partial S_G(A)}{\partial A} - 2\mathrm{Re}\left(X^\dagger \frac{\partial K}{\partial A} Y\right)\right) = 0 \quad , \tag{5.22}$$

that is

$$\dot{h} = -\frac{\partial S_G(A)}{\partial A} + 2\mathrm{Re}\left(X^\dagger \frac{\partial K}{\partial A} Y\right) = F_{bos} + F_{ferm} = F \quad . \tag{5.23}$$

Then the equation for the evolution of h is

$$h' = h + \Delta t F \quad . \tag{5.24}$$

Let us derive explicitly the form of the bosonic and fermionic forces, F_{bos} and F_{ferm}. Up to constants

$$\begin{aligned} S_G(U) &= -\frac{\beta}{2}\sum_P (U_P + U_P^\dagger) \\ &= -\frac{\beta}{2}\sum_{n,\mu} (U_\mu(n)V_\mu(n) + U_\mu(n)^* V_\mu(n)^*) \\ &= -\frac{\beta}{2}\sum_{n,\mu} (e^{iA_\mu(n)}V_\mu(n) + e^{-iA_\mu(n)}V_\mu(n)^*) \end{aligned} \tag{5.25}$$

where $V_\mu(n)$ are the sum of the staples, or product of the other three links in the plaquettes containing $U_\mu(n)$. Then one obtains

$$\frac{\partial S_G(A)}{\partial A_\mu(n)} = \beta \quad \mathrm{Im}(U_\mu(n)V_\mu(n)) \quad . \tag{5.26}$$

For the fermionic force, recalling that

$$K_{ik} = \delta_{ik} - k \sum_{\nu} [(1-\gamma_\nu) e^{iA_\nu(i)} \delta_{k,i+\hat{\nu}} + (1+\gamma_\nu) e^{-iA_\nu(i-\nu)} \delta_{k,i-\hat{\nu}}] \quad , \tag{5.27}$$

one obtains, finally

$$\frac{\partial K_{ik}}{\partial A_\mu(j)} = -\kappa i (1-\gamma_\mu) \delta_{ij} e^{iA_\nu(i)} \delta_{i+\mu,k} + \kappa i (1+\gamma_\mu) \delta_{i+\mu,k} e^{-iA_\mu(i-\mu)} \delta_{k,i-\hat{\mu}} \quad . \tag{5.28}$$

It is then clear after (5.17) and (5.24) that one needs the evolved field h to update the field A and the evolved field A to update the field h. The iteration of this mechanism defines a trajectory at the end of which, one has a new configuration for the link variables U_μ. Since we are moving along trajectories satisfying the condition $\dot{H} = 0$, it follows that the probability distribution e^{-H} does not change. This ensures that the detailed balance holds. However, after the molecular dynamics steps, we did an acceptance decision at the ens of each trajectory.

5.4 Results

For the matrix inversion defined in (5.21) we used the conjugate gradient method (see [81] and references therein). The convergence of this numerical method is controlled by a tolerance parameter, which ensures that solutions in two subsequent iterations are close enough. In our case, we fixed the tolerance to 10^{-5}.

For the generation of gauge field configurations, we let the system evolve through typically $N = 50$ trajectories and choose Δt in order to have $N\Delta t \sim 1$.

For the characterization of the transition lines, we focus above all on the study of the plaquette

$$\langle P \rangle = \frac{1}{N_P} \langle \sum_P \mathrm{Re} U_P \rangle \quad , \tag{5.29}$$

and its susceptibility

$$\chi = V(\langle P^2 \rangle - \langle P \rangle^2) \quad . \tag{5.30}$$

They are, in general, good quantities for the location of transitions. N_P is the total number of plaquettes on the lattice, while $V = N_t N_s^3$ is the total volume. In all simu-

lations we use $N_t = 12$ and vary N_s from 4 to 10. In particular, we concentrate on the analysis of the Binder cumulant B_4 [82]. For a general observable O, it is defined as

$$B_4 = 1 - \frac{\langle O \rangle^4}{3\langle O^2 \rangle^2} \quad . \tag{5.31}$$

This parameter takes the value 2/3, for gaussian distributions of the observable in the thermodynamical limit. For finite volumes it falls down corresponding to the transition. It allows for the discrimination between one-peak and two-peaks distributions, the former being characteristic of second or higher transitions, the latter of first order transitions. If the depth of the fall decreases towards zero, after increasing the volume, one can conclude that transition is first order. Otherwise, if the depth increases towards the value 2/3 with increasing volumes, then the limit distribution will be one-peak-like. In this case transition must be either second or higher order (crossover). This is the way in which we want to use the Binder cumulant. We study, furthermore, the chiral condensate

$$\langle \overline{\psi}\psi \rangle = \frac{1}{4V} \langle \mathrm{Tr} K^{-1} \rangle \quad . \tag{5.32}$$

Let us now consider separately the regions candidate for a more precise numerical study of the critical properties.

5.4.1 Chiral transition: $\beta = 1.2$

For the specific study of chiral line $\kappa = \kappa_c$, we study both the chiral condensate and the pion norm defined as

$$\langle \Pi \rangle = \frac{1}{4V} \langle \mathrm{Tr}(K^{-1}\gamma_5 K^{-1}\gamma_5) \rangle \quad . \tag{5.33}$$

This quantity is to be handled very carefully, since the expected critical behavior turns out to be deviated, due to the effect of zero-modes of the gauge field [83]. As a consequence, it can be used for the location of the chiral transition, but it cannot be used for a scaling analysis, in order to find out the nature of the transition.

In particular at $\beta = 1.2$ we locate the transition point looking at the peak of $\langle \Pi \rangle$, under variation of κ. In the central part of Fig. 5.3 it is possible to see that $\kappa_c(\beta = 1.2) \sim 0.15$.

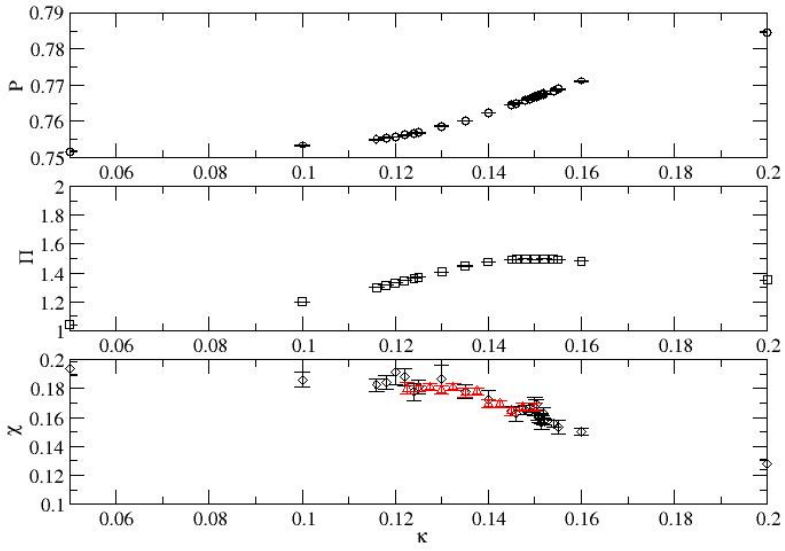

Figure 5.3: $\beta = 1.20$: the plaquette (top), the pion norm (center) and the susceptibility (bottom) for $N_s = 8$ (diamonds) and $N_s = 10$ (triangles).

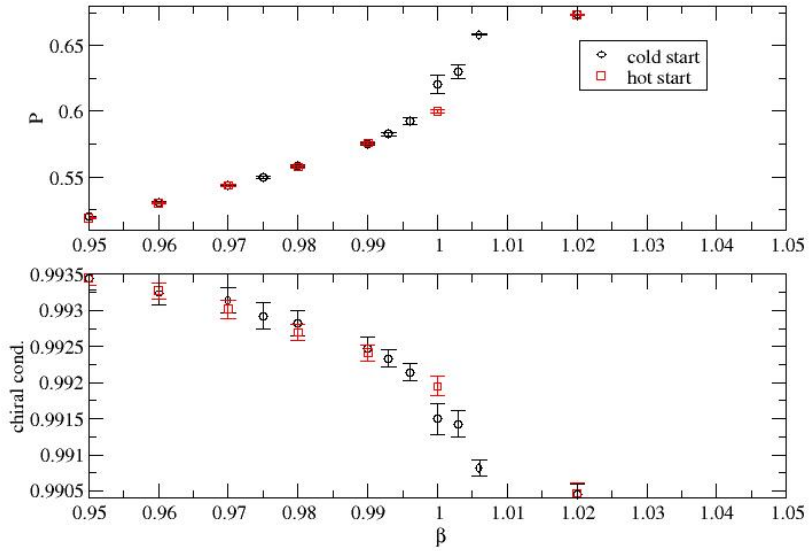

Figure 5.4: P and $\overline{\psi}\psi$ at $\kappa = 0.1$ and $N_s = 8$. Hysteresis is present around $\beta \sim 1$.

Corresponding to this value, neither P nor $\overline{\psi}\psi$ show any jump or rapid change. All seems to suggest that here no transition occurs. Indeed, looking at the plaquette susceptibility for $N_s = 8$ and $N_s = 10$ (lower part of Fig. 5.3) a very small peak is present around $\kappa = 0.15$, but its height does not increase if the volume is increased. This suggests that the chiral line is actually a crossover line. This is in agreement with analogous conclusion based on the behavior of the Π variance under variation of the volume [71], which, as stated above, cannot be used to determine the nature of the transition.

5.4.2 Confinement transition: $\kappa = 0.1$

Let us now study the confinement transition. Let us cross this line at $\kappa = 0.1$ by varying β. From short simulations, it is possible to see (Fig. 5.4) that hysteresis effects are present both for P and $\overline{\psi}\psi$ around $\beta \sim 1$. This is a typical feature of first order transition. In Fig. 5.5 it is shown the plaquette distribution around transition. The peak

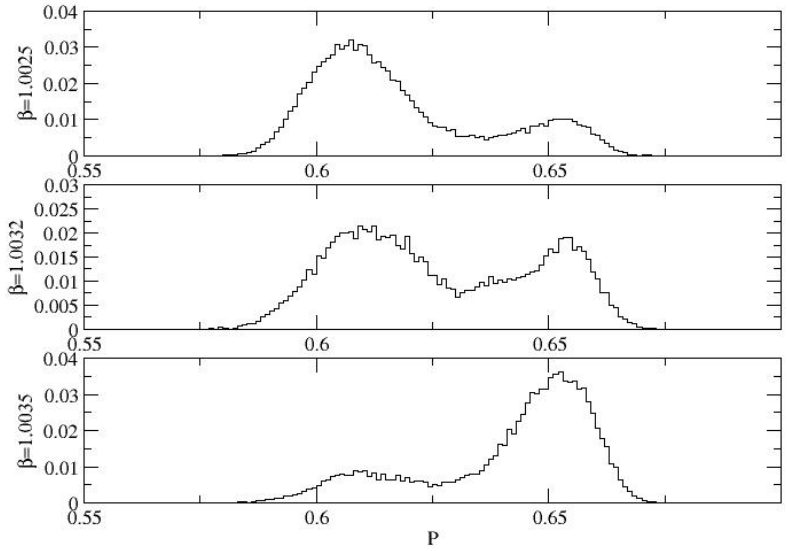

Figure 5.5: P distribution around transition. Here $\kappa = 0.1$ and $N_s = 8$.

dynamics is first order in the sense that one passes discontinuously from the lower peak to the higher one, increasing β. The fact that the two peaks are quite close supports the idea of weakly first order transition in the pure gauge case ($\kappa = 0$) [71, 73, 74, 75]. Looking at Fig. 5.6, one sees that the height of susceptibility increases, increasing the volume. This suggests that a true transition occurs. For a more stringent argument about the nature of the transition one should keep on increasing volume and do a finite size scaling analysis. At the moment let us try to single out a first order behavior through the Binder cumulant, as explained above. B_4 presents the behavior of Fig. 5.7. The most important information can be extracted from the depth of the cumulant for several volumes. In Fig. 5.8 one sees that the minimum of B_4 increases with the volume, suggesting either a second order transition or a crossover. This seems in contrast with the previous expectations. A possible solution to this controversy can be the fact that when transition is weakly first order, the correlation length becomes rather large compared with the lattice spacing. If the volume is too small, the correlation length could saturate

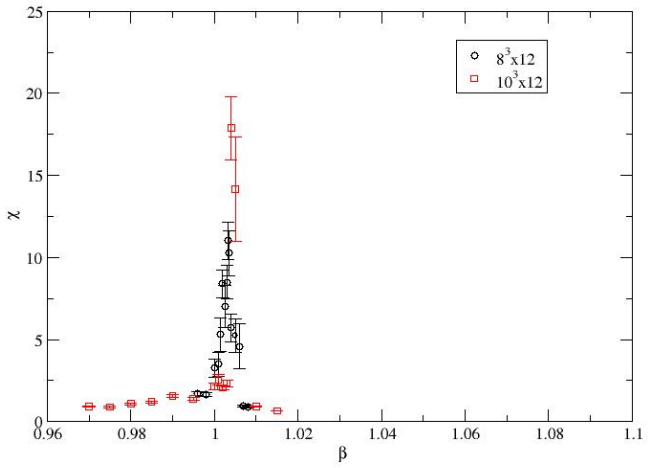

Figure 5.6: Plaquette susceptibility around transition at $\kappa = 0.1$ for $N_s = 8$ (circles) and $N_s = 10$ (squares).

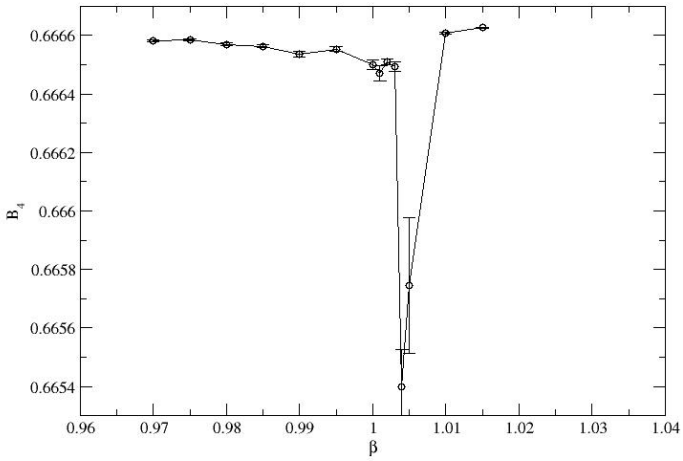

Figure 5.7: Binder cumulant for several β at $\kappa = 0.1$ and $N_s = 8$.

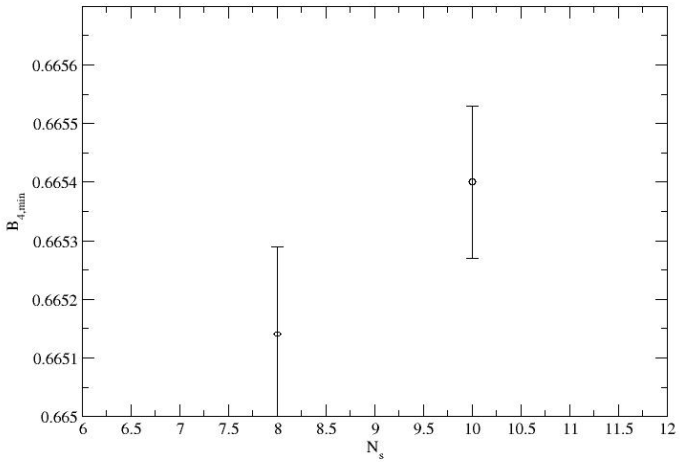

Figure 5.8: Minimum of B_4 for two values of lattice size at $\kappa = 0.1$.

the available space, inducing a second order transition behavior. This means that one needs to analyze larger volumes to really reveal the nature of the transition.

5.4.3 $\beta = 0.85$

Let us now consider the transition line which separates the confinement phase from the high-κ one. Let us cross this line at $\beta = 0.85$ by varying κ. We observe the hysteresis effects even stronger that those we have seen in the previous section, thus suggesting a first order transition. This picture is supported by the sharp jump which is present in the plaquette (see Fig. 5.9). The well separated peaks in the plaquette distribution also indicate a first order transition. This is shown in Fig. 5.10. One could be tempted to give the same conclusion looking at the minimum of the Binder cumulant (see Fig. 5.11). Indeed the depth of the cumulant decreases, increasing the lattice size. In this context it should be stressed that for $N_s = 8$ a two-peak structure is not realized in our simulations. In Fig. 5.10 the two peaks do not appear at the same time, producing an increasing in the minimum of B_4. Then, one should scan more accurately in β, in order to find

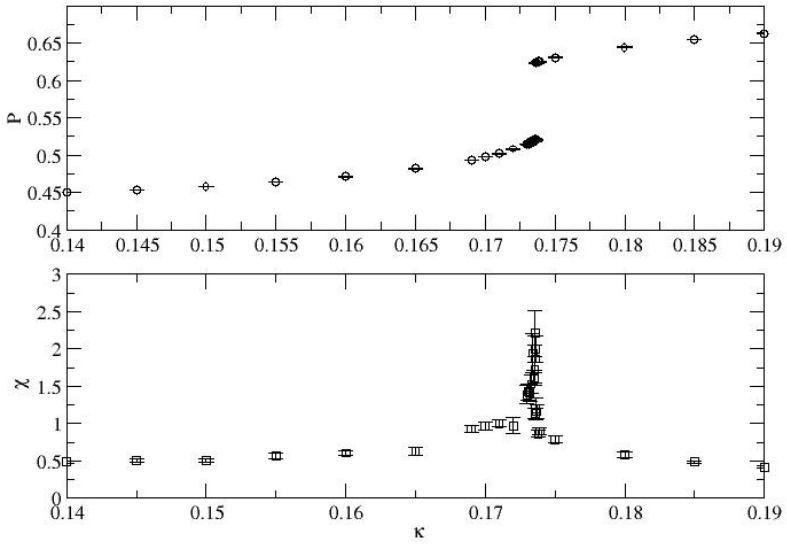

Figure 5.9: Plaquette and its susceptibility for several κ at $\beta = 0.85$. The lattice size is $N_s = 8$.

the point where the phase mixing occurs and subsequently calculate the B_4 depth for $N_s = 8$. The situation is different for $N_s = 10$ where the phase mixing point has been already singled out. In all cases, a larger volume analysis is needed.

5.4.4 Crossing point

In the last sections we have considered the branches around the crossing point between chiral and confinement lines. Here we address the question about the position of the crossing point which is a good candidate for the resolution of the Landau problem.
First we simulate at $\beta = 1.001$ for a range of κ large enough. ¿From Fig. 5.12 it is evident that confinement and chiral line are still separated. Indeed, the pion norm shows a peak at $\kappa \sim 0.15$, while the plaquette has a rapid increase around $\kappa \sim 0.11$. The picture is different at $\beta = 0.95$, where P and Π locate the transition approximately at the same point $\kappa \sim 0.146$ (see Fig. 5.13). Then ($\beta = 0.95$, $\kappa = 0.145$) is our first estimation

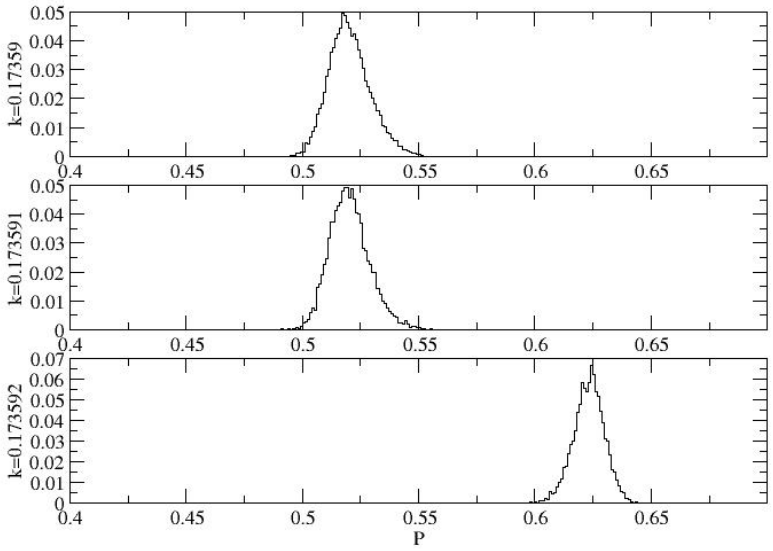

Figure 5.10: Plaquette distribution around transition at $\beta = 0.85$ for $N_s = 8$.

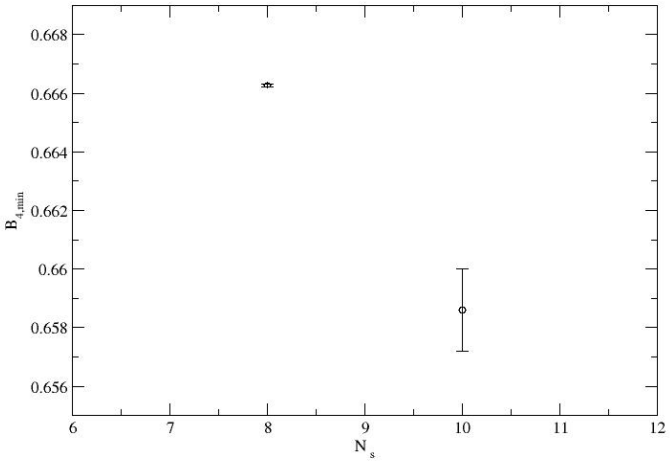

Figure 5.11: Minimum of B_4 for two values of lattice size at $\beta = 0.85$.

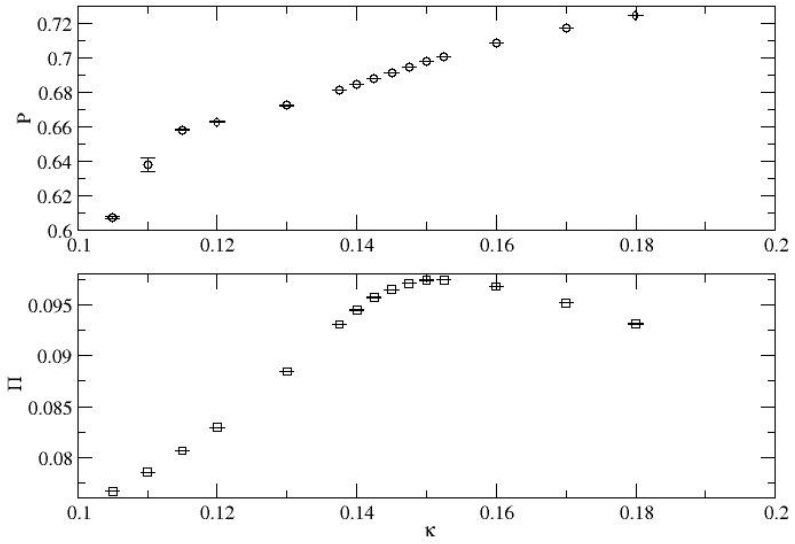

Figure 5.12: Plaquette and pion norm for several κ at $\beta = 1.001$ for $N_s = 10$.

of the crossing point. The plaquette distribution around the point $\kappa = 0.146$ is shown in Fig. 5.14. The well separated peaks reveal a clear first order dynamics, while the strange behavior in Fig. 5.15 for the minimum of B_4 suggests a more precise analysis is needed. The picture can be clarified going to larger lattices and studying, for example, the scaling of susceptibilities and the behavior of the B_4 depth.

5.5 Conclusions

In this work the problem of the existence of a second order transition point in the phase diagram of QED with Wilson fermion is addressed. Our preliminary results indicate that the confinement transition is weakly first order, while the transition between the confinement phase and the high-κ one is first order. No transition is found, instead, on the chiral line.

We locate the crossing point between confinement and chiral line at ($\beta = 0.95$, $\kappa =$

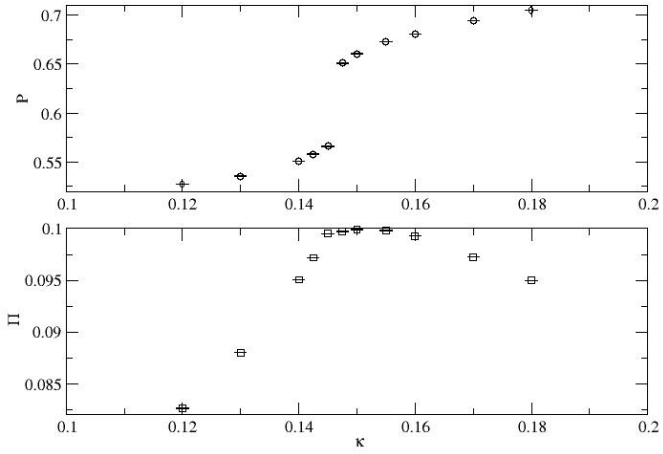

Figure 5.13: Plaquette and pion norm for several κ at $\beta = 0.95$ for $N_s = 8$.

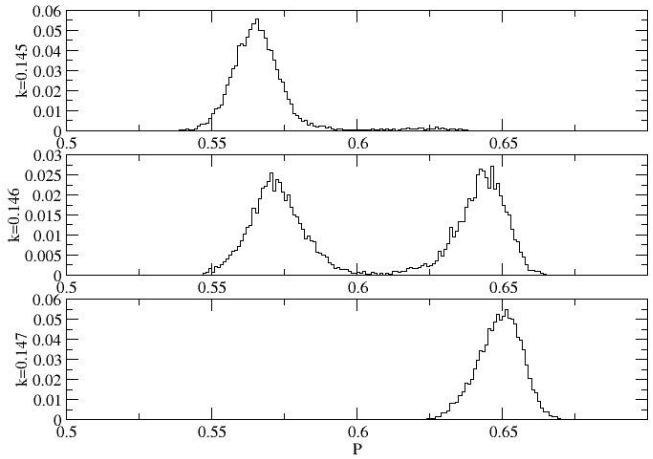

Figure 5.14: Plaquette distribution around the transition at $\beta = 0.95$ for $N_s = 8$.

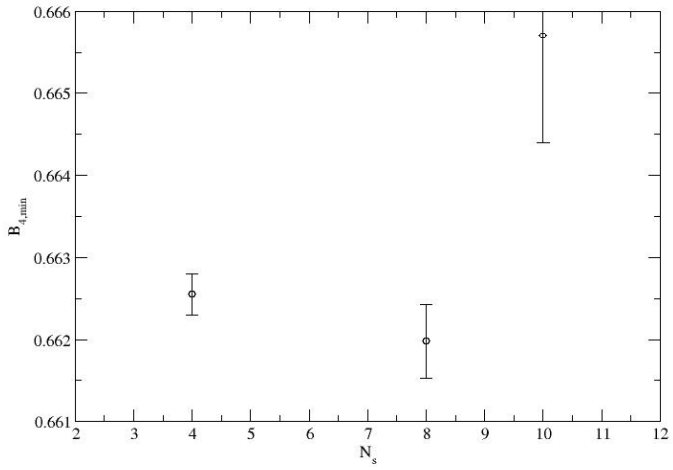

Figure 5.15: Minimum of B_4 for three values of lattice size at $\beta = 0.95$.

0.145) and try to find out the nature of the transition. There are signals indicating a first order transition.

In all cases, our results turns out to be only preliminary and call for larger lattices to become conclusive.

Bibliography

[1] H. E. Stanley, *Introduction to Phase Transitions and Critical Phenomena*, Oxford University Press, New York (1971).

[2] D. Chandler, *Introduction to Modern Statistical Mechanics*, Oxford University Press, New York (1987).

[3] J. Cardy, *Scaling and Renormalization in Statistical Physics*, Cambridge University Press, Cambridge (1996).

[4] A. Pelissetto and E. Vicari, Phys. Rept. **368** (2002) 549.

[5] L. Onsager, Phys. Rev. **65** (1944) 117.

[6] N. D. Mermin and H. Wagner, Phys. Rev. Lett. **17** (1966) 1133.

[7] W. Janke and K. Nather, Phys. Rev. B **48** (1993) 7419.

[8] V. L. Berezinsky, Sov. Phys. JETP **32** (1971) 493.

[9] J. M. Kosterlitz and D. J. Thouless, J. Phys. C **6** (1973) 1181.

[10] C. Itzykson and J. M. Drouffe, *Statistical Field Theory*, Cambridge University Press, Cambridge (1989).

[11] R. P. Feynman, Rev. Mod. Phys. **20** (1948) 367.

[12] R. P. Feynman and A. R. Hibbs, *Quantum Mechanics and Path Integrals*, New York, USA, McGraw-Hill (1965).

[13] H. J. Rothe, *Lattice Gauge Theories An Introduction*, World Scientific (1992).

[14] I. Montvay and G. Münster, *Quantum Fields on a Lattice*, Cambridge University Press, Cambridge (1994).

[15] C. N. Yang and R. L. Mills, Phys. Rev. **96** (1954) 191.

[16] T. Muta, *Foundations of Quantum Cromodynamics. Second Edition*, World Sci. Lect. Notes Phys. **57** (1998).

[17] K. Wilson, Phys. Rev. D **10** (1974) 2445.

[18] J. B. Kogut and L. Susskind, Phys. Rev. D **11** (1975) 395.

[19] L. Susskind, Phys. Rev. D **20** (1979) 2610.

[20] S. D. Katz, Nucl. Phys. Proc. Suppl. **129** (2004) 60.

[21] F. Karsch, E. Laermann, A. Peikert, C. Schmidt and S. Stickan, hep-lat/0010027.

[22] L. D. McLarren and B. Svetitsky, Phys. Rev. D **24** (1981) 450.

[23] E. Laermann and O. Philipsen, Ann. Rev. Nucl. Part. Sci. **53** (2003) 163.

[24] B. Svetitsky and L.G. Yaffe, Nucl. Phys. B **210** (1982) 423.

[25] S. Fortunato, F. Karsch, P. Petreczky and H. Satz, Nucl. Phys. Proc. Suppl. **94** (2001) 398.

[26] R. Fiore, A. Papa and P. Provero, Nucl. Phys. Proc. Suppl. **106** (2002) 486.

[27] J. M. Hammersley, D. C. Handscomb, *Monte Carlo Methods*, Methuen's Monographs, London (1975).

[28] A. B. Clarke, R. L. Disney, *Probability and Random Processes: a First Course With Aapplications*, John Wiley and Sons (1985).

[29] N. Metropolis, A. W. Rosenbluth, M. N. Rosenbluth, A. H. Teller and E. Teller, J. Chem. Phys. **21** (1953) 1087.

[30] S. Basak and K. De Asit, Phys. Lett. B **430** (1998) 320.

[31] R. Falcone, R. Fiore, M. Gravina and A. Papa, Nucl. Phys. B **767** (2007) 385.

[32] R. Falcone, R. Fiore, M. Gravina and A. Papa, Nucl. Phys. B **785** (2007) 13.

[33] A. M. Polyakov, Phys. Lett. B **72** (1978) 477.

[34] L. Susskind, Phys. Rev. D **20** (1979) 2610.

[35] F. Gliozzi and P. Provero, Phys. Rev. D **56** (1997) 1131.

[36] R. Fiore, F. Gliozzi and P. Provero, Phys. Rev. D **58** (1998) 114502.

[37] J. Engels and T. Scheideler, Nucl. Phys. B **539** (1999) 557.

[38] S. Fortunato, F. Karsch, P. Petreczky and H. Satz, Nucl. Phys. (Proc. Suppl.) **94** (2001) 398.

[39] R. Fiore, A. Papa and P. Provero, Nucl. Phys. (Proc. Suppl.) **106** (2002) 486.

[40] R. Fiore, A. Papa and P. Provero, Phys. Rev. D **63** (2001) 117503.

[41] A. Papa and C. Vena, Int. J. Mod. Phys. A **19** (2004) 3209.

[42] A. Pelissetto and E. Vicari, Phys. Rept. **368** (2002) 549.

[43] M. Caselle, M. Hasenbusch and P. Provero, Nucl. Phys. B **556** (1999) 575.

[44] M. Caselle, M. Hasenbusch, P. Provero and K. Zarembo, Nucl. Phys. B **623** (2002) 474.

[45] R. Fiore, A. Papa and P. Provero, Nucl. Phys. (Proc. Suppl.) **119** (2003) 490.

[46] R. Fiore, A. Papa and P. Provero, Phys. Rev. D **67** (2003) 114508.

[47] F. Karsch and S. Stickan, Phys. Lett. B **488** (2000) 319.

[48] H. W. J. Blöte and R. H. Swendsen, Phys. Rev. Lett. **43** (1979) 779.

[49] W. Janke and R. Villanova, Nucl. Phys. B **489** (1997) 679 and references therein.

[50] R. V. Gavai, F. Karsch and B. Petersson, Nucl. Phys. B **322** (1989) 738.

[51] A. S. Kronfeld, Nucl. Phys. (Proc. Suppl.) **17** (1990) 313.

[52] M. Lüscher and U. Wolff, Nucl. Phys. B **339** (1990) 222.

[53] R. H. Swendsen and J. S. Wang, Phys. Rev. Lett. **58** (1987) 86.

[54] P. W. Kasteleyn and C. M. Fortuin, J. Phys. Soc. Jpn. Suppl. **26** (1969) 11.

[55] M. N. Chernodub, E. M. Ilgenfritz, A. Schiller, Phys. Rev. D **64** (2001) 054507; Phys. Rev. Lett. **88** (2002) 231601; Phys. Rev. D **67** (2003) 034502.

[56] A. Polyakov, Nucl. Phys. B **120** (1977) 429; M. Göpfert, G. Mack, Commun. Math. Phys. **81** (1981) 97; **82** (1982) 545.

[57] N. Parga, Phys. Lett. B **107** (1981) 442.

[58] P. D. Coddington, A. J. G. Hey, A. A. Middleton and J. S. Townsend, Phys. Lett. B **175** (1986) 64.

[59] R. Kenna, arXiv:cond-mat/0512356.

[60] A. C. D. van Enter and S. B. Shlosman, Phys. Rev. Lett. **89** (2002) 285702.

[61] O. Borisenko, M. Gravina and A. Papa, J. Stat. Mech. **2008** (2008) P08009.

[62] A. M. Ferrenberg and R. H. Swendsen, Phys. Rev. Lett. **63** (1989) 1195.

[63] M. Hasenbusch and K. Pinn, J. Phys. A **30** (1997) 63.

[64] R. Kenna and A. C. Irving, Nucl. Phys. B **485** (1997) 583.

[65] M. Hasenbusch, J. Phys. A **38** (2005) 5869.

[66] H. Weber and P. Minnhagen, Phys. Rev. B **37** (1988) 5986.

[67] M. Hasenbusch, arXiv:cond-mat/0804.1880.

[68] T. A. DeGrand and D. Toussaint, Phys. Rev. D **22** (1980) 2478.

[69] N. Kawamoto and J. Smit, Nucl. Phys. B **192** (1981) 100.

[70] N. Kawamoto, Nucl. Phys. B **190** (1981) 617.

[71] A. Hoferichter, V. K. Mitrjushkin, T. Neuhaus and H. Stuben, Nucl. Phys. B **434** (1995) 358.

[72] A. Hoferichter, V. K. Mitrjushkin, M. Mueller-Preussker and H. Stuben, Nucl. Phys. Proc. Suppl. **63** (1998) 454.

[73] I. Campos, A. Cruz and A. Tarancon, Phys. Lett. B **424** (1998) 328.

[74] I. Campos, A. Cruz and A. Tarancon, Nucl. Phys. Proc. Suppl. **73** (1999) 715.

[75] M. Baig, Nucl. Phys. Proc. Suppl. **42** (1995) 654.

[76] J. Jersak, hep-lat/0010014 (2000).

[77] C. B. Lang, J. Jersak and T. Neuhaus, Phys. Rev. Lett. **77** (1996) 1933.

[78] S. Gottlieb, W. Liu, D. Toussaint, R. L. Renken and R. L. Sugar, Phys. Rev. D **35** (1987) 2531.

[79] S. Duane and J. Kogut, Nucl. Phys. B **275** (1986) 398.

[80] D. Callaway and A. Rahman, Phys. Rev. Lett. **49** (1982) 613.

[81] R. H. Hestenes and E. Stiefel, Journal of Research of the NBS **49** (1952) 409.

[82] K. Binder and D. W. Heermann, *Monte Carlo Simulation in Statistical Physics - an Introduction*, Springer-Verlag Berlin Heidelberg (2002).

[83] I. L. Bogolubsky, V. K. Mitrjushkin, M. Mueller-Preussker and N. V. Zverev, Nucl. Phys. Proc. Suppl. **94** (2001) 661.

Acknowledgment

I ringraziamenti sono dovuti ai due compagni di questo bellissimo percorso: Alessandro e Rossella. Grazie ad entrambi per il tempo, la pazienza e l'affetto che mi hanno dedicato. Grazie ad entrambi per i buoni consigli che mi hanno saputo dare.
Un augurio per tutti in questi tempi di partenza: a presto!